(12) INTERNATIONAL APPLICATION PUBLISHED UNDER THE PATENT COOPERATION TREATY (PCT)

(51) International Patent Classification:
G01S 19/37 (2010.01)   *G01S 19/20* (2010.01)

(21) International Application Number:
PCT/US2010/002565

(22) International Filing Date:
19 September 2010 (19.09.2010)

(25) Filing Language: English

(26) Publication Language: English

(30) Priority Data:
61/277,184   19 September 2009 (19.09.2009)   US

(71) Applicant *(for all designated States except US)*: TRIMBLE NAVIGATION LIMITED [US/US]; 935 Stewart Drive, Sunnyvale, CA 94085 (US).

(72) Inventor; and
(75) Inventor/Applicant *(for US only)*: SEEGER, Stephan [DE/DE]; Brotmannstrasse 29, 85635 Hoehenkirchen-Siegertsbrunn (DE).

(74) Agent: RITER, Bruce, D.; 101 First Street PMB 208, Los Altos, CA 94022 (US).

(81) Designated States *(unless otherwise indicated, for every kind of national protection available)*: AE, AG, AL, AM,

AO, AT, AU, AZ, BA, BB, BG, BH, BR, BW, BY, BZ, CA, CH, CL, CN, CO, CR, CU, CZ, DE, DK, DM, DO, DZ, EC, EE, EG, ES, FI, GB, GD, GE, GH, GM, GT, HN, HR, HU, ID, IL, IN, IS, JP, KE, KG, KM, KN, KP, KR, KZ, LA, LC, LK, LR, LS, LT, LU, LY, MA, MD, ME, MG, MK, MN, MW, MX, MY, MZ, NA, NG, NI, NO, NZ, OM, PE, PG, PH, PL, PT, RO, RS, RU, SC, SD, SE, SG, SK, SL, SM, ST, SV, SY, TH, TJ, TM, TN, TR, TT, TZ, UA, UG, US, UZ, VC, VN, ZA, ZM, ZW.

(84) Designated States *(unless otherwise indicated, for every kind of regional protection available)*: ARIPO (BW, GH, GM, KE, LR, LS, MW, MZ, NA, SD, SL, SZ, TZ, UG, ZM, ZW), Eurasian (AM, AZ, BY, KG, KZ, MD, RU, TJ, TM), European (AL, AT, BE, BG, CH, CY, CZ, DE, DK, EE, ES, FI, FR, GB, GR, HR, HU, IE, IS, IT, LT, LU, LV, MC, MK, MT, NL, NO, PL, PT, RO, SE, SI, SK, SM, TR), OAPI (BF, BJ, CF, CG, CI, CM, GA, GN, GQ, GW, ML, MR, NE, SN, TD, TG).

Declarations under Rule 4.17:
— of inventorship (Rule 4.17(iv))

Published:
— without international search report and to be republished upon receipt of that report (Rule 48.2(g))

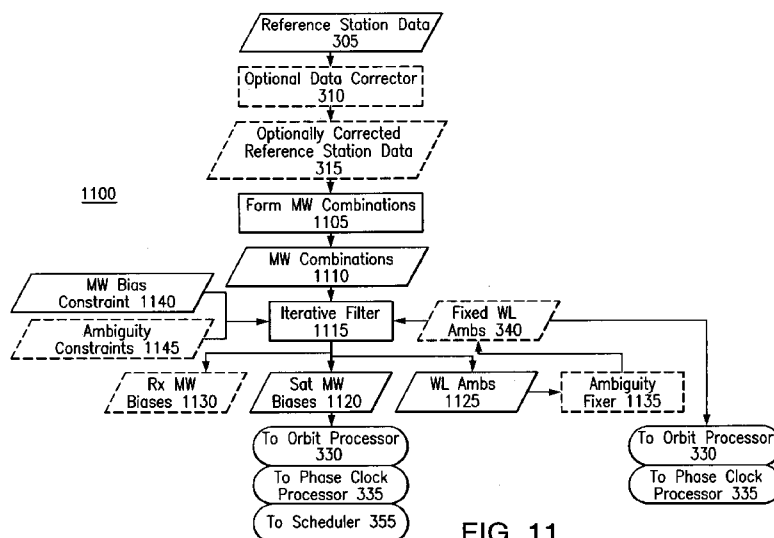(54) Title: GNSS SIGNAL PROCESSING TO ESTIMATE MW BIASES

FIG. 11

(57) Abstract: Methods and apparatus are described for processing a set of GNSS signal data derived from code observations and carrier-phase observations at multiple receivers of GNSS signals of multiple satellites over multiple epochs, the GNSS signals having at least two carrier frequencies, comprising: forming an MW (Melbourne- Wübbena) combination per receiver-satellite pairing at each epoch to obtain a MW data set per epoch, and estimating from the MW data set per epoch an MW bias per satellite which may vary from epoch to epoch, and a set of WL (widelane) ambiguities, each WL ambiguity corresponding to one of a receiver-satellite link and a satellite- receiver-satellite link, wherein the MW bias per satellite is modeled as one of (i) a single estimation parameter and (ii) an estimated offset plus harmonic variations with estimated amplitudes.

GNSS SIGNAL PROCESSING TO ESTIMATE MW BIASES

CROSS-REFERENCE TO RELATED APPLICATIONS

[001] The following are related hereto and incorporated herein in their entirety by this reference: United States Patent Application 12/660,091 filed 20 February 2010 (TNL A-2549US); United States Patent Application 12/660,080 filed 20 February 2010 (TNL A-2555US); United States Provisional Application for Patent No. 61/277,184 filed 19 September 2009 (TNL A-2585P); International Patent Application PCT/US2009/059552 filed 5 October 2009, published as WO 2010/042441 on 15 April 2010 (TNL A-2288PCT); United States Provisional Application for Patent No. 61/195,276 filed 6 October 2008 (TNL A-2288P); International Patent Application PCT/US/2009/004471 filed 5 August 2009, published as WO 2010/021656 on 25 February 2010 (TNL A-2526PCT); International Patent Application PCT/US/2009/004473 filed 5 August 2009, published as WO 2010/021658 on 25 February 2010 (TNL A-2525PCT); International Patent Application PCT/US/2009/004474 filed 5 August 2009, published as WO 2010/021659 on 25 February 2010 (TNL A-2524PCT); International Patent Application PCT/US/2009/004472 filed 5 August 2009, published as WO 2010/021657 on 25 February 2010 (TNL A-2523PCT); International Patent Application PCT/US/2009/004476 filed 5 August 2009 published as WO 2010/021660 A3 on 25 February 2010 (TNL A-2339PCT); United States Provisional Application for Patent No. 61/189,382 filed 19 August 2008 (TNL A-2339P); United States Patent 7,576,690 issued 18 August 2009 (TNL A-1805US); United States Patent Application 12/451,513 filed 22 June 2007, published as US 2010/0141515 on 10 June 2010; United States Patent 7,755,542 issued 13 July 2010 (TNL A-1789US); International Patent Application PCT/US07/05874 filed 7 March 2007, published as WO 2008/008099 on 17 January 2008 (TNL A-1789PCT); United States Patent Application No. 11/988,763 filed 14 January 2008, published as US 2009/0224969 A1 on 10 September 2009 (TNL A-1743US); International Patent Application No. PCT/US/2006/034433 filed 5 September 2006, published as WO 2007/032947 on 22 March 2007 (TNL A-1743PCT); United States Patent No. 7,432,853 granted 7 October 2008; (TNL A-1403US); International Patent Application No. PCT/US2004/035263 filed 22 October 2004, published as WO 2005/045463 on 19 May 2005 (TNL A-1403PCT); United States Patent No. 6,862,526 granted 1 March 2005 (TNL A-1006US).

[002] Priority benefit of United States Provisional Application for Patent No. 61/277,184 filed 19 September 2009 (TNL A-2585P) is hereby claimed.

BACKGROUND

[003]   The invention relates to GNSS signal processing, and particularly to GNSS signal processing involving precise satellite data.

5   BRIEF SUMMARY

[004]   Methods and apparatus are described for processing a set of GNSS signal data derived from code observations and carrier-phase observations at multiple receivers of GNSS signals of multiple satellites over multiple epochs, the GNSS signals having at least two carrier frequencies, comprising: forming an MW (Melbourne-Wübbena) combination per receiver-satellite pairing at

10   each epoch to obtain a MW data set per epoch, and estimating from the MW data set per epoch an MW bias per satellite which may vary from epoch to epoch, and a set of WL (widelane) ambiguities, each WL ambiguity corresponding to one of a receiver-satellite link and a satellite-receiver-satellite link, wherein the MW bias per satellite is modeled as one of (i) a single estimation parameter and (ii) an estimated offset plus harmonic variations with estimated

15   amplitudes.

[005]   In some embodiments, corrections are applied to the GNSS signal data. In some embodiments, at least one linear combination of GNSS signal data is smoothed before estimating an MW bias per satellite. In some embodiments, at least one MW bias constraint is applied. In some embodiments, at least one integer WL ambiguity constraint is applied. In some

20   embodiments, a spanning tree (ST) is used over one of an observation graph and a filter graph for constraining the WL ambiguities. In some embodiments, a minimum spanning tree (MST) is used on one of an observation graph and a filter graph for constraining the WL ambiguities.

[006]   In some embodiments, the minimum spanning tree is based on edge weights, each edge weight derived from receiver-satellite geometry. In some embodiments, the edge weight is

25   defined with respect to one of (i) a geometric distance from receiver to satellite, (ii) a satellite elevation angle, and (iii) a geometric distance from satellite to receiver to satellite, and (iv) a combination of the elevations under which the two satellites in a single differenced combination are seen at a station. In some embodiments, the minimum spanning tree is based on edge weights, with each edge weight based on WL ambiguity information, defined with respect to one

30   of (i) difference of a WL ambiguity to integer, (ii) WL ambiguity variance, and (iii) a combination of (i) and (ii).

[007]   In some embodiments, at least one of the WL ambiguities is fixed as an integer value. In some embodiments, candidate sets of WL integer ambiguity values are determined, a weighted combination of the candidate sets is formed, and at least one of the WL ambiguities is fixed as a

- 3 -

value taken from the weighted combination. In some embodiments, the estimating step comprises introducing fixed WL ambiguities so as to estimate MW biases which are compatible with fixed WL ambiguities. In some embodiments,the estimating step comprises applying an iterative filter to the MW data per epoch and wherein introducing fixed WL ambiguities

5   comprises one of (i) putting the fixed WL ambiguities as observations into the filter, (ii) putting the fixed WL ambiguities as observations into a copy of the filter generated after each of a plurality of observation updates, and (iii) reducing the MW combinations by the fixed WL ambiguities and putting the resulting reduced MW combinations into a second filter without ambiguity states to estimate at least one MW bias per satellite.

10   [008]   In some embodiments, at least one MW bias is shifted by an integer number of WL cycles. In some embodiments, at least one MW bias and its respective WL ambiguity are shifted by an integer number of WL cycles. In some embodiments, the navigation message comprises orbit information.

       Some embodiments provide apparatus for performing one or more of the described methods.

15   Some embodiments provide a computer program comprising instructions configured, when executed on a computer processing unit, to carry out one or more of the described methods. Some embodiments provide a tangible computer-readable medium embodying such a computer program.

BRIEF DESCRIPTION OF DRAWINGS

[009]   These and other aspects and features of the present invention will be more readily understood from the embodiments described below with reference to the drawings, in which:

FIG. 1 shows a high-level view of a system in accordance with some embodiments of the
5   invention;
FIG. 2 shows a high-level view of a system and system data in accordance with some embodiments of the invention;
FIG. 3 is a schematic diagram of network processor architecture in accordance with some embodiments of the invention;
10   FIG. 4 is a schematic diagram of data correction in accordance with some embodiments of the invention;
FIG. 5 is a schematic view of linear combinations of observations in accordance with some embodiments of the invention;
FIG. 6 is a schematic view of a generic Kalman filter process;
15   FIG. 7 is a schematic diagram of a code-leveled clock processor in accordance with some embodiments of the invention;
FIG. 8, FIG. 9 and FIG. 10 are deleted;
FIG. 11 is a schematic diagram of a Melbourne-Wübbena bias process flow in accordance with some embodiments of the invention;
20   FIG. 12 is a schematic diagram of a Melbourne-Wübbena bias process flow in accordance with some embodiments of the invention;
FIG. 13A shows filter states of an undifferenced Melbourne-Wübbena bias processor in accordance with some embodiments of the invention;
FIG. 13B shows filter states of a single-differenced Melbourne-Wübbena bias processor in
25   accordance with some embodiments of the invention;
FIG. 14 is a schematic diagram of a Melbourne-Wübbena bias processor in accordance with some embodiments of the invention;
FIG. 15 is a schematic diagram of a Melbourne-Wübbena bias processor in accordance with some embodiments of the invention;
30   FIG. 16 is a schematic diagram of a Melbourne-Wübbena bias processor in accordance with some embodiments of the invention;
FIG. 17 is a schematic diagram of a Melbourne-Wübbena bias processor in accordance with some embodiments of the invention;

FIG. 18 is a schematic diagram of a Melbourne-Wübbena bias processor in accordance with some embodiments of the invention;

FIG. 19A is an observation graph of GNSS stations and satellites;

FIG. 19B is an abstract graph showing stations and satellites as vertices and station-satellite

5   observations as edges;

FIG. 19C depicts a minimum spanning tree of the graph of FIG. 19B;

FIG. 19D depicts a minimum spanning tree with constrained edges;

FIG. 19E is an undifferenced observation graph of GNSS stations and satellites;

FIG. 19F is an filter graph corresponding to the observation graph of FIG. 19E;

10   FIG. 19G is a single-differenced observation graph of GNSS stations and satellites;

FIG. 19H is a filter graph corresponding to the observation graph of FIG. 19G;

FIG. 19I is a set of observations graphs comparing constraints in undifferenced and single-differenced processing;

FIG. 20 is a schematic diagram of a Melbourne-Wübbena bias processor in accordance with some

15   embodiments of the invention;

FIG. 21A shows a spanning tree on an undifferenced observation graph;

FIG. 21B shows a minimum spanning tree on an undifferenced observation graph;

FIG. 21C shows a spanning tree on a single-differenced observation graph;

FIG. 21D shows a minimum spanning tree on a single-differenced observation graph;

20   FIG. 22 is a schematic diagram of a Melbourne-Wübbena bias processor in accordance with some embodiments of the invention;

FIG. 23A is a schematic diagram of a Melbourne-Wübbena bias processor in accordance with some embodiments of the invention;

FIG. 23B is a schematic diagram of a Melbourne-Wübbena bias processor in accordance with

25   some embodiments of the invention;

FIG. 24A is a schematic diagram of a Melbourne-Wübbena bias processor in accordance with some embodiments of the invention;

FIG. 24B is a schematic diagram of a Melbourne-Wübbena filtering process in accordance with some embodiments of the invention;

30   FIG. 24C is a schematic diagram of a Melbourne-Wübbena filtering process in accordance with some embodiments of the invention;

FIG. 24D is a schematic diagram of a Melbourne-Wübbena filtering process in accordance with some embodiments of the invention;

FIG. 25A is a schematic diagram of a Melbourne-Wübbena bias processor in accordance with some embodiments of the invention;

FIG. 25B illustrates the effect of shifting biases in accordance with some embodiments of the invention;

FIG. 25C is a schematic diagram of a Melbourne-Wübbena bias processor in accordance with some embodiments of the invention;

FIG. 26A is a schematic diagram of the startup of an orbit processor in accordance with some embodiments of the invention;

FIG. 26B is a schematic diagram of an orbit processor in accordance with some embodiments of the invention;

FIG. 26C is a schematic diagram of an orbit mapper of an orbit processor in accordance with some embodiments of the invention;

FIG. 26D is a schematic diagram of an orbit mapper of an orbit processor in accordance with some embodiments of the invention;

FIG. 27 is a timing diagram of code-leveled clock processing in accordance with some embodiments of the invention;

FIG. 28A is a schematic diagram of a high-rate code-leveled satellite clock processor in accordance with some embodiments of the invention;

FIG. 28B is a schematic diagram of a high-rate code-leveled satellite clock processor in accordance with some embodiments of the invention;

FIG. 28C is a schematic diagram of a high-rate code-leveled satellite clock processor in accordance with some embodiments of the invention;

FIG. 29 is a schematic diagram of a high-rate phase-leveled satellite clock processor in accordance with some embodiments of the invention;

FIG. 30A is a schematic diagram of a high-rate phase-leveled satellite clock processor in accordance with some embodiments of the invention;

FIG. 30B is a schematic diagram of a high-rate phase-leveled satellite clock processor in accordance with some embodiments of the invention;

FIG. 30C is a schematic diagram of a high-rate phase-leveled satellite clock processor in accordance with some embodiments of the invention;

FIG. 31 is a schematic diagram of a high-rate phase-leveled satellite clock processor in accordance with some embodiments of the invention;

FIG. 32 is a schematic diagram of a high-rate phase-leveled satellite clock processor in accordance with some embodiments of the invention;

FIG. 33 is a schematic diagram of a high-rate phase-leveled satellite clock processor in accordance with some embodiments of the invention;

FIG. 34 is a schematic diagram of a high-rate phase-leveled satellite clock processor in accordance with some embodiments of the invention;

5 FIG. 35 is deleted;

FIG. 36 is a schematic diagram of a network processor computer system in accordance with some embodiments of the invention;

FIG. 37 is a simplified schematic diagram of an integrated GNSS receiver system in accordance with some embodiments of the invention;

10 FIG. 38 is a schematic diagram of a GNSS rover process with synthesized base station data in accordance with some embodiments of the invention;

FIG. 39 depicts observation clock prediction in accordance with some embodiments of the invention;

FIG. 40 is a schematic diagram of a process for generating synthesized base station data in

15 accordance with some embodiments of the invention;

FIG. 41 is deleted;

FIG. 42 is a schematic diagram of an alternate GNSS rover process with synthesized base station data in accordance with some embodiments of the invention;

FIG. 43 is a simplified schematic diagram of a GNSS rover process with synthesized base station

20 data in accordance with some embodiments of the invention;

FIG. 44 is a timing diagram of a low-latency GNSS rover process with synthesized base station data in accordance with some embodiments of the invention;

FIG. 45 is a timing diagram of a high-accuracy GNSS rover process with synthesized base station data in accordance with some embodiments of the invention;

25 FIG. 46 is a schematic diagram of an alternate GNSS rover process with synthesized base station data in accordance with some embodiments of the invention;

FIG. 47 depicts performance of a GNSS rover process with ambiguity fixing in accordance with some embodiments of the invention in relation to a GNSS rover process without ambiguity fixing;

30 FIG. 48 is a schematic diagram of a GNSS rover process with ambiguity fixing in accordance with some embodiments of the invention;

FIG. 49 is a schematic diagram of a GNSS rover process with ambiguity fixing in accordance with some embodiments of the invention;

- 8 -

FIG. 50 is a schematic diagram of a GNSS rover process with ambiguity fixing in accordance with some embodiments of the invention;

FIG. 51 is a schematic diagram of a GNSS rover process with ambiguity fixing in accordance with some embodiments of the invention;

5 FIG. 52 is a schematic diagram of a GNSS rover process with ambiguity fixing in accordance with some embodiments of the invention;

FIG. 53 is a schematic diagram of a GNSS rover process with ambiguity fixing in accordance with some embodiments of the invention;

FIG. 54 is a schematic diagram of a GNSS rover process with ambiguity fixing in accordance

10 with some embodiments of the invention;

FIG. 55 is a schematic diagram of a GNSS rover process with ambiguity fixing in accordance with some embodiments of the invention;

FIG. 56 is a schematic diagram of a GNSS rover process with ambiguity fixing in accordance with some embodiments of the invention;

15 FIG. 57 is a schematic diagram of a GNSS rover process with ambiguity fixing in accordance with some embodiments of the invention;

FIG. 58 is a schematic diagram of a GNSS rover process with ambiguity fixing in accordance with some embodiments of the invention;

FIG. 59 is a schematic diagram of a GNSS rover process with ambiguity fixing in accordance

20 with some embodiments of the invention;

FIG. 60 is a schematic diagram of a GNSS rover process with ambiguity fixing in accordance with some embodiments of the invention;

FIG. 61 is a schematic diagram of a GNSS rover process with ambiguity fixing in accordance with some embodiments of the invention; and

25 FIG. 62 is a schematic diagram of a GNSS rover process with ambiguity fixing in accordance with some embodiments of the invention.

DETAILED DESCRIPTION

Part 1: System Overview

[0010]   Global Navigation Satellite Systems (GNSS) include GPS, Galileo, Glonass, Compass and other similar positioning systems. While the examples given here are directed to GPS processing the principles are applicable to any such positioning system.

[0011]   Definition of Real time: In this document the term "Real time" is mentioned several times. In the scope of the inventions covered by the following embodiments this term means that there is an action (e.g., data is processed, results are computed) as soon the required information for that action is available. Therefore, certain latency exists, and it depends on different aspects depending on the component of the system. The required information for the application covered in this document is usually GNSS data, and/or GNSS corrections, as described below.

[0012]   The network processors running in real time are able to provide results for one epoch of data from a network of monitoring receivers after: (1a) The data is collected by each of the monitoring receivers (typically less than 1 msec); (1b) The data is transmitted from each receiver to the processing center (typically less than 2 sec); (1c) The data is processed by the processor. The computation of the results by the network processors typically takes between 0.5 and 5 seconds depending on the processor type, and amount of data to be used.

[0013]   It is usual that data that do not follow certain restrictions in transmission delay (e.g., 3 sec) are rejected or buffered and therefore not immediately used for the current epoch update. This avoids the enlargement of the latency of the system in case one or more stations are transmitting data with an unacceptable amount of delay.

[0014]   A rover receiver running in real time is able to provide results for one epoch of data after the data is collected by receiver (typically less than 1 msec) and: (2a) The correction data is generated by the processing center (see 1a,1b,1c); (2b) The correction data (if required) is received from the processing center (typically less than 5 sec); (2c) The data is processed (typically less than 1 msec).

[0015]   To avoid or minimize the effect of data latency caused by (2a) and (2b), a delta phase approach can be used so updated receiver positions can be computed (typically in less than 1 msec) immediately after the data is collected and with correction data streams. The delta phase approach is described for example in US Patent 7,576,690 granted August 18, 2009 to U. Vollath.

[0016]   FIG. 1 and FIG. 2 show high level views of a system 100 in accordance with some embodiments of the invention. Reference stations of a worldwide tracking network, such as reference stations 105, 110, ... 115, are distributed about the Earth. The position of each

reference station is known very precisely, e.g., within less than 2 cm. Each reference station is

equipped with an antenna and tracks the GNSS signals transmitted by the satellites in view at that

station, such as GNS satellites 120, 125, ... 130. The GNSS signals have codes modulated on

each of two or more carrier frequencies. Each reference station acquires GNSS data 205

5   representing, for each satellite in view at each epoch, carrier-phase (carrier) observations 210 of

at least two carriers, and pseudorange (code) observations 215 of the respective codes modulated

on at least two carriers. The reference stations also obtain the almanac and ephemerides 220 of

the satellites from the satellite signals. The almanac contains the rough position of all satellites of

the GNSS, while the so-called broadcast ephemerides provide more precise predictions (ca. 1 m)

10   of the satellites' positions and the satellites' clock error (ca. 1.5 m) over specific time intervals.

[0017]   GNSS data collected at the reference stations is transmitted via communications channels

135 to a network processor 140. Network processor 140 uses the GNSS data from the reference

stations with other information to generate a correction message containing precise satellite

position and clock data, as detailed below. The correction message is transmitted for use by any

15   number of GNSS rover receivers. The correction message is transmitted as shown in FIG. 1 via

an uplink 150 and communications satellite 155 for broadcast over a wide area; any other suitable

transmission medium may be used including but not limited to radio broadcast or mobile

telephone link. Rover 160 is example of a GNSS rover receiver having a GNSS antenna 165 for

receiving and tracking the signals of GNSS satellites in view at its location, and optionally having

20   a communications antenna 170. Depending on the transmission band of the correction message,

it can be received by rover 160 via GNSS antenna 165 or communications antenna 170.

Part 2: Network Architecture

25   [0018]   FIG. 3 is a schematic diagram showing principal components of the process flow 300 of a

network processor 140 in accordance with some embodiments of the invention. GNSS data from

the global network of reference stations 310 is supplied without corrections as GNSS data 305 or

after correction by an optional data corrector 310 as corrected GNSS data 315, to four processors:

a standard clock processor 320, a Melbourne-Wübbena (MW) bias processor 325, an orbit

30   processor 330, and a phase clock processor 335.

[0019]   Data corrector 310 optionally analyzes the raw GNSS data 305 from each reference

station to check for quality of the received observations and, where possible, to correct the data

for cycle slips, which are jumps in the carrier-phase observations occurring, e.g., each time the

receiver has a loss of lock. Commercially-available reference stations typically detect cycle slips

and flag the data accordingly. Cycle slip detection and correction techniques are summarized, for example, in *G. Seeber*, SATELLITE GEODESY, 2nd Ed. (2003) at pages 277-281. Data corrector 310 optionally applies other corrections. Though not all corrections are needed for all the processors, they do no harm if applied to the data. For example as described below some

5   processors use a linear combination of code and carrier observations in which some uncorrected errors are canceled in forming the combinations.

[0020] Observations are acquired epoch by epoch at each reference station and transmitted with time tags to the network processor 140. For some stations the observations arrive delayed. This delay can range between milliseconds and minutes. Therefore an optional synchronizer 318

10   collects the data of the corrected reference station data within a predefined time span and passes the observations for each epoch as a set to the processor. This allows data arriving with a reasonable delay to be included in an epoch of data.

[0021] The MW bias processor 325 takes either uncorrected GNSS data 305 or corrected GNSS data 315 as input, since it uses the Melbourne-Wübbena linear combination which cancels out all

15   but the ambiguities and the biases of the phase and code observations. Thus only receiver and satellite antenna corrections are important for the widelane processor 325. Based on this linear combination, one MW bias per satellite and one widelane ambiguity per receiver-satellite pairing are computed. The biases are smooth (not noisy) and exhibit only some sub-daily low-rate variations. The widelane ambiguities are constant and can be used as long as no cycle slip occurs

20   in the observations on the respective satellite-receiver link. Thus the bias estimation is not very time critical and can be run, e.g., with a 15 minute update rate. This is advantageous because the computation time grows with the third power of the number of stations and satellites. As an example, the computation time for a reasonable network with 80 stations can be about 15 seconds. The values of fixed widelane ambiguities 340 and/or widelane biases 345 are optionally

25   used in the orbit processor 330 and/or the phase clock processor 335, and/or are supplied to a scheduler 355. MW bias processor 325 is described in detail in Part 7 below.

[0022] Some embodiments of orbit processor 330 are based on a prediction-correction strategy. Using a precise force model and starting with an initial guess of the unknown values of the satellite's parameters (initial position, initial velocity and dynamic force model parameters), the

30   orbit of each satellite is predicted by integration of the satellite's nonlinear dynamic system. The sensitivity matrix containing the partial derivatives of the current position to the unknown parameters is computed at the same time. Sensitivities of the initial satellite state are computed at the same time for the whole prediction. That is, starting with a prediction for the unknown parameters, the differential equation system is solved, integrating the orbit to the current time or

into the future. This prediction can be linearized into the direction of the unknown parameters. Thus the partial derivatives (sensitivities) serve as a measure of the size of the change in the current satellite states if the unknown parameters are changed, or vice versa.

[0023] In some embodiments these partial derivatives are used in a Kalman filter to improve the initial guess by projecting the GNSS observations to the satellite's unknown parameters. This precise initial state estimate is used to again integrate the satellite's dynamic system and determine a precise orbit. A time update of the initial satellite state to the current epoch is performed from time to time. In some embodiments, ionospheric-free ambiguities are also states of the Kalman filter. The fixed widelane ambiguity values 340 are used to fix the ionospheric-free ambiguities of the orbit processor 330 to enhance the accuracy of the estimated orbits. A satellite orbit is very smooth and can be predicted for minutes and hours. The precise orbit predictions 350 are optionally forwarded to the standard clock processor 320 and to the phase clock processor 335 as well as to a scheduler 355.

[0024] Ultra-rapid orbits 360, such as IGU orbits provided by the International GNSS Service (IGS), can be used as an alternative to the precise orbit predictions 355. The IGU orbits are updated four times a day and are available with a three hour delay.

[0025] Standard clock processor 320 computes code-leveled satellite clocks 360 (also called standard satellite clocks), using GNSS data 305 or corrected GNSS data 315 and using precise orbit predictions 355 or ultra-rapid orbits 365. Code-leveled means that the clocks are sufficient for use with ionospheric-free code observations, but not with carrier-phase observations, because the code-leveled clocks do not preserve the integer nature of the ambiguities. The code-leveled clocks 360 computed by standard clock processor 320 represent clock-error differences between satellites. The standard clock processor 320 uses the clock errors of the broadcast ephemerides as pseudo observations and steers the estimated clocks to GPS time so that they can be used to compute, e.g., the exact time of transmission of a satellite's signal. The clock errors change rapidly, but for the use with code measurements, which are quite noisy, an accuracy of some centimeter is enough. Thus a "low rate" update rate of 30 seconds to 60 seconds is adequate. This is advantageous because computation time grows with the third power of number of stations and satellites. The standard clock processor 325 also determines troposphere zenith delays 365 as a byproduct of the estimation process. The troposphere zenith delays and the code-leveled clocks are sent to the phase clock processor 335. Standard clock processor 320 is described in detail in Part 6 below.

[0026] The phase clock processor 335 optionally uses the fixed widelane ambiguities 340 and/or MW biases 345 from widelane processor 325 together with the troposphere zenith delays 365 and

the precise orbits 350 or IGU orbits 360 to estimate single-differenced clock errors and narrowlane ambiguities for each pairing of satellites. The single-differenced clock errors and narrowlane ambiguities are combined to obtain single-differenced phase-leveled clock errors 370 for each satellite (except for a reference satellite) which are single-differenced relative to the

5   reference satellite. The low-rate code leveled clocks 360, the troposphere zenith delays 365 and the precise orbits 350 or IGU orbits 360 are used to estimate high-rate code-leveled clocks 375. Here, the computational effort is linear with the number of stations and to the third power with the number of satellites. The rapidly-changing phase-leveled clocks 370 and code-leveled clocks 375 are available, for example, with a delay of 0.1 sec – 0.2 sec. The high-rate phase-leveled

10   clocks 370 and the high-rate code-leveled clocks 375 are sent to the scheduler 355 together with the MW biases 340. Phase clock processor 340 is described in detail in Part 9 below.

[0027] Scheduler 355 receives the orbits (precise orbits 350 or IGU orbits 360), the MW biases 340, the high-rate phase-leveled clocks 370 and the high-rate code-leveled clock 375. Scheduler 355 packs these together and forwards the packed orbits and clocks and biases 380 to a message

15   encoder 385 which prepares a correction message 390 in compressed format for transmission to the rover. Transmission to a rover takes for example about 10 sec – 20 sec over a satellite link, but can also be done using a mobile phone or a direct internet connection or other suitable communication link.

20   **Part 3: Observation Data Corrector**

[0028] FIG. 4 is a schematic diagram of data correction in accordance with some embodiments of the invention. Optional observation corrector 310 corrects the GNSS signals collected at a reference station for displacements of the station due to centrifugal, gyroscopic and gravitational forces acting on the Earth, the location of the station's antenna phase center relative to the

25   station's antenna mounting point, the location of the satellite's antenna phase center relative to the satellite's center of mass given by the satellite's orbit, and variations of those phase centers depending on the alignment of the station's antenna and the satellite's antenna.

[0029] The main contributors to station displacements are solid Earth tides up to 500 mm, ocean tidal loadings up to 100 mm, and pole tides up to 10 mm. All of these depend on where the

30   station is located. More description is found in McCarthy, D.D., Petit, G. (eds.), *IERS Conventions (2003)*, IERS Technical Note No. 32, and references cited therein.

[0030] Ocean tides caused by the forces of astronomical bodies – mainly the moon – acting on the Earth's loose masses, also cause the Earth's tectonic plates to be lifted and lowered. This well-known effect shows up as recurring variations of the reference stations' locations. The solid

Earth tides are optionally computed for network processing as well as for rover processing, as the effect should not be neglected and the computational effort is minor.

[0031] The second largest effect is the deformation of the Earth's tectonic plates due to the load of the oceans varying over time with the tides. Ocean tide loading parameters used to quickly

5   compute the displacement of a station over time depend on the location of the station. The computational effort to derive these parameters is quite high. They can be computed for a given location, using any of the well-known models available at the online ocean-tide-loading service provided by the Onsala Space Observatory Ocean, http://www.oso.chalmers.se/~loading/, Chalmers: Onsala Space Observatory, 2009. The lower accuracy parameters, e.g., from

10   interpolation of a precomputed grid, are sufficient for the applications discussed here.

[0032] The smallest effect mentioned here is that due to pole tides. This displacement is due to the lift of a tectonic plate caused by the centrifugal and gyroscopic effects generated by the polar motion of the Earth. Earth orientation parameters are used for this computation. These are updated regularly at the International Earth Rotation & Reference System Service, International

15   Earth Rotation & Reference System Service, http://hpiers.obspm.fr/, L'Observatoire de Paris, 2009, and are not easily computed. This minor effect is therefore optionally neglected in the rover processing.

[0033] Absolute calibrated antenna models are used to compute the offsets and variations of receiver and satellite antenna phase centers. A description is found at J. Kouba, *A Guide to Using*

20   *International GPS Service (IGS) Products, Geodetic Survey Division Natural Resources Canada*, February 2003. Calibration data collected by the IGS is made available in antex files at http://igscb.jpl.nasa.gov/, 2009; satellite antenna offset information is found for example in the IGS absolute antenna file igs05.atx.

[0034] Another effect is the antenna phase wind-up. If a receiver antenna is moving relative to

25   the sender antenna the recorded data shows a phase shift. If this effect is neglected, a full turn of the satellite around the sending axis will cause an error of one cycle in the carrier-phase detected at the receiver. Since the satellite's orientation relative to the receiver is well known most of the time, this effect can be modeled as described in Wu J.T., Hajj G.A., Bertiger W.I., & Lichten S.M., *Effects of antenna orientation on GPS carrier phase*, MANUSCRIPTA GEODAETICA, Vol. 18,

30   pp. 91 – 98 (1993).

[0035] The relative movement of the station and the satellite is mainly due to the orbiting satellite. If a satellite is eclipsing - this means the satellite's orbit crosses the Earth's shadow - additional turns of the satellite around its sending axis are possible. For example, GPS Block IIA satellites have a noon turn and a shadow crossing maneuver, while GPS Block IIR satellites have

a noon turn and a midnight turn. If the sun, the Earth and the satellite are nearly collinear it is hard to compute the direction of the turn maneuvers, and an incorrect direction will cause an error in the carrier-phase of one cycle. The satellite's yaw attitude influences the phase wind-up and the satellite antenna corrections. More detailed descriptions are found in Kouba, J., *A simplified*

5   *yaw-attitude model for eclipsing GPS satellites*, GPS SOLUTIONS (2008) and Bar-Sever, Y.E., *A new model for GPS yaw attitude*, JOURNAL OF GEODESY, Vol. 70, pp. 714-723 (1996).

[0036]   In the case of only using phase observations, the effect of an unmodeled satellite turn maneuver can not be separated from the satellite clock. Thus in a phase clock error estimation the effect of the turn maneuver is included in the estimated satellite clock error. If a rover uses those

10   clocks it must not correct for satellite turn maneuver either.

[0037]   The sun position is needed to compute the satellite's body-fixed coordinate frame, since the x axis is defined by the cross product of the satellite's position and the sun's position. This coordinate system is used to compute the yaw attitude, the satellite's antenna correction (offset and variations, mapped into sine of sight) and the phase wind-up correction. The moon's position

15   is also needed for the solid Earth tides. How to compute the position of the sun and the moon is found, for example, in Seidelmann, P.K. (ed.), *Explanatory Supplement to the Astronomical Almanac*, University Science Books, U.S. (1992).

[0038]   Further corrections can also be applied, though these are of only minor interest for the positioning accuracy level demanded by the marketplace.

20   [0039]   Additional effects as corrections for relativistic effects, ionospheric and troposphere delays do not need to be considered in the optional data corrector 310. Relativistic corrections are usually applied to the satellite clocks. The major first order effect due to the ionosphere is eliminated using an ionospheric free combination of the GNSS observations, and the effect due to the troposphere is in some embodiments partly modeled and partly estimated.

25

Part 4: Forming Linear Combinations

    4.1 Basic Modeling Equations

[0040]   For code $P_{i,km}^{j}$ and carrier phase $\Phi_{i,km}^{j}$ observations between receiver i and satellite j

30   on frequency band k and modulation type m the following observation model is assumed that relates the observations to certain physical quantities,

$$P_{i,km}^{j} = \rho_{i}^{j} + c\Delta t_{i} - c\Delta t^{j} + T_{i}^{j} + I_{P,i,k}^{j} + b_{P,i,km} - b_{P,km}^{j} + m_{P,i,km}^{j} + \varepsilon_{P,i,km}^{j}.$$ (1)

$$\Phi^j_{i,km} = \rho^j_i + c\Delta t_i - c\Delta t^j + T^j_i + I^j_{\Phi,i,k} + b_{\Phi,i,k} - b^j_{\Phi,k} + \lambda_k N^j_{i,k} + m^j_{\Phi,i,km} + \varepsilon^j_{\Phi,i,km} \, . \qquad (2)$$

with

ρ^j_i	geometrical range from satellite j to receiver i
c	speed of light
Δt_i	receiver i clock error
Δt^j	satellite j clock error
T^j_i	tropospheric delay from satellite j to receiver i
$I^j_{P,i,k} = \dfrac{I^j_{1i}}{f^2_k} + \dfrac{2I^j_{2i}}{f^3_k} + \dfrac{3I^j_{3i}}{f^4_k}$	code ionospheric delay on frequency f_k
$I^j_{\Phi,i,k} = -\dfrac{I^j_{1i}}{f^2_k} - \dfrac{I^j_{2i}}{f^3_k} - \dfrac{I^j_{3i}}{f^4_k}$	carrier phase ionospheric delay on frequency f_k
$b_{P,i,km}$	code receiver bias
$b^j_{P,km}$	code satellite bias
$b_{\Phi,i,k}$	phase receiver bias (independent of modulation type m)
$b^j_{\Phi,k}$	phase satellite bias (independent of modulation type m)
$N^j_{i,k}$	integer ambiguity term from satellite j to receiver i on wavelength λ_k
$m^j_{P,i,km}$	code multipath from satellite j to receiver i
$m^j_{\Phi,i,km}$	phase multipath from satellite j to receiver i
$\varepsilon^j_{P,i,km}$	code random noise term
$\varepsilon^j_{\Phi,i,km}$	phase random noise term

The modulation type dependency in the phase observation can be suppressed by assuming that the different phase signals on a frequency band are already shifted to a common base inside the receiver, e.g. L2C is assumed to be shifted by -0.25 cycles to compensate the 90 degrees rotation of the quadrature phase on which it is modulated. However, noise and multipath terms (that are usually not modeled) still have a different contribution to the phase observation for different modulation types.

[0041] Examples of different modulation types (also called code types) are in case of GPS L1C/A, L1P, L1C on L1-frequency band and L2C, L2P on L2-frequency band and in case of

Glonass L1C/A, L1P and L2C/A, L2P.   For the Glonass satellite system, wavelength λ_k and

frequency f_k also depend on a satellite specific frequency channel number so that the notation

could be extended to $\lambda_k^{(j)}$ and $f_k^{(j)}$. In addition, especially the code receiver biases $b_{P,i,km}$ also

have a channel and therefore satellite dependency (as can be seen in a zero-baseline processing

5   with some averaging over time so that $P_{i_1i_2,km}^{j} = b_{P,i_1i_2,km}$). Therefore a more precise formulation

for the code receiver bias would be $b_{P,i,km}^{j} = b_{P,i,km} + \Delta b_{P,i,km}^{j}$.

[0042]   The symbol Φ used here for carrier phase observations, is also used for the time

transition matrix in the Kalman filter context. For both cases, Φ is the standard symbol used in

the scientific literature and we adopted this notation. The meaning of Φ will be always clear from

10   the context.

[0043]   In the following we neglect the second order $\dfrac{I_{2i}^{j}}{f_k^3}$ and third order $\dfrac{I_{3i}^{j}}{f_k^4}$ ionospheric terms

that are typically in the range of less than 2 cm (Morton, van Graas, Zhou, & Herdtner, 2008),

(Datta-Barua, Walter, Blanch, & Enge, 2007). In this way, $I_{P,i,k}^{j} = \dfrac{I_i^{j}}{f_k^2} = -I_{\Phi,i,k}^{j}$ with $I_i^{j} := I_{1i}^{j}$.

Only under very severe geomagnetic active conditions the second and third order terms can reach

15   tens of centimeters. However, these conditions occur only for a few days in many years. The

higher order ionospheric terms can be taken into account by ionospheric models based on the

Appleton-Hartree equation that relates the phase index of refraction of a right hand circularly

polarized wave propagating through the ionosphere to the wave frequency f_k, the electron

density and the earth magnetic field. Approximations to the Appleton-Hartree equation allow to

20   relate the parameters I_{2i}^{j}, I_{3i}^{j} of the second and third order ionospheric terms to the first order

ionospheric estimation parameter $I_i^{j} := I_{1i}^{j}$ that is a measure of the total electron content along the

signal propagation path. Thus higher order ionospheric terms can be corrected on base of

observation data on at least two frequencies.

[0044]   In the following we will often talk about ionospheric-free (IF) linear combinations.

25   However, notice that these linear combinations only cancel the first order ionospheric term and

are thus not completely ionospheric-free.

Linear Combinations of Observations

[0045] By combining several code $P_{i,km}^{j}$ and carrier phase $\Phi_{i,km}^{j}$ observations in a linear way

$$LC = \sum_{i,j,k,m} a_{P,i,km}^{j} P_{i,km}^{j} + a_{\Phi,i,km}^{j} \Phi_{i,km}^{j} \quad \text{with } a_{P,i,km}^{j}, a_{\Phi,i,km}^{j} \in R \text{ for all } i,j,k,m \tag{3}$$

some of the physical quantities can be eliminated from the linear combination LC so that these quantities do not have to be estimated if the linear combination is used as the observation input for an estimator. In this way some linear combinations are of special importance.

[0046] Single difference (SD) observations between two satellites j_1 and j_2 eliminate all quantities that are not satellite dependent, i.e. that do not have a satellite index j.

[0047] Defining $X^{j_1 j_2} := X^{j_2} - X^{j_1}$, the between satellite SD observations are formally obtained by substituting each index j by $j_1 j_2$ and ignoring all terms without a satellite index j

$$P_{i,km}^{j_1 j_2} = \rho_i^{j_1 j_2} - c\Delta t^{j_1 j_2} + T_i^{j_1 j_2} + I_{P,i,k}^{j_1 j_2} - b_{P,km}^{j_1 j_2} + m_{P,i,km}^{j_1 j_2} + \varepsilon_{P,i,km}^{j_1 j_2}. \tag{4}$$

$$\Phi_{i,km}^{j_1 j_2} = \rho_i^{j_1 j_2} - c\Delta t^{j_1 j_2} + T_i^{j_1 j_2} + I_{\Phi,i,k}^{j_1 j_2} - b_{\Phi,k}^{j_1 j_2} + \lambda_k N_{i,k}^{j_1 j_2} + m_{\Phi,i,km}^{j_1 j_2} + \varepsilon_{\Phi,i,km}^{j_1 j_2}. \tag{5}$$

In this way the receiver clock and receiver bias terms have been eliminated in the linear combination.

[0048] In the same way single difference observations between two receivers i_1 and i_2 eliminate all quantities that are not receiver dependent, i.e. that have no receiver index i.

[0049] By generating the difference between two receivers i_1 and i_2 on the between satellite single difference observations (4) and (5), double difference (DD) observations are obtained that also eliminate all receiver dependent terms from (4) and (5).

[0050] Defining $X_{i_1 i_2}^{j_1 j_2} := X_{i_2}^{j_1 j_2} - X_{i_1}^{j_1 j_2} = \left(X_{i_2}^{j_2} - X_{i_2}^{j_1} \right) - \left(X_{i_1}^{j_2} - X_{i_1}^{j_1} \right)$, the DD observations are formally obtained from (4) and (5) by substituting each index i by $i_1 i_2$ and ignoring all terms without a receiver index i

$$P_{i_1 i_2,km}^{j_1 j_2} = \rho_{i_1 i_2}^{j_1 j_2} + T_{i_1 i_2}^{j_1 j_2} + I_{P,i_1 i_2,k}^{j_1 j_2} + m_{P,i_1 i_2,km}^{j_1 j_2} + \varepsilon_{P,i_1 i_2,km}^{j_1 j_2}. \tag{6}$$

$$\Phi_{i_1 i_2,km}^{j_1 j_2} = \rho_{i_1 i_2}^{j_1 j_2} + T_{i_1 i_2}^{j_1 j_2} + I_{\Phi,i_1 i_2,k}^{j_1 j_2} + \lambda_k N_{i_1 i_2,k}^{j_1 j_2} + m_{\Phi,i_1 i_2,km}^{j_1 j_2} + \varepsilon_{\Phi,i_1 i_2,km}^{j_1 j_2}. \tag{7}$$

In this way also the satellite clock and the satellite biases have been eliminated in the linear combination.

[0051] In the following we assume that all code observations $P^j_{i,km}$ correspond to the same modulation type and that all phase observations $\Phi^j_{i,km}$ correspond to the same observation type that may differ from the modulation type of the code observations. Since the modulation type dependency for the phase observations occurs only in the unmodeled multipath and random noise terms, in this way the modulation type index m can be suppressed.

[0052] For our purposes two linear combinations that cancel the first order ionospheric delay $\dfrac{I^j_i}{f^2_k}$ in different ways are of special importance, the iono-free linear combination for code and carrier phase and the Melbourne-Wübbena (MW) linear combination $\Phi^j_{i,WL} - P^j_{i,NL}$ consisting of the widelane (WL) carrier phase $\dfrac{\Phi^j_{i,WL}}{\lambda_{WL}} := \dfrac{\Phi^j_{i,1}}{\lambda_1} - \dfrac{\Phi^j_{i,2}}{\lambda_2}$ and narrowlane (NL) code

$\dfrac{P^j_{i,NL}}{\lambda_{NL}} := \dfrac{P^j_{i,1}}{\lambda_1} + \dfrac{P^j_{i,2}}{\lambda_2}$ observations with wavelengths $\lambda_{WL} = \dfrac{c}{f_{WL}} := \dfrac{c}{f_1 - f_2}$ and

$\lambda_{NL} = \dfrac{c}{f_{NL}} := \dfrac{c}{f_1 + f_2}$, (Melbourne, 1985), (Wübbena, 1985),

$$P^j_{i,NL} = \rho^j_i + c\Delta t_i - c\Delta t^j + T^j_i + \lambda_{NL}\left(\frac{b_{P,i,1}}{\lambda_1} + \frac{b_{P,i,2}}{\lambda_2}\right) - \lambda_{NL}\left(\frac{b^j_{P,1}}{\lambda_1} + \frac{b^j_{P,2}}{\lambda_2}\right)$$
$$+ \lambda_{NL}\left(\frac{I^j_i}{\lambda_1 f^2_1} + \frac{I^j_i}{\lambda_2 f^2_2}\right) + \lambda_{NL}\left(\frac{m^j_{P,i,1} + \varepsilon^j_{P,i,1}}{\lambda_1} + \frac{m^j_{P,i,2} + \varepsilon^j_{P,i,2}}{\lambda_2}\right) \tag{8}$$

$$\Phi^j_{i,WL} = \rho^j_i + c\Delta t_i - c\Delta t^j + T^j_i + \lambda_{WL}\left(\frac{b_{\Phi,i,1}}{\lambda_1} - \frac{b_{\Phi,i,2}}{\lambda_2}\right) - \lambda_{WL}\left(\frac{b^j_{\Phi,1}}{\lambda_1} - \frac{b^j_{\Phi,2}}{\lambda_2}\right)$$
$$- \lambda_{WL}\left(\frac{I^j_i}{\lambda_1 f^2_1} - \frac{I^j_i}{\lambda_2 f^2_2}\right) + \lambda_{WL}\underbrace{\left(N^j_{i1} - N^j_{i2}\right)}_{=:N^j_{i,WL}} + \lambda_{WL}\left(\frac{m^j_{\Phi,i,1} + \varepsilon^j_{\Phi,i,1}}{\lambda_1} - \frac{m^j_{\Phi,i,2} + \varepsilon^j_{\Phi,i,2}}{\lambda_2}\right) \tag{9}$$

so that

$$\Phi_{i,WL}^{j} - P_{i,NL}^{j} = \underbrace{\lambda_{WL}\left(\frac{b_{\Phi,i,1}}{\lambda_1} - \frac{b_{\Phi,i,2}}{\lambda_2}\right) - \lambda_{NL}\left(\frac{b_{P,i,1}}{\lambda_1} + \frac{b_{P,i,2}}{\lambda_2}\right)}_{=:\, b_{i,MW}} +$$

$$\underbrace{-\left[\lambda_{WL}\left(\frac{b_{\Phi,1}^{j}}{\lambda_1} - \frac{b_{\Phi,2}^{j}}{\lambda_2}\right) - \lambda_{NL}\left(\frac{b_{P,1}^{j}}{\lambda_1} + \frac{b_{P,2}^{j}}{\lambda_2}\right)\right]}_{=:\, b_{MW}^{j}} + \lambda_{WL}N_{i,WL}^{j} +$$

$$\underbrace{+\lambda_{WL}\left(\frac{m_{\Phi,i,1}^{j}}{\lambda_1} - \frac{m_{\Phi,i,2}^{j}}{\lambda_2}\right) - \lambda_{NL}\left(\frac{m_{P,i,1}^{j}}{\lambda_1} + \frac{m_{P,i,2}^{j}}{\lambda_2}\right)}_{=:\, m_{i,MW}^{j}} +$$

$$\underbrace{+\lambda_{WL}\left(\frac{\varepsilon_{\Phi,i,1}^{j}}{\lambda_1} - \frac{\varepsilon_{\Phi,i,2}^{j}}{\lambda_2}\right) - \lambda_{NL}\left(\frac{\varepsilon_{P,i,1}^{j}}{\lambda_1} + \frac{\varepsilon_{P,i,2}^{j}}{\lambda_2}\right)}_{=:\, \varepsilon_{i,MW}^{j}} +$$

$$= \quad b_{i,MW} - b_{MW}^{j} + \lambda_{WL}N_{i,WL}^{j} + m_{i,MW}^{j} + \varepsilon_{i,MW}^{j} \tag{10}$$

where the ionospheric term in the WL-phase cancels with the ionospheric term in the NL-code
due to

$$-\lambda_{WL}\left(\frac{1}{\lambda_1 f_1^2} - \frac{1}{\lambda_2 f_2^2}\right) - \lambda_{NL}\left(\frac{1}{\lambda_1 f_1^2} + \frac{1}{\lambda_2 f_2^2}\right) = -\frac{c}{f_1 - f_2}\left(\frac{c}{f_1} - \frac{c}{f_2}\right) - \frac{c}{f_1 + f_2}\left(\frac{c}{f_1} + \right.$$

$$= -\frac{c^2}{f_1 - f_2}\frac{f_2 - f_1}{f_1 f_2} - \frac{c^2}{f_1 + f_2}\frac{f_2 + }{f_1 f_2}$$

$$= +\frac{c^2}{f_1 f_2} - \frac{c^2}{f_1 f_2}$$

$$= 0$$

[0053] Neglecting the usually unmodeled multipath $m_{i,MW}^{j}$ and random noise terms $\varepsilon_{i,MW}^{j}$,
equation (10) simplifies to

$$\Phi_{i,WL}^{j} - P_{i,NL}^{j} = b_{i,MW} - b_{MW}^{j} + \lambda_{WL}N_{i,WL}^{j} \tag{11}$$

or in a between satellite single difference (SD) version to

$$\Phi_{i,WL}^{j_1j_2} - P_{i,NL}^{j_1j_2} = -b_{MW}^{j_1j_2} + \lambda_{WL}N_{i,WL}^{j_1j_2} \tag{12}$$

[0054] Note that the satellite bias cancels in the double difference (DD) (between receivers and
between satellites) Melbourne-Wübbena (MW) observation,

$$\Phi^{j_1 j_2}_{i_1 i_2, WL} - P^{j_1 j_2}_{i_1 i_2, NL} = \lambda_{WL} N^{j_1 j_2}_{i_1 i_2, WL} \tag{13}$$

Thus the DD-WL ambiguities $N^{j_1 j_2}_{i_1 i_2, WL}$ are directly observed by the DD-MW observations.

[0055] The iono-free linear combination on code $P^j_{i,IF} := \dfrac{f_1^2 P^j_{i,1} - f_2^2 P^j_{i,2}}{f_1^2 - f_2^2}$ and carrier phase

$\Phi^j_{i,IF} := \dfrac{f_1^2 \Phi^j_{i,1} - f_2^2 \Phi^j_{i,2}}{f_1^2 - f_2^2}$ results in

$$
\begin{aligned}
P^j_{i,IF} &= \rho^j_i + c\Delta t_i - c\Delta t^j + T^j_i + \underbrace{\frac{f_1^2 b_{P,i,1} - f_2^2 b_{P,i,2}}{f_1^2 - f_2^2}}_{=: b_{P,i,IF}} - \underbrace{\frac{f_1^2 b^j_{P,1} - f_2^2 b^j_{P,2}}{f_1^2 - f_2^2}}_{=: b^j_{P,IF}} \\
&\quad + \underbrace{\frac{f_1^2 m^j_{P,i,1} - f_2^2 m^j_{P,i,2}}{f_1^2 - f_2^2}}_{=: m^j_{P,i,IF}} + \underbrace{\frac{f_1^2 \varepsilon^j_{P,i,1} - f_2^2 \varepsilon^j_{P,i,2}}{f_1^2 - f_2^2}}_{=: \varepsilon^j_{P,i,IF}} \\
&= \rho^j_i + c\Delta t_i - c\Delta t^j + T^j_i + b_{P,i,IF} - b^j_{P,IF} + m^j_{P,i,IF} + \varepsilon^j_{P,i,IF}
\end{aligned}
\tag{14}
$$

and

$$
\begin{aligned}
\Phi^j_{i,IF} &= \rho^j_i + c\Delta t_i - c\Delta t^j + T^j_i + \underbrace{\frac{f_1^2 b_{\Phi,i,1} - f_2^2 b_{\Phi,i,2}}{f_1^2 - f_2^2}}_{=: b_{\Phi,i,IF}} - \underbrace{\frac{f_1^2 b^j_{\Phi,1} - f_2^2 b^j_{P,2}}{f_1^2 - f_2^2}}_{=: b^j_{\Phi,IF}} \\
&\quad + \underbrace{\frac{f_1^2 \lambda_1 N^j_{i,1} - f_2^2 \lambda_2 N^j_{i,2}}{f_1^2 - f_2^2}}_{=: \lambda_{IF} N^j_{i,IF}} + \underbrace{\frac{f_1^2 m^j_{\Phi,i,1} - f_2^2 m^j_{\Phi,i,2}}{f_1^2 - f_2^2}}_{=: m^j_{\Phi,i,IF}} + \underbrace{\frac{f_1^2 \varepsilon^j_{\Phi,i,1} - f_2^2 \varepsilon^j_{\Phi,i,2}}{f_1^2 - f_2^2}}_{=: \varepsilon^j_{\Phi,i,IF}} \\
&= \rho^j_i + c\Delta t_i - c\Delta t^j + T^j_i + b_{\Phi,i,IF} - b^j_{\Phi,IF} + \lambda_{IF} N^j_{i,IF} + m^j_{\Phi,i,IF} + \varepsilon^j_{\Phi,i,IF}
\end{aligned}
\tag{15}
$$

[0056] Neglecting the usually unmodeled multipath $m^j_{P,i,IF}$, $m^j_{\Phi,i,IF}$ and random noise terms

$\varepsilon^j_{P,i,IF}$, $\varepsilon^j_{\Phi,i,IF}$, (14) and (15) simplify to

$$P^j_{i,IF} = \rho^j_i + c\Delta t_i - c\Delta t^j + T^j_i + b_{P,i,IF} - b^j_{P,IF}. \tag{16}$$

$$\Phi^j_{i,IF} = \rho^j_i + c\Delta t_i - c\Delta t^j + T^j_i + b_{\Phi,i,IF} - b^j_{\Phi,IF} + \lambda_{IF} N^j_{i,IF}. \tag{17}$$

or in a between satellite single difference (SD) version to

$$P^{j_1 j_2}_{i,IF} = \rho^{j_1 j_2}_i - c\Delta t^{j_1 j_2} + T^{j_1 j_2}_i - b^{j_1 j_2}_{P,IF}. \tag{18}$$

$$\Phi^{j_1 j_2}_{i,IF} = \rho^{j_1 j_2}_i - c\Delta t^{j_1 j_2} + T^{j_1 j_2}_i - b^{j_1 j_2}_{\Phi,IF} + \lambda_{IF} N^{j_1 j_2}_{i,IF}. \tag{19}$$

[0057] The iono-free wavelength λ_{IF} just depends on the ratio of the involved frequencies that are listed for different GNSS in Table 1 and Table 2.

Table 1

	GPS			Galileo				
	L1	L2	L5	E2L1E1	E5a	E5b	E5a/b	E6
10.23 MHz ·	154	120	115	154	115	118	116.5	125

Table 2

	Glonass	$(k = -7,...,+6)$	$\dfrac{L1}{L2} = \dfrac{9}{7}$
L1	L2		
$(1602 + k \cdot 9/16)$ MHz	$(1246 + k \cdot 7/16)$ MHz		

[0058] Defining $F_1, F_2 \in N$ by

$$\begin{aligned} f_1 &=: F_1 \gcd(f_1, f_2) \\ f_2 &=: F_2 \gcd(f_1, f_2) \end{aligned} \qquad \Rightarrow \quad \frac{f_1}{f_2} = \frac{F_1}{F_2} \tag{20}$$

where gcd is an abbreviation for the greatest common divisor, it follows for the iono-free wavelength

$$\begin{aligned} \lambda_{IF} N_{i,IF}^j &:= \frac{f_1^2 \lambda_1 N_{i,1}^j - f_2^2 \lambda_2 N_{i,2}^j}{f_1^2 - f_2^2} = \lambda_1 \frac{f_1^2 N_{i,1}^j - f_2^2 \frac{\lambda_2}{\lambda_1} N_{i,2}^j}{f_1^2 - f_2^2} = \lambda_1 \frac{f_1^2 N_{i,1}^j - f_2^2 \frac{f_1}{f_2} N_{i,2}^j}{f_1^2 - f_2^2} \\ &= \lambda_1 \frac{\frac{f_1^2}{f_2^2} N_{i,1}^j - \frac{f_1}{f_2} N_{i,2}^j}{\frac{f_1^2}{f_2^2} - 1} = \lambda_1 \frac{\frac{F_1^2}{F_2^2} N_{i,1}^j - \frac{F_1}{F_2} N_{i,2}^j}{\frac{F_1^2}{F_2^2} - 1} = \lambda_1 \frac{F_1}{F_2^2} \frac{F_1 N_{i,1}^j - F_2 N_{i,2}^j}{\frac{F_1^2 - F_2^2}{F_2^2}} \\ &= \underbrace{\lambda_1 \frac{F_1}{F_1^2 - F_2^2}}_{=: \lambda_{IF}} \underbrace{\left(F_1 N_{i,1}^j - F_2 N_{i,2}^j \right)}_{:= N_{i,IF}^j} \end{aligned} \tag{21}$$

[0059] The factors F_1, F_2 are listed for different GNSS frequency combinations together with the resulting iono-free wavelengths in Table 3.

Table 3

GNSS	Freq. bands	F_1 / F_2	λ_1 / m	λ_{NL} / m	$\dfrac{\lambda_{IF}}{\lambda_1} = \dfrac{F_1}{F_1^2 - F_2^2}$
GPS	L1-L2	77/60	0.1903	0.1070	0.0331
	L1-L5	154/115	0.1903	0.1089	0.0147
	L2-L5	24/23	0.2442	0.1247	0.5106

Galileo	L1-E5a	154/115	0.1903	0.1089	0.0147
	L1-E5b	77/59	0.1903	0.1077	0.0315
	L1-E6	154/125	0.1903	0.1050	0.019
	E5b-E5a	118/115	0.2483	0.1258	0.1688
	E6-E5a	25/23	0.2344	0.1221	0.2604
	E6-E5b	125/118	0.2344	0.1206	0.0735
Glonass	L1-L2	9/7	$\dfrac{c}{(1602 + k \cdot 9/16) \cdot 10^6}$	$\dfrac{c}{(2848 + k) \cdot 10^6}$	0.2813

(22)

[0060] Since for most frequency combinations the iono-free wavelength λ_{IF} is too small for reliable ambiguity resolution (the frequency combination L2-L5 is a mentionable exception), the following relation between the iono-free ambiguity $N_{i,IF}^j$ and the widelane ambiguity $N_{i,WL}^j$ is of special importance. By using the definitions

$$\left. \begin{array}{rcl} N_{i,WL}^j &:=& N_{i,1}^j - N_{i,2}^j \\ N_{i,NL}^j &:=& N_{i,1}^j + N_{i,2}^j \end{array} \right\} \quad \Leftrightarrow \quad \begin{array}{rcl} N_{i,1}^j &=& \frac{1}{2}\left(N_{i,NL}^j + N_{i,WL}^j\right) \\ N_{i,2}^j &=& \frac{1}{2}\left(N_{i,NL}^j - N_{i,WL}^j\right) \end{array}$$

(23)

the iono-free ambiguity term can be rewritten as

$$\begin{aligned} \lambda_{IF} N_{i,IF}^j &:= \frac{f_1^2}{f_1^2 - f_2^2}\lambda_1 N_{i,1}^j - \frac{f_2^2}{f_1^2 - f_2^2}\lambda_2 N_{i,2}^j \\ &= \underbrace{\left(\frac{f_1^2}{f_1^2 - f_2^2}\frac{c}{f_1} + \frac{f_2^2}{f_1^2 - f_2^2}\frac{c}{f_2}\right)}_{\frac{cf_1}{(f_1-f_2)(f_1+f_2)} + \frac{cf_2}{(f_1-f_2)(f_1+f_2)} = \frac{c}{f_1-f_2} =: \lambda_{WL}}\frac{1}{2}N_{i,WL}^j + \underbrace{\left(\frac{f_1^2}{f_1^2 - f_2^2}\frac{c}{f_1} - \frac{f_2^2}{f_1^2 - f_2^2}\frac{c}{f_2}\right)}_{\frac{cf_1}{(f_1-f_2)(f_1+f_2)} - \frac{cf_2}{(f_1-f_2)(f_1+f_2)} = \frac{c}{f_1+f_2} =: \lambda_{NL}}\frac{1}{2}N_{i,NL}^j \\ &= \frac{1}{2}\lambda_{NL}N_{i,NL}^j + \frac{1}{2}\lambda_{WL}N_{i,WL}^j \quad ; \quad N_{i,NL}^j = N_{i,1}^j + N_{i,2}^j = N_{i,1}^j + \frac{1}{2}\left(N_{i,NL}^j - N_{i,WL}^j\right) \\ &= \lambda_{NL}N_{i,1}^j + \frac{1}{2}(\lambda_{WL} - \lambda_{NL})N_{i,WL}^j \end{aligned}$$

(24)

[0061] Thus, once the widelane ambiguity $N_{i,WL}^j$ has been fixed to integer on base of the Melbourne-Wübbena linear combination (11), the relation (24) can be used for integer resolution of the unconstrained narrowlane ambiguity $N_{i,1}^j$ (especially when $\lambda_{NL} \gg \lambda_{IF}$, see Table 3),

$$N_{i,1}^{j} = \frac{1}{\lambda_{NL}}\left(\lambda_{IF}N_{i,IF}^{j} - \frac{1}{2}(\lambda_{WL} - \lambda_{NL})N_{i,WL}^{j}\right)$$

(25)

[0062]   We call $N_{i,1}^{j}$ the unconstrained or free narrowlane ambiguity since it occurs in (24) in combination with the narrowlane wavelength λ_{NL} and does not depend on whether the fixed widelane is even or odd. Since $N_{NL} = N_{WL} + 2N_{2}$ (see (23)), N_{NL} always has to have for consistency reasons the same even/odd status as N_{WL} and is therefore already constrained to some extent.

Part 5: Kalman Filter Overview

[0063]   Some embodiments of the standard clock processor 320, the MW bias processor 325, the orbit processor 330 and the phase clock processor 335 use a Kalman filter approach.

[0064]   FIG. 6 shows a diagram of the Kalman filter algorithm 600. The modeling underlying the Kalman filter equations relate the state vector x_{k} at time step k (containing the unknown parameters) to the observations (measurements) z_{k} via the design matrix H_{k} and to the state vector at time step $k-1$ via the state transition matrix Φ_{k-1} together with process noise w_{k-1} and observation noise v_{k} whose covariance matrices are assumed to be known as Q_{k}, R_{k}, respectively. Then the Kalman filter equations predict the estimated state $\hat{x}_{k-1}$ together with its covariance matrix P_{k-1} via the state transition matrix Φ_{k-1} and process noise input described by covariance matrix Q_{k-1} to time step k resulting in predicted state $\hat{x}_{k}^{-}$ and predicted covariance matrix P_{k}^{-}. Predicted state matrix and state covariance matrix are then corrected by the observation z_{k} in the Kalman filter measurement update where the gain matrix K_{k} plays a central role in the state update as well as in the state covariance update.

Part 6: Code-Leveled Clock Processor

[0065]   The estimated absolute code-leveled low-rate satellite clocks 365 are used in positioning solutions, for example to compute the precise send time of the GNSS signal and also to obtain a quick convergence of float position solutions, e.g., in precise point positioning. For send time computation a rough, but absolute, satellite clock error estimate can be used. Even the satellite clocks from the broadcast message are good enough for this purpose. However, the quality of

single-differenced pairs of satellite clock errors is important to achieve rapid convergence in

positioning applications. For this purpose a clock accuracy level of ca. 10 cm is desired.

[0066]   Some embodiments use quality-controlled ionospheric-free combinations of GNSS

observations from a global tracking network, optionally corrected for known effects, to estimate

5   (mostly) uninterrupted absolute code-leveled satellite clock errors.

[0067]   The raw GNSS reference station data 305 are optionally corrected by data corrector 310

to obtain corrected network data 315 as described in Part 3 above.

[0068]   For each station, ionospheric-free combinations derived from observation of signals with

different wavelengths (e.g. L1 and L2) and the broadcasted clock error predictions are used as an

10   input for the filter:

$$P_{r,IF}^{s} - c\Delta t_{rel}^{s} = \rho_{r}^{s} + c\Delta t_{P,r} - c\Delta t_{P}^{s} + T_{r}^{s} + \varepsilon_{P,r,IF}^{s} \qquad (26)$$

$$\Phi_{r,IF}^{s} - c\Delta t_{rel}^{s} = \rho_{r}^{s} + c\Delta t_{P,r} - c\Delta t_{P}^{s} + T_{r}^{s} + \lambda N_{r}^{s} + \varepsilon_{\Phi,r,IF}^{s} \qquad (27)$$

$$\Delta t_{brc}^{s} \approx \Delta t_{P}^{s} \qquad (28)$$

where

15     $P_{r,IF}^{s}$ is the ionospheric-free code combination for each receiver-satellite pair r,s

$\Phi_{r,IF}^{s}$ is the ionospheric-free phase observation for each receiver-satellite pair r,s

Δt_{brc}^{s} is the broadcast satellite clock error prediction

ρ_{r}^{s} is the geometric range from satellite s to receiver r

Δt_{rel}^{s} represents the relativistic effects for satellite s

20     $c\Delta t_{P,r} := c\Delta t_{r} + b_{P,r,IF}$ is the clock error for receiver r

$c\Delta t_{P}^{s} := c\Delta t^{s} + b_{P,IF}^{s}$ is the clock error for satellite s

T_{r}^{s} is the troposphere delay observed at receiver r

$\varepsilon_{P,r,IF}^{s}$ represents noise in the code measurement

$\varepsilon_{\Phi,r,IF}^{s}$ represents noise in the carrier measurement

25     $\lambda N_{r}^{s} := \lambda_{IF} N_{r,IF}^{s} + b_{\Phi,r,IF} - b_{P,r,IF} - \left(b_{\Phi,IF}^{s} - b_{P,IF}^{s}\right)$ is the float carrier ambiguity from satellite s

to receiver r

[0069]   The code and carrier observations are corrected for relativistic effects Δt_{rel}^{s}, computed

based on satellite orbits, when estimating the satellite clock error. Afterwards this term can be

added to the estimated clock error to allow the rover using those satellites to correct for all time related effects at once.

[0070] The geometric range ρ_r^s at each epoch can be computed from a precise satellite orbit and a precise reference station location. The respective noise terms $\varepsilon_{P,r,IF}^s$ and $\varepsilon_{\Phi,r,IF}^s$ are not the same for code and carrier observations. Differencing the phase observation and code observation directly leads to a rough estimate of the carrier ambiguity N_r^s though influenced by measurement noise $\varepsilon_{P,r,IF}^s$ and $\varepsilon_{\Phi,r,IF}^s$:

$$\Phi_{r,IF}^s - P_{r,IF}^s = \lambda N_r^s + \varepsilon_{\Phi,r,IF}^s + \varepsilon_{P,r,IF}^s . \tag{29}$$

Thus as an input for the filter this difference $\Phi_{r,IF}^s - P_{r,IF}^s$, the phase measurement $\Phi_{r,IF}^s$ and the broadcasted satellite clock error prediction Δt_{brc}^s is used. The difference $\Phi_{r,IF}^s - P_{r,IF}^s$ is a pseudo measurement for the ambiguities, which are modeled as constants. As due to the biases the float ambiguity is not really a constant the estimated value represents the ambiguity together with a constant part of the biases. The non-constant part of the biases will end up in the residuals. This approximation leads to acceptable results as long as the biases are more or less constant values. The converged float ambiguities are used to define the level of the clock errors.

[0071] Once the ambiguities are converged, the phase measurement $\Phi_{r,IF}^s$ provides a measurement for the clock errors and the troposphere. For the troposphere $T_r^s = (1 + c_{T,r})\hat{T}_r^s$ it is sufficient to estimate only one scaling factor per receiver $c_{T,r}$. A mapping to different elevations is computed using a troposphere model $\hat{T}_r^s$. The scaling factor can be assumed to vary over time like a random walk process.

[0072] For the satellite clocks a linear time discrete process is assumed

$$\Delta t_P^s(t_{i+1}) = \Delta t_P^s(t_i) + w_1^s(t_i) + (\Delta \dot{t}_P^s(t_i) + w_2^s(t_i))(t_{i+1} - t_i) \tag{30}$$

with random walks w_1^s and w_2^s overlaid on the clock error Δt_P^s and on the clock error rate $\Delta \dot{t}_P^s$. The receiver clocks are usually not as precise as the satellite clocks and are often unpredictable. Thus the receiver clocks are modeled as white noise to account for any behavior they might exhibit.

[0073] The system of receiver and satellite clocks is underdetermined if only code and phase observations are used. Thus all clock estimates can have a common trend (any arbitrary function added to each of the clocks). In a single difference this trend cancels out and each single

difference clock is correct. To overcome this lack of information the broadcast clock error predictions can be used as pseudo observations for the satellite clock errors to keep the system close to GPS time.

[0074]   The assumption of a random walk on the clock rate is equal to the assumption of a
5   random run on the clock error itself. Optionally a quadratic clock error model is used to model changes in the clock rate. This additional parameter for clock rate changes can also be modeled , as a random walk. The noise input used for the filter can be derived by an analysis of the clock errors using for example the (modified) Allan deviation or the Hadamard variance. The Allan deviation is described in *A. van Dierendonck, Relationship between Allan Variances and Kalman*
10   *Filter Parameters*, PROCEEDINGS OF THE 16TH ANNUAL PRECISE TIME AND TIME INTERVAL (PTTI) SYSTEMS AND APPLICATION MEETING 1984, pp. 273-292. The Hadamard variance is described in *S. Hutsell, Relating the Hadamard variance to MCS Kalman filter clock estimation*, 27TH ANNUAL PRECISE TIME AND TIME INTERVAL (PTTI) APPLICATIONS AND PLANNING MEETING 1996, pp. 291-301.

15   [0075]   There are many different approaches to overcome the underdetermined clock system besides adding the broadcasted satellite clock errors as pseudo-observations. One is to fix one of the satellite or receiver clock errors to the values of an arbitrarily chosen function (e.g. 0 or additional measurements of a good receiver clock). Another is to fix the mean of all clocks to some value, for example to the mean of broadcasted or ultra-rapid clock errors as done in *A.*
20   *Hausschild, Real-time Clock Estimation for Precise Orbit Determination of LEO-Satellites*, ION GNSS 2008, Sept. 16–19, 2008, Savannah, Georgia, 9 pp. This is taken into account in deriving the clock models; the system model and the noise model fits the clock error difference to the fixed clock error and no longer to the original clock error.

[0076]   FIG. 7A is a schematic diagram of a "standard" code-leveled clock processor 320 in
25   accordance with some embodiments of the invention. An iterative filter such as a Kalman filter 705 uses for example ionospheric-free linear combinations 710 of the reference station observations and clock error models 715 with broadcast satellite clocks 720 as pseudo-observations to estimate low-rate code-leveled (standard) satellite clocks 365, tropospheric delays 370, receiver clocks 725, satellite clock rates 730, (optionally) ionospheric-free float ambiguities
30   374, and (optionally) ionospheric-free code-carrier biases 372.

[0077]   Further improvements can be made to quality of the clocks. Single differences of the estimated clock errors can exhibit a slow drift due to remaining errors in the corrected observations, errors in the orbits, and long term drift of the biases. After some time the single differences of the estimated clock errors no longer match a code-leveled clock. To account for

such a drift, the mismatch between code and phase measurements is optionally estimated and applied to the estimated clock errors. In some embodiments this is done by setting up an additional filter such as filter 735 of FIG. 7A with only one bias per satellite and one per receiver, to estimate the ionospheric-free code-carrier biases 372 as indicated by "option 1." The receiver

5   biases are modeled for example as white noise processes. The satellite biases are modeled for example as random walk with an appropriate small input noise, because only low rate variations of the satellite biases are expected. Observations used for this filter are, for example, an ionospheric-free code combination 740, reduced by the tropospheric delay 370, the satellite clock errors 365 and the receiver clock errors 725 estimated in the above standard code-leveled clock

10   filter 705. Rather than setting up the additional filter such as filter 730, the iono-free code-carrier biases are in some embodiments modeled as additional states in the code-leveled clock estimation filter 705, as indicated by "option 2."

Part 7: MW (Melbourne-Wübbena) Bias Processor

15   **Part 7.1   MW Bias: Motivation**

[0078]   The range signals emitted by navigation satellites and received by GNSS receivers contain a part for which delays in the satellite hardware are responsible. These hardware delays are usually just called satellite biases or uncalibrated delays. In differential GNSS processing the satellite biases do not play any role when both receivers receive the same code signals (e.g. in

20   case of GPS both L1C/A or both L1P). However, the biases are always important for Precise Point Positioning (PPP) applications where the precise positioning of a single rover receiver is achieved with the help of precise satellite clocks and precise orbits determined on base of a global network of reference stations (as e.g. by the International GNSS service (IGS)) (Zumberge, Heflin, Jefferson, Watkins, & Webb, 1997), (Héroux & Kouba, 2001). Here the knowledge of

25   satellite biases can allow to resolve undifferenced (or between satellite single differenced) integer ambiguities on the rover which is the key to fast high precision positioning without a reference station (Mervart, Lukes, Rocken, & Iwabuchi, 2008), (Collins, Lahaye, Héroux, & Bisnath, 2008).

[0079]   Usually the satellite biases are assumed to be almost constant over time periods of weeks

30   (Ge, Gendt, Rothacher, Shi, & Liu, 2008), and their variations can be neglected (Laurichesse & Mercier, 2007), (Laurichesse, Mercier, Berthias, & Bijac, 2008). Our own intensive studies revealed by processing in the here proposed way GPS data of a global network of reference stations over several months that there are daily repeating patterns in the Melbourne-Wübbena (MW) linear combination of satellite biases of size up to about 14 cm over 6 hours, as well as

drifts over a month of up to about 17 cm and sometimes sudden bias level changes (of arbitrary size) of individual satellites within seconds (e.g. GPS PRN 24 on 2008.06.26). Nevertheless, the daily repeatability of the MW satellite biases is usually in the range of 2 to 3 cm which is consistent with the literature. Therefore the real-time estimation of satellite biases as a dynamical
5   system in a sequential least squares filter (like e.g. a Kalman filter ((Grewal & Andrews, 2001), (Bierman, 1977)) and the transmission of these biases to PPP based rover receivers (in addition to precise satellite clocks and orbits) becomes important for integer ambiguity resolution on the rover.

10   **Part 7.2   MW Bias: Process Flow**

[0080]   FIG. 11 is a schematic diagram of a process flow 1100 for MW satellite bias and WL ambiguity determination in accordance with some embodiments. GNSS observation data 305 on code and carrier phase on at least two frequencies from a number of reference station receivers is used as the main input into the process. These observations are optionally corrected at 310 for
15   effects that do not require estimation of any model parameters. Among the corrections typically used in PPP applications for the MW linear combination, especially the receiver and satellite antenna offsets and variations are of importance. Higher order ionospheric terms do not cancel in this linear combination. The optionally corrected GNSS observation data 315 is then forwarded to a module 1105 that generates linear combinations 1110 of the code and phase observations on
20   two frequencies. The determined MW observation combinations 1110 are then input into a sequential filter 1115 (such as a Kalman filter) that relates MW observations $\Phi^j_{i,WL} - P^j_{i,NL}$ to the estimation parameters, i.e., the MW satellite biases b^j_{MW} 1120, WL ambiguities $N^j_{i,WL}$ 1125 and optionally MW receiver biases $b_{i,MW}$ 1130 via Equation (11) in the undifferenced case or via Equation (12) in the between satellite single difference case.

25   [0081]   Importantly, process noise input on the MW satellite biases b^j_{MW} ensures that the biases can vary over time. Due to the periodic behavior of satellite biases, optionally the biases may also be modeled by harmonic functions, e.g. as

$$b^j_{MW} = b^j_0 + b^j_1 \sin(\alpha^j) + b^j_2 \cos(\alpha^j) \tag{31}$$

where α^j defines the position of satellite j in the orbit (e.g. α^j could be the argument of latitude or the true anomaly) and b^j_0, b^j_1, b^j_2 are the estimated parameters that need much less process
30   noise than a single parameter b^j_{MW} and can therefore further stabilize the estimation process.

[0082]   In addition to the observation data, a single MW bias constraint 1140 and several ambiguity constraints 1145 are input to the filter [935]. These constraints are additional arbitrary equations that are e.g. of the form

$$b_{WL}^{j_0} = 0 \tag{32}$$

$$N_{i,WL}^{j} = \text{round}(N_{i,WL}^{j}) \tag{33}$$

and that are added to the filter with a very low observation variance of e.g. $10^{-30} m^2$. The constraints ensure that the system of linear equations in the filter 1115 is not underdetermined so that the variances of the model parameters immediately become of the same order as the observation variance. They have to be chosen in a careful way so that the system of linear equations is not over-constrained by constraining a double-difference WL ambiguity which is directly given by the MW observations (see equation (13). By constraining the ambiguities to an arbitrary integer, information about the integer nature of the ambiguities comes into the system. In a Kalman filter approach where the system of equations in (11) or (12) (optionally together with (31)) is extended by arbitrary equations for the initial values of all parameters so that always a well defined float solution (with variances of the size of the initial variances) exists, it is preferable to constrain the ambiguities to the closest integer of the Kalman filter float solution.

[0083]   The estimated MW satellite biases 1120 are either directly used as the process output or after an optional additional WL ambiguity fixing step. Therefore the estimated WL ambiguities 1125 are optionally put into an ambiguity fixer module 1135. The resulting fixed WL ambiguities 340 (that are either fixed to integer or float values) are used as the second process output. Optionally the fixed WL ambiguities 340 are fed back into the filter 1115 (or into a filter copy or a secondary filter without ambiguity states (compare FIG. 24A – FIG. 25D) to get satellite MW bias output 1120 which is consistent with integer WL ambiguities.

[0084]   The MW satellite biases 1120 are transferred for example via the scheduler 355 to rover receivers where they help in fixing WL ambiguities at the rover. Network WL ambiguities 1125 or 340 can be forwarded to the phase clock processor 335 and orbit processor 330 where they help in fixing iono-free (IF) ambiguities when the reference station data 305 from the same receiver network is used in these processors. Alternatively, instead of the network WL ambiguities 1125 or 340], MW satellite biases 1120 are transferred to orbit processor 330 and phase clock processor 335 to derive WL ambiguities in a station-wise process for the network receivers in the same way as it is done on the rover. Then the derived WL ambiguities help in fixing IF ambiguities. With such an approach, GNSS data from different reference station networks can be used in the different processors.

[0085]   FIG. 12 shows a schematic diagram of a processing architecture 1200 in accordance with some embodiments. Code and carrier phase observations 1205 (e.g., from reference station data 305) on at least two frequencies from a number of reference station receivers are put into a linear combiner 1210 that generates a set of Melbourne-Wübbena (MW) linear combinations 1220, one

5   such MW combination for each station-satellite pairing from code and carrier phase observations on two frequencies. If more than two frequencies are available several MW combinations can be generated for a single station-satellite pairing. These MW observations are then put into a processor 1225 that estimates at least MW biases per satellite 1230 and WL ambiguities per station-satellite pairing 1235 based on modeling equations (11) in the undifferenced case or (12)

10   in the between satellite single difference case (both optionally together with (31)). The processor is usually one or more sequential filters such as one or more Kalman filters. Since it can also consist of several filters, here the more general term processor is used. Process noise 1240 input on the MW satellite biases in the processor allows them to vary from epoch to epoch even after the convergence phase of filtering. The outputs of the process are the estimated satellite MW

15   biases 1230 and network WL ambiguities 1235.

[0086]   Thus, some embodiments provide a method of processing a set of GNSS signal data derived from code observations and carrier-phase observations at multiple receivers of GNSS signals of multiple satellites over multiple epochs, the GNSS signals having at least two carrier frequencies, comprising: forming an MW (Melbourne-Wübbena) combination per receiver-

20   satellite pairing at each epoch to obtain a MW data set per epoch; and estimating from the MW data set per epoch an MW bias per satellite which may vary from epoch to epoch, and a set of WL (widelane) ambiguities, each WL ambiguity corresponding to one of a receiver-satellite link and a satellite-receiver-satellite link, wherein the MW bias per satellite is modeled as one of (i) a single estimation parameter and (ii) an estimated offset plus harmonic variations with estimated

25   amplitudes.

[0087]   Broadcast satellite orbits 1245 contained in the navigation message are optionally used, for example with coarse receiver positions 1250, to reduce the incoming observations to a minimal elevation angle under which a satellite is seen at a station. The receiver positions 1250 are optionally given as an additional input, or alternatively can be derived as known in the art

30   from the code observations and the broadcast satellite orbit. The restriction to observations of a minimal elevation can be done at any place before putting the observations into the processor. However, performing the restriction directly after pushing the code and carrier phase observations into the process avoids unnecessary computations.

[0088]   FIG. 13A and FIG. 13B show respectively the state vectors for the undifferenced (= zero-differenced (ZD)) and single differenced embodiments, listing parameters to be estimated.

The ZD state vector 1310 comprises n satellite bias states b_{MW}^{j}, a number of ambiguity states

$N_{i,WL}^{j}$ that changes over time with the number of satellites visible at the stations, and m receiver

5   bias states $b_{i,MW}$. The SD state vector 1320 comprises n satellite bias states $b_{MW}^{jj_0}$ to a fixed

reference satellite j_0 that can be either a physical or an artificial satellite. In addition, the SD

state vector comprises the same number of ambiguity states as in the ZD case. However, here

each ambiguity represents an SD ambiguity to a physical or artificial satellite. Each station can

have its own choice of reference satellite. In the SD case no receiver bias states are necessary, so

10   that there are always m less states in the SD state vector 1320 than in the comparable ZD state

vector 1310. More details about artificial reference satellites follow in Part 7.4.

Part 7.3   MW Process: Correcting and Smoothing

[0089]   FIG. 14 shows a process 1400 with the addition of observation correction to the MW

15   process of FIG. 12. Some embodiments add the observation data corrector module 310 of FIG. 3.

Code and carrier phase observations 1205 on at least two frequencies from a number of reference

stations (e.g., from reference station data 305) are corrected in the optional observation data

corrector 310 for effects that do not require estimation of any model parameters (especially

receiver and satellite antenna offsets and variations, and higher order ionospheric effects).

20   Knowledge of the broadcast satellite orbits 1245 and the coarse receiver positions 1250 is used

for this. The corrected observation data 1310 are then optionally fed into the process of FIG. 12

to produce MW satellite biases 1330 and widelane ambiguities 1335.

[0090]   In FIG. 15, code and carrier phase observations 1205 on at least two frequencies from a

number of reference stations (e.g., from reference station data 305) are optionally corrected in the

25   observation data corrector 310, then combined in a linear combiner 1210 to form Melbourne-

Wübbena linear combinations 1220 and finally smoothed over several epochs in a smoother 1410

to form smoothed Melbourne-Wübbena combinations 1420. Alternatively, smoothing can be

done on the original observations or on any other linear combination of the original observations

before generating the MW linear combination. In any case, the resulting smoothed MW

30   observations are put into the processor 1225 for estimating MW satellite biases 1430 and WL

ambiguities 1435 as in the embodiments of FIG. 12 and FIG. 14.

[0091]   Smoothing means to combine multiple observations over time, e.g. by a simple averaging

operation, to obtain a reduced-noise observation. MW smoothing is done to reduce the multipath

error present in (10) that is not explicitly modeled in the processor 1225, e.g., as in modeling

equations (11) and (12). Smoothing is motivated by the expectation that the MW observation is

almost constant over short time periods since the MW observation only consists of hardware

biases and a (constant) ambiguity term. A reasonable smoothing interval is, for example, 900

5   seconds. An additional advantage of smoothing the MW observations is that an observation

variance can be derived for the smoothed observation from the input data by the variance of the

mean value,

$$\sigma^2_{obs,MW} = \frac{\sum_{t=1}^{n}(x_t - \bar{x})^2}{(n-1)n} \quad \text{with} \quad \bar{x} = \frac{1}{n}\sum_{t=1}^{n}x_t \tag{34}$$

where x_t is the MW observation at smoothing epoch t and n is the number of observations used

in the smoothing interval. To ensure that this variance really reflects multipath and not just a too-

10   small number of possibly unreliable observations in the smoothing interval, it is advantageous to

accept a smoothed observation as filter input only when a minimal number of observations is

available, e.g. 80% of the theoretical maximum. Note that the statistical data that holds mean

value and variance of the Melbourne-Wübbena observation has to be reset in case of an

unrepaired cycle slip since this observation contains an ambiguity term. Of course, a cycle slip

15   also requires a reset of the corresponding ambiguity in the filter.

[0092] If smoothing is done by a simple averaging operation over a fixed time interval,

smoothing implies different data rates in the process. Observations 1205 are coming in with a

high data rate, while smoothed MW observations 1420 are forwarded to the processor with a

lower data rate. This kind of smoothing has the advantage that observations put into the processor

20   are not correlated and can therefore be handled in a mathematically correct way. The alternative

of using some kind of a (weighted) moving average allows to stay with a single (high) data rate,

but has the disadvantage that the resulting smoothed observations become mathematically

correlated.

25   **Part 7.4 MW Process: MW Bias Constraint**

[0093] FIG. 16 shows a process 1600 with the addition of one or more MW bias constraints to

the process of FIG. 15, which can similarly be added to the embodiments shown in FIG. 12, FIG.

14. At least one MW bias constraint 1605 like (32) is put into the processor to reduce the rank

defect in modeling equations (11) or (12).

30   [0094] The rank defect in (11) or (12) becomes apparent by counting the number of observations

and the number of unknowns in these equations. For example in (11), if there are

$i = 1, \ldots, m$ stations and $j = 1, \ldots, n$ satellites and it is assumed that all satellites are seen at all stations, there will be $m \cdot n$ Melbourne-Wübbena observations. However, at the same time there are also $m \cdot n$ unknown ambiguities $N_{i,WL}^{j}$ in addition to m receiver biases $b_{i,MW}$ and n satellite biases b_{MW}^{j}, resulting in $m \cdot n + m + n$ unknowns. Thus the system of equations defined by (11)

5   can only be solved if the number of arbitrary constraints introduced into the system is the number of unknowns minus the number of observations, i.e. $(m \cdot n + m + n) - (m \cdot n) = m + n$.

[0095] Most of these constraints should be ambiguity constraints as the following consideration demonstrates. For n satellites $n - 1$ independent between-satellite single differences can be generated. In the same way, from m stations $m - 1$ between station single differences can be

10   derived. In a double difference (DD) between stations and satellites these independent single differences are combined, resulting in $(m - 1) \cdot (n - 1) = m \cdot n - (m + n - 1)$ double difference observations. Since as in (13) the DD ambiguities are uniquely determined by the DD-MW observations, the difference between the $m \cdot n$ ambiguities in (11) and the $m \cdot n - (m + n - 1)$ unique DD ambiguities should be constrained, resulting in $m + n - 1$ ambiguity constraints. Thus

15   from the $m + n$ required constraints all but one should be ambiguity constraints. The remaining arbitrary constraint should be a constraint on the biases. This statement remains true in the more general case when not all satellites are seen at all stations and thus the number of required constraints can no longer be counted in the demonstrated simple way. The constraint on the biases itself is an arbitrary equation like (32) or more generally of the form

$$\sum_i a_i b_{i,MW} + \sum_j a^j b_{MW}^j = b \quad \text{with} \quad a_i, a^j, b \in R \tag{35}$$

20   [0096] In the single difference case (12) the constraint on the biases is more straightforward. The state vector of the satellite biases does not contain all possible SD biases but only the independent ones. This is achieved by taking an arbitrary reference satellite and choosing as states only the SD biases to the reference. To be prepared for a changing reference satellite in case the old reference satellite is not observed anymore, it is preferable to also have a state for the

25   reference satellite. However, the SD bias of the reference to itself has to be zero.

$$b_{MW}^{j_{ref}j_{ref}} = b_{MW}^{j_{ref}} - b_{MW}^{j_{ref}} \equiv 0 \tag{36}$$

This equation is added as a constraint. Note, however, that the SD bias states are not necessarily interpreted as SDs to a physical reference satellite. It is also possible to have an artificial reference satellite with a bias that is related to the biases of the physical satellites (this ensures that the artificial satellite is connected to the physical satellites)

$$\sum_{j} a^{j} b_{MW}^{j} = b \quad \text{with} \quad a^{j}, b \in R \tag{37}$$

[0097] By specifying arbitrary values for a^{j}, b (with at least one $a^{j} \neq 0$) and introducing (37) as a constraint into (12), the information about the bias of the reference satellite comes into the system.

[0098] With knowledge of MW satellite biases (as they are derived from the system proposed here) from a different source, it is also reasonable to introduce more than one bias constraint into the system. For example, if all MW satellite biases are constrained, it is in a single-difference approach not necessary to introduce any ambiguity constraints into the system, since (12) can be rewritten as

$$\Phi_{i,WL}^{j_1 j_2} - P_{i,NL}^{j_1 j_2} + b_{MW}^{j_1 j_2} = \lambda_{WL} N_{i,WL}^{j_1 j_2} \tag{38}$$

[0099] Thus all SD ambiguities $N_{i,WL}^{j_1 j_2}$ are uniquely determined with knowledge of the SD-MW satellite biases. It is exactly this relation that helps a rover receiver to solve for its WL ambiguities with the help of the here derived MW satellite biases.

[00100] In the undifferenced approach, one ambiguity constraint per station is introduced when the MW satellite biases for all satellites are introduced as constraints into the system.

[00101] All bias constraints to handle the rank defect in modeling equations (11) or (12) are avoided if one additional ambiguity constraint is introduced instead. However, this additional ambiguity constraint is not arbitrary. It is chosen such that the double difference relation (13) is fulfilled. However, (13) does not contain the unmodeled multipath and just determines a float value for the DD ambiguity. Thus, deriving an integer DD ambiguity value from (13) is prone to error.

[00102] To better distinguish between arbitrary ambiguity constraints and ambiguity constraints that have to fulfill the DD ambiguity relation (13), we usually call the second kind of constraints ambiguity fixes. While constraints are arbitrary and do not depend on the actual observations, fixes do. Constraints cannot be made to a wrong value, fixes can. Which of the ambiguities can be constrained to an arbitrary value is described in Part 7.6.

Part 7.5 MW Bias Process: WL Ambiguity Constraints

[00103] FIG. 17 shows a process 1700 with the addition of one or more WL ambiguity constraints to the process of FIG. 16, which can similarly be added to the embodiments shown in FIG. 12, FIG. 14 and FIG. 15. At least one WL ambiguity integer constraint 1705 as in Equation (33) is put into the processor 1225 to further reduce the rank defect in modeling equations (11) or (12).

As for FIG. 16, the correct number of arbitrary ambiguity constraints in a network with

$i = 1, \ldots, m$ stations and $j = 1, \ldots, n$ satellites, where all satellites are seen at all stations, is

$m + n - 1$. However, in a global network with reference stations distributed over the whole Earth

not all satellites are seen at all stations. For this case, choosing the correct number of arbitrary

5   ambiguity constraints and determining the exact combinations that are not restricted by the DD

ambiguity relation (13) is described in Part 7.6.

[00104] Although the constrained ambiguities that are not restricted by the DD ambiguity relation

(13) could be constrained to any value in order to reduce the rank effect in the modeling

equations (11) or (12), it is desirable to constrain these ambiguities to an integer value so that the

10   integer nature of the ambiguities comes into the system. This helps later on when for the

remaining unconstrained float ambiguities, integer values are searched that are consistent with

(13) and to which these ambiguities can be fixed.

[00105] In a Kalman filter approach where equations (11) or (12) are extended by equations for

the initial values of the parameters, there is always a well defined float solution for all parameters

15   (that has, however, a large variance if the initial variances of the parameters have also been

chosen with large values). In this case it is reasonable to constrain the ambiguities to the closest

integer of their Kalman filter float solution since this disturbs the filter in the least way and gives

the solution that is closest to the initial values of the parameters. It is also advantageous to

constrain the ambiguities one after the other, looking up after each constraint the updated float

20   ambiguity of the next ambiguity to be constrained. Such a procedure helps to stabilize the filter

in cases of network outages where many ambiguities are lost, receiver biases are modeled as

white noise parameters and just already converged satellite biases have a defined value.

Part 7.6   MW Bias Process: Determining WL Ambiguity Constraints

25   [00106] FIG. 18 shows a process 1800 with the addition of determining one or more WL

ambiguity constraints for the process of FIG. 17 so as to avoid under- and over-constraining of

the modeling equations (11) or (12).

[00107] Under-constraining means that too few constraints have been introduced to overcome the

rank defect in (11) or (12). Over-constraining means that arbitrary constraints have been

30   introduced that are inconsistent with the DD ambiguity relation (13). Thus, a system can be at the

same time over- and under-constrained.

[00108] The MW observation input 1420 defines an observation graph, 1805, i.e. a number of

edges given by observed station-satellite links. Based on this graph a spanning tree (ST) 1815 is

generated by an ST generator 1810 that connects all stations and satellites (in the undifferenced

case (11)) or just all satellites (in the between satellite single differenced case (12)) without introducing loops.The resulting ST 1815 defines the WL ambiguity constraints 1705, i.e., which WL ambiguities are constrained.

[00109] FIG. 19A shows at 1900 how observed station-satellite links can be interpreted as an

5   abstract graph, i.e. a number of vertices connected by edges. The stations at the bottom of FIG. 19A and the satellites at the top of FIG. 19A are identified as vertices and the station-satellite pairs (each pair corresponding to observations at a station of a satellite's signals) as edges. The abstract graph 1910 of FIG. 19B does not distinguish any more between stations and satellites and instead shows the edges as links between vertices.

10   [00110] In graph theory a tree is a graph without closed loops. An example is shown at 1920 in FIG. 19C, where the tree is marked with bold lines. A spanning tree on a graph is a tree that connects (or spans) all vertices, as in FIG. 19C.

[00111] Instead of building the spanning tree based on the current observation graph, it can alternatively be based on all station-satellite ambiguities that are currently in the filter. These

15   ambiguities correspond to station-satellite links that were observed in the past but that are not necessarily observed anymore in the current epoch. We call the station-satellite links defined by the filter ambiguities the filter graph. Notice that it is a bit arbitrary for how long ambiguities are kept in the filter when they are no longer observed. If a fixed slot management for the ambiguities in the filter is used that holds a maximal number of ambiguities for each station so

20   that a newly observed ambiguity on a rising satellite will throw out the oldest ambiguity if all slots are already used, this time of keeping a certain ambiguity does not have to be specified. It will be different for each satellite on each station. However, such a slot management guarantees that after some time each station holds the same number of ambiguities.

[00112] In general the filter graph contains more station-satellite links than the observation graph.

25   It contains in addition stations that are not observed anymore (which often occurs for short time periods in a global network), satellites no longer observed at any station (e.g. since a satellite became unhealthy for a short time period), or just station-satellite links that fall below the elevation cutoff. Working on the filter graph is of special importance when the later described ambiguity fixing is also done on the filter graph and ambiguity constraints and fixes are

30   introduced on the original filter and not on a filter copy.

[00113] In the single-differenced observation graph 1960 of FIG. 19G two satellites are usually connected by several edges since the two satellites are usually observed at several stations. Each edge connecting two satellites corresponds to an (at least in the past) observed satellite-station-

satellite link, i.e., a single-difference observation. Of course, also the SD filter graph 1970 of FIG. 19H contains more edges than the SD observation graph 1960.

[00114] Constraining the ambiguities determined by a spanning tree over the observation or the filter graph can avoid under- and over-constraining of modeling equations (11) or (12). This is

5   illustrated for the undifferenced case in FIG. 19D. A spanning tree (ST) on the observation graph or filter graph connects all vertices without introducing loops (see emphasized edges in FIG. 19C). FIG. 19D shows at 1930 in addition to the spanning tree edges (in dark grey) that are constrained to an arbitrary integer value, also a single satellite bias constraint S1 depicted in dark grey. The satellite bias is visualized as a circle since its contribution to the observation is the

10   same for all receiver observations of this satellite.

[00115] Constraining the ST edges together with one additional satellite bias S1 allows to resolve the underdetermined linear system of equations (11): The observation R1-S1 together with the satellite bias constraint S1 and the ambiguity constraint R1-S1 allows to uniquely solve for receiver bias R1 (compare equation (11)). Once receiver bias R1 is known, the observation R1-

15   S2 together with the ambiguity constraint R1-S2 allows to solve for satellite bias S2. In the same way all other receiver and satellite biases can be computed with the help of the ST constrained ambiguities. The spanning property of the ST ensures that all satellite and receiver biases are reached while the tree property ensures that there are no loops that would constrain a double difference observation (13). Once all satellite and receiver biases are known, the remaining

20   ambiguities (e.g. R2-S1, R2-S4 and R2-S5 in FIG. 19D) can be directly computed from the remaining observations one after the other.

[00116] In the SD case shown in FIG. 19G and 19H the argumentation is quite similar. Constraining one SD satellite bias to an arbitrary value (e.g., constraining the bias of a physical reference satellite to 0), the SD satellite bias of the next satellite can be determined with the help

25   of an SD observation between the first and second satellite and the ambiguity constraint from the SD spanning tree between the two satellites (compare equation (12)). Once the second satellite bias is known the third bias can be calculated. In the same way all other satellite biases are determined with the help of the SD spanning tree constraints. By adding one ambiguity constraint per station to an arbitrary satellite, all remaining SD ambiguities (single-differenced

30   against a station-specific reference satellite) in the filter can be resolved one after the other.

[00117] The relation underlying this description between an undifferenced (= zero-differenced (ZD)) spanning tree 1975 and a SD spanning tree 1980 is depicted in FIG. 19I. Connecting each station with a single satellite by introducing one ambiguity constraint per station and adding to

these constraints the ones given by an ST on the SD observation graph (or filter graph), defines

the same constraints that are given by an ST on a ZD observation graph (or filter graph) 1985.

Building up a spanning tree on a graph is not a unique process. For a given graph there exist

many trees that span the graph. To make the generation of a spanning tree more unique the use of

5   a minimum spanning tree (with respect to some criterion) is proposed in Part 7.7.

Part 7.7 MW Bias Process: Minimum Spanning Tree

[00118] Fig. 21A shows at 2110 a spanning tree (ST) on an undifferenced observation graph.

FIG. 21B shows at 2120 a minimum spanning tree (MST) (Cormen, Leiserson, Rivest, & Stein,

10   2001) on the undifferenced observation graph of FIG. 21A. FIG. 20 shows the ST generator 1810

of FIG. 18 replaced with an MST generator 2010. For building up an MST on a graph, each edge

has an edge weight resulting in a so-called weighted graph. The MST is defined as the spanning

tree with the overall minimal edge weight. The edge weight can be assigned in any of a variety of

ways. One possible way is based on the current receiver-satellite geometry and therefore use the

15   station positions 1250 and the satellite positions 1245 as inputs. The connections between the

coarse receiver positions 1250, the broadcast satellite orbits 1245 and the MST generator 2010

are depicted in FIG. 20.

[00119] The edges in the undifferenced observation graph or filter graph are given by station-

satellite links. In some embodiments the edge weight is the geometric distance from receiver to

20   satellite or a satellite-elevation-angle-related quantity (like the inverse elevation angle or the

zenith distance (=90°-elevation)).

[00120] The edges in the single-differenced observation graph or filter graph are given by

satellite-receiver-satellite links connecting two different satellites over a station. In some

embodiments the edge weight is the geometric distance from satellite to receiver to satellite, or a

25   combination of the elevations under which the two satellites are seen at the receiver. In some

embodiments the combination of the two elevations is the sum of the inverse elevations, the sum

of the zenith distances, the minimal inverse elevation, or the minimal zenith distance.

[00121] In FIG. 21 A and FIG. 21B the ST and MST edges are marked with an "X." The ST

2110 in FIG. 21A and the MST 2120 in FIG. 21B are identical, and the ST 2130 in FIG. 21C and

30   the MST 2140 in FIG. 21D are identical, reflecting the fact that each ST can be obtained as an

MST by definition of suitable edge weights.

[00122] An MST is well defined (i.e. it is unique) if all edge weights are different. Assigning the weights to the edges allows control on how the spanning tree is generated. In embodiments using geometrical based weights the MST is generated in a way that highest satellites (having smallest geometrical distance and smallest zenith distance, or smallest value of 1/elevation) are preferred. These are also the station-satellite links that are least influenced by the unmodeled multipath. In these embodiments the weights prefer those edges for constraining which should shift the least multipath into other links when constraining the ambiguities to an integer value. In embodiments using low elevation station-satellite links with high multipath for constraining, the multipath is shifted to links with higher elevation satellites. This can result in the counter-intuitive effect that ambiguities on high elevation satellites become more difficult to fix to an integer value.

[00123] Generating an MST on a given weighted graph is a standard task in computer science for which very efficient algorithms exist. Examples are Kruskal's, Prim's, and Boruvka's algorithms.

[00124] FIG. 22 shows an alternative way of choosing the edge weights of the observation graph or filter graph on which the MST (defining the constrained ambiguities) is generated. In some embodiments, the edge weights are derived from the ambiguity information in the filter, i.e. from the values of the WL ambiguities 1435, or from the variances 2210 of the WL ambiguities, or from both.

[00125] A particular interesting edge weight used in some embodiments is the distance of the corresponding ambiguity to its closest integer value. In this way the MST chooses the ambiguities for constraining that span the observation/filter graph and that are as close as possible to integer. Thus the states in the processor are influenced in a minimal way by the constraints to integer. An additional advantage is that the constraints of the last epoch will also be favored in the new epoch since their distance to integer is zero which prevents from over-constraining the filter when the constraints are directly applied to the filter and no filter copy is used. The same goal is reached by using the variance of the ambiguity as an edge weight. Constrained ambiguities have a variance of the size of the constraining variance, e.g., $10^{-30} \, m^2$, and are thus favored in the MST generation in some embodiments. In some embodiments each combination of ambiguity distance to integer and ambiguity variance is used as an edge weight. In some embodiments the combination of an edge weight derived from the station-satellite geometry and from ambiguity information is used. In some embodiments for example, in the first epoch a geometrically motivated weight is chosen (to minimize effects from unmodeled multipath and to ensure that constraints stay in the system for a long time) and in later epochs an ambiguity-derived weight (to avoid over-constraining) is chosen.

Part 7.8   MW Bias Process: WL Ambiguity Fixing

[00126] FIG. 23 shows fixing of the WL ambiguities before they are sent out (e.g. for use in the phase clock processor 335 or orbit processor 300). In some embodiments the WL ambiguity state values 1435 are forwarded together with at least the WL ambiguity variances 2210 from the filter
5   to an ambiguity fixer 2305 module. The ambiguity fixer module 2305 outputs the fixed WL ambiguities 2310.

[00127] The ambiguity fixer module 2305 can be implemented in a variety of ways:

[00128] **Threshold based integer rounding:** In some embodiments a simple fixer module checks each individual ambiguity to determine whether it is closer to integer than a given
10   threshold (e.g., closer than $a = 0.12$ WL cycles). If also the standard deviation of the ambiguity is below a second given threshold (e.g , $\sigma = 0.04$ so that $a = 3\sigma$) the ambiguity is rounded to the next integer for fixing. Ambiguities that do not fulfill these fixing criteria remain unfixed. In some embodiments the satellite elevation angle corresponding to the ambiguity is taken into account as an additional fixing criterion so that e.g. only ambiguities above $15°$ are fixed.

15   [00129] **Optimized sequence, threshold based integer bootstrapping:** A slightly advanced approach used in some embodiments fixes ambiguities in a sequential way. After the fix of one component of the ambiguity vector, the fix is reintroduced into the filter so that all other not yet fixed ambiguity components are influenced over their correlations to the fixed ambiguity. Then the next ambiguity is checked for fulfilling the fixing criteria of distance to integer and standard
20   deviation. In some embodiments the sequence for checking ambiguity components is chosen in an optimal way by ordering the ambiguities with respect to a cost function, e.g. distance to integer plus three times standard deviation. In this way the most reliable ambiguities are fixed first. After each fix the cost function for all ambiguities is reevaluated. After that, again the ambiguity with the smallest costs is checked for fulfilling the fixing criteria. The fixing process stops when
25   the best ambiguity fixing candidate does not fulfill the fixing criteria. All remaining ambiguities remain unfixed.

[00130] **Integer least squares, (generalized) partial fixing:** A more sophisticated approach used in some embodiments takes the covariance information of the ambiguities from the filter into account. The best integer candidate N_1 is the closest integer vector to the least squares float
30   ambiguity vector $\hat{N} \in R^v$ in the metric defined by the ambiguity part of the (unconstrained) state covariance matrix $P_{\hat{N}} \in R^v \times R^v$, both obtained from the filter, i.e.

$$N_1 = \arg \min_{N \in Z^v} \left(N - \hat{N} \right) P_{\hat{N}}^{-1} \left(N - \hat{N} \right) \tag{39}$$

[00131] However, since the observation input to the filter is, due to measurement noise, only precise to a certain level also the resulting estimated float ambiguity vector $\hat{N}$ is only reliable to a certain level. Then a slightly different $\hat{N}$ may lead to a different $N \in Z^\nu$ that minimizes (39). Therefore in some embodiments the best integer candidate is exchanged with e.g. the second best integer candidate by putting other noisy measurements (e.g. from other receivers) into the filter. To identify the reliable components in the ambiguity vector that can be fixed to a unique integer with a high probability, the minimized quantity $\left(N - \hat{N}\right)^T P_{\hat{N}}^{-1}\left(N - \hat{N}\right)$ is compared in some embodiments under the best integer candidates in a statistical test like the ratio test. If N_i is the i'th best $(i > 1)$ integer candidate this implies that

$$\left(N_i - \hat{N}\right)^T P_{\hat{N}}^{-1}\left(N_i - \hat{N}\right) > \left(N_1 - \hat{N}\right)^T P_{\hat{N}}^{-1}\left(N_1 - \hat{N}\right), \text{ or}$$

$$F_i := \frac{\left(N_i - \hat{N}\right)^T P_{\hat{N}}^{-1}\left(N_i - \hat{N}\right)}{\left(N_1 - \hat{N}\right)^T P_{\hat{N}}^{-1}\left(N_1 - \hat{N}\right)} > 1 \tag{40}$$

[00132] The quotient in (40) is a random variable that follows an F-distribution. Some embodiments basically follow the description in (Press, Teukolsky, Vetterling, & Flannery, 1996). The probability that F_i would be as large as it is if $\left(N_i - \hat{N}\right)^T P_{\hat{N}}^{-1}\left(N_i - \hat{N}\right)$ is smaller than $\left(N_1 - \hat{N}\right)^T P_{\hat{N}}^{-1}\left(N_1 - \hat{N}\right)$ is denoted as $Q(F_i|\nu,\nu)$ whose relation to the beta function and precise algorithmic determination is given in (Press, Teukolsky, Vetterling, & Flannery, 1996). In other words, $Q(F_i|\nu,\nu)$ is the significance level at which the hypothesis $\left(N_i - \hat{N}\right)^T P_{\hat{N}}^{-1}\left(N_i - \hat{N}\right) < \left(N_1 - \hat{N}\right)^T P_{\hat{N}}^{-1}\left(N_1 - \hat{N}\right)$ can be rejected. Thus each candidate for which e.g. $Q(F_i|\nu,\nu) \geq 0.05$ can be declared as comparable good as N_1. The first candidate $i_0 + 1$ for which $Q(F_{i_0+1}|\nu,\nu) < 0.05$ is accepted as significantly worse than N_1.

[00133] Then all the components in the vectors $N_1, N_2, \ldots, N_{i_0}$ that have the same value can be taken as reliable integer fixes. The components in which these ambiguity vectors differ should not be fixed to an integer. However, among these components there can exist certain linear combinations that are the same for all vectors $N_1, N_2, \ldots, N_{i_0}$. These linear combinations can also be reliably fixed to an integer.

[00134] In some embodiments determination of the best integer candidate vectors is performed via the efficient LAMBDA method (Teunissen, 1995).

[00135] **Best integer equivariant approach:** In some embodiments the components of the high-dimensional ambiguity vector are fixed to float values that are given by a linear combination of the best integer candidates. FIG. 23B shows the WL ambiguities are sent out (e.g. for use in the phase clock processor 335 or orbit processor 300).

[00136] In these embodiments the WL ambiguity state values 1435 are forwarded together with the ambiguity variance-covariance matrix 2210 from the filter to an integer ambiguity searcher module 2320. Integer ambiguity searcher module 2320 outputs a number of integer ambiguity candidate sets 2323 that are then forwarded to an ambiguity combiner module 2325 that also gets the least squares ambiguity float solution 1435 and the ambiguity variance-covariance matrix 2210 from the filter as an input. The least squares ambiguity float solution 1435 is used together with the ambiguity variance-covariance matrix 2210 for forming a weight for each integer ambiguity candidate. In the ambiguity combiner module 2325 the weighted integer ambiguity candidates are summed up. The output is a fixed WL ambiguity vector 2330 that can then be forwarded to the phase clock processor 335 and orbit processor 330.

[00137] To derive the weights for the integer ambiguity vectors, note that the least squares ambiguity float vector $\hat{N}$ is the expectation value of a multidimensional Gaussian probability function $p(N)$, i.e.

$$\hat{N} = \int_{N \in R^\nu} N\, p(N)\, dN \quad \text{with} \quad p(N) = \frac{e^{-\frac{1}{2}(N-\hat{N})^T P_{\hat{N}}^{-1}(N-\hat{N})}}{\int_{N \in R^\nu} e^{-\frac{1}{2}(N-\hat{N})^T P_{\hat{N}}^{-1}(N-\hat{N})}\, dN} \tag{41}$$

[00138] Thus an ambiguity expectation value that recognizes the integer nature of the ambiguities is given by

$$\check{N} := \sum_{N \in Z^\nu} N\, \check{p}(N) \quad \text{with} \quad \check{p}(N) = \frac{e^{-\frac{1}{2}(N-\hat{N})^T P_{\hat{N}}^{-1}(N-\hat{N})}}{\sum_{N \in Z^\nu} e^{-\frac{1}{2}(N-\hat{N})^T P_{\hat{N}}^{-1}(N-\hat{N})}} \tag{42}$$

[00139] Since the summation over the whole integer grid $N \in Z^\nu$ cannot be computed in practice, the sum is in some embodiments restricted to the best integer ambiguity candidates

$$\check{N} \approx \sum_{i \text{ with } F_i < 1+\varepsilon} N_i\, \check{p}(N_i) \quad \text{with} \quad \check{p}(N_i) \approx \frac{e^{-\frac{1}{2}(N_i-\hat{N})^T P_{\hat{N}}^{-1}(N_i-\hat{N})}}{\sum_{i \text{ with } F_i < 1+\varepsilon} e^{-\frac{1}{2}(N_i-\hat{N})^T P_{\hat{N}}^{-1}(N_i-\hat{N})}} \tag{45}$$

with F_i from (40). The $\check{p}(N_i)$ are the desired weights for the best integer ambiguity

candidates. Thereby a reasonable value for ε follows from the following

consideration. In the sum in (42) ambiguity vectors N can be neglected if the

relative weight to the largest $\bar{p}(N)$ is small, i.e. if $\bar{p}(N)/\bar{p}(N_1) \leq \delta$ with e.g.

$\delta = e^{-q}; q = 25$. In other words, all ambiguity vectors with $\bar{p}(N)/\bar{p}(N_1) > \delta$ have

to be recognized. Writing out this condition for $N = N_i$ with the definition for

$\bar{p}(N)$ from (42) results in

$$\delta < \frac{\bar{p}(N_i)}{\bar{p}(N_1)} = \frac{e^{-\frac{1}{2}(N_i-\hat{N})' P_{\hat{N}}^{-1}(N_i-\hat{N})}}{e^{-\frac{1}{2}(N_1-\hat{N})' P_{\hat{N}}^{-1}(N_1-\hat{N})}} \tag{43}$$

$$= e^{\frac{1}{2}(N_1-\hat{N})' P_{\hat{N}}^{-1}(N_1-\hat{N})-\frac{1}{2}(N_i-\hat{N})' P_{\hat{N}}^{-1}(N_i-\hat{N})}$$

$$\Leftrightarrow \ln\delta = -q < \frac{1}{2}(N_1-\hat{N})' P_{\hat{N}}^{-1}(N_1-\hat{N})-\frac{1}{2}(N_i-\hat{N})' P_{\hat{N}}^{-1}(N_i-\hat{N})$$

$$\Leftrightarrow \frac{-q}{\frac{1}{2}(N_1-\hat{N})' P_{\hat{N}}^{-1}(N_1-\hat{N})} < \underbrace{1-\frac{\frac{1}{2}(N_i-\hat{N})' P_{\hat{N}}^{-1}(N_i-\hat{N})}{\frac{1}{2}(N_1-\hat{N})' P_{\hat{N}}^{-1}(N_1-\hat{N})}}_{=:F_i}$$

$$\Leftrightarrow F_i < 1+\frac{q}{\frac{1}{2}(N_1-\hat{N})' P_{\hat{N}}^{-1}(N_1-\hat{N})}$$

Thus

$$\varepsilon := \frac{q}{\frac{1}{2}(N_1-\hat{N})' P_{\hat{N}}^{-1}(N_1-\hat{N})} \tag{44}$$

is a reasonable value for ε.

[00140] The $\bar{p}(N_i)$ are the desired weights for the best integer ambiguity candidates. The ambiguity candidates themselves can be determined in an efficient way with the LAMBDA method (Teunissen, 1995).

Part 7.9   MW Bias Process: Using Fixed WL Ambiguities

[00141] FIG. 24A shows an embodiment 2400. In this way the estimated MW biases 1430 are made consistent with the fixed WL ambiguities 2330. These fixed-nature MW satellite biases from the network are transferred to the rover receiver where they help in fixing WL ambiguities. [00142] The fixed WL ambiguities 2330 can be introduced into the processor 1225 in several different ways. FIG. 24B, FIG. 24C and FIG. 24D show details of three possible realizations of the processor 1225 that differ in the manner of feeding back the fixed WL ambiguities into the MW bias estimation process.

[00143] In the embodiment 2400 the processor 1225 comprises a single sequential filter 2410 (such as a Kalman filter) that holds states 2415 for satellite MW biases, states 2420 for WL ambiguities and - in case of the undifferenced observation model (11) - also states 2425 for receiver MW biases. In the single differenced (SD) observation model (12) no receiver bias

5   states occur. In addition to these states, which contain the values of the least-squares best solution of the model parameters for the given observations, the filter also contains variance-covariance (vc) information 2430 of the states. The vc-information is usually given as a symmetric matrix and shows the uncertainty in the states and their correlations. It does not directly depend on the observations but only on the observation variance, process noise,

10   observation model and initial variances. However, since the observation variance is derived from the observations when smoothing is enabled (see Part 7.3), there can also be an indirect dependence of the vc-matrix 2430 on the observations.

[00144] The filter input comprises MW observations (e.g., smoothed MW observations 1420) and satellite MW-bias process noise 1240 (see Part 7.2), a MW bias constraint 1605 (see Part 7.4),

15   integer WL ambiguity constraints 1705 (see Part 7.5) and, optionally, shifts from a bias and ambiguity shifter 24 (discussed in Part 7.10).

[00145] The filter output of primary importance comprises the satellite MW biases 1430, the (float) WL ambiguities 1430 and the (unconstrained) WL ambiguity part 2210 of the vc-matrix 2430. The ambiguity information is forwarded to an ambiguity fixer module (see Part 7.8) that

20   outputs (float or integer) fixed WL ambiguities 2310. These fixed WL ambiguities 2310 are output for use in the orbit processor 330 and the phase clock processor 335. In addition, the fixed WL ambiguities 2310 are reintroduced into the filter by adding them as pseudo observations with a very small observation variance (of e.g. $10^{-30} \, m^2$). The resulting satellite MW biases 1430 are output to the rover and, optionally, to the orbit processor 330 and the phase clock processor 335.

25   Since they are consistent with the fixed WL ambiguities, we call them fixed MW biases.

[00146] Note that, if an ambiguity were fixed to a wrong integer, the wrong ambiguity would remain in the filter 2410 until a cycle slip on that ambiguity occurs or it is thrown out of the filter (such as when it has not been observed anymore for a certain time period or another ambiguity has taken over its ambiguity slot in the filter 2410). If this were to occur the MW biases would be

30   disturbed for a long time. However, an advantage of this approach is that also ambiguity fixes remain in the filter that have been fixed to integer when the satellites were observed at high elevations but having meanwhile moved to low elevations and could not be fixed anymore or that are even no longer observed. These ambiguity fixes on setting satellites can stabilize the solution of MW biases a lot.

[00147] Note also that a float ambiguity should not be fixed with a very small variance (of e.g. $10^{-30} m^2$) in the single filter 2410 since in this way new observations cannot improve anymore the ambiguity states by bringing them closer to an integer. In some embodiments the float ambiguity is fixed with a variance that depends on its distance to integer so that the observation variance tends to zero when the distance to the closest integer tends to zero and tends to infinity when the distance to the closest integer tends to 0.5. However, for fixing float ambiguities the approaches used in the embodiments of FIG. 24C and FIG. 24D are more suitable.

[00148] In the embodiment 2440 of FIG 24C the processor 1225 comprises two sequential filters 2445 and 2450 where the process flow for the first filter 2445 is almost identical with the filter 2410 of FIG. 24B. The difference is that no fixed WL ambiguities 1430 are fed back into filter 2445. Instead, each time new fixed WL ambiguities 2310 are available (e.g. after each observation update), a filter copy 2450 of the first filter 2445 is made and then the fixed WL ambiguities 2310 are introduced as pseudo-observations into the filter copy 2450. The original filter 2445 thus remains untouched so that no wrong fixes can be introduced into it. The filter copy 2450 outputs fixed satellite MW biases 2455 (e.g., as MW biases 345).

[00149] A disadvantage of this approach is that only currently observed ambiguities can be fixed and introduced into the filter copy 2550. All prior ambiguity fixes are lost. However, this is a preferred way of processing when the whole ambiguity space is analyzed at once as it is done in the integer least squares partial fixing and integer candidate combination approaches (see Part 7.8).

[00150] Embodiment 2460 of FIG. 24D shows an alternative approach to feed the fixed WL ambiguities into the estimation process. Here the fixed WL ambiguities 2310 are forwarded to an ambiguity subtracter module 2665 that reduces the MW observations 1420 by the ambiguities. The resulting ambiguity-reduced MW observations 2670 are put into a second filter 2475 that does not have any ambiguity states but only satellite MW bias states 2480 and - in the undifferenced approach (11) - also receiver MW bias states 2485. This second filter 2475 just needs a single MW bias constraint 2490 and process noise on satellite MW biases 2480 as additional inputs. In case biases are shifted in the first filter 2440 they also have to be shifted in the second filter 2475.

[00151] The second filter 2475 outputs fixed satellite MW biases 2450.

[00152] Note that in this approach the ambiguities are not fixed with a very small observation variance (of e.g. $10^{-30} m^2$) but only with the usual observation variance of the MW observations. By inserting observations over time with the same fixed ambiguity, the weak ambiguity constraint is more and more tightened. All prior ambiguity fixes remain in the filter to some extent. A

wrong fix that is detected after some time will be smoothed out. Thus it is also quite reasonable to put float-ambiguity-reduced MW observations into the filter.

[00153] Since the second filter 2475 does not have ambiguity states that build the majority of states in the first filter, the second filter 2475 is very small and can be updated at a very high rate

5   of, e.g. every second, without running into performance problems. Thus in some embodiments the original MW observations without any prior smoothing are input into this filter.

Part 7.10 MW Bias Process: Shifting MW Biases

[00154] FIG. 25A shows an embodiment 2500 in which the process described in Part 7.8 is

10   augmented with an external satellite MW bias shifter module 2505. The term *external* means, in contrast to the shifting module shown in FIG. 25C where the shifting is applied on the filter. Note that all the ambiguity constraining and fixing related steps as well as the correction and smoothing steps are optional.

[00155] The bias shifter module 2505 shifts the satellite MW biases 1430 to produce satellite MW

15   biases 2510 in a desired range of at least one WL cycle. This is possible since as seen from Equation (11) a shift in a satellite bias by n WL cycles are absorbed by the WL ambiguities corresponding to this satellite, e.g.

$$
\begin{aligned}
\Phi^j_{i,WL} - P^j_{i,NL} &= b_{i,MW} - b^j_{MW} + \lambda_{WL} N^j_{i,WL} \\
&= b_{i,MW} - \underbrace{\left(b^j_{MW} + n\lambda_{WL}\right)}_{=: \tilde{b}^j_{MW}} + \lambda_{WL} \underbrace{\left(N^j_{i,WL} - n\right)}_{=: \tilde{N}^j_{i,WL}}
\end{aligned}
\tag{46}
$$

Similar shifts are possible for receiver biases.

[00156] FIG. 25B shows the impact of shifting MW biases as in equation (46). Each MW

20   combination is depicted in FIG. 25B as the distance between a receiver (e.g., one of receivers 2525, 2530, 2535, 2540) and a satellite 2545. This distance is represented by the sum of a receiver bias (which is the same for all satellites and therefore visualized as a circle around the receiver such as 2550), a satellite bias (that is the same for all receivers and therefore visualized as a circle 2555 around the satellite) and an ambiguity (that depends on the receiver-satellite pair

25   and is therefore visualized as a bar such as bar 2560 for the pairing of receiver 2525 and satellite 2545). Reducing the satellite bias by the wavelength of one WL cycle (as depicted by smaller circle 2565) increases all related ambiguities by the wavelength of one WL cycle. The receiver biases are untouched by this operation.

[00157] An advantage of shifting satellite MW biases into a defined range is that in this way the

30   biases can be encoded with a fixed number of bits for a given resolution. This allows to reduce

the necessary bandwidth for transferring satellite MW biases to the rover which is in some

embodiments done over expensive satellite links.

[00158] Although all satellite biases b_{MW}^j / λ_{WL} can be mapped for a certain fixed time e.g. into the

range $[-0.5,+0.5[$ it is preferable to extend this range e.g. to $[-1,+1[$ in order to avoid frequent

5   jumps in the MW satellite biases when they leave the defined range. Due to the oscillating

behavior of MW satellite biases, the satellite biases at the border of the defined range close to -0.5

or +0.5 might often leave this range. For example, a bias moving to $-0.5 - \varepsilon$ is then mapped to

$+0.5 - \varepsilon$. Then the bias oscillates back to $+0.5 + \varepsilon$ and is then mapped back to $-0.5 + \varepsilon$. In

practice, it has been found that with a range of $[-1,+1[$ bias jumps can be avoided for several

10   months.

[00159] Note that MW bias jumps can also be handled at the rover by comparing the latest

received MW bias value with the previous one. If the values differ by approximately one cycle a

bias jump is detected and the correct bias reconstructed. The situation is complicated by the fact

that WL ambiguities consistent with shifted satellite MW biases are used in the phase clock

15   processor to determine iono-free (IF) biases that are also sent to the rover. Reconstructing the

MW bias at the rover after a jump requires also an adaptation of the IF bias by $\frac{1}{2}(\lambda_{WL} - \lambda_{NL})$.

[00160] FIG. 25C shows an alternative to the external satellite MW bias shifter module 2505 of

FIG. 25A. Satellite MW biases 1430 and WL-ambiguities 1435 are sent to an internal shifter

module 2580 that determines on the basis of equation (46) shifts for MW biases and WL

20   ambiguities such that the biases are mapped to the desired range. Then all these shifts are applied

to the bias and ambiguity states in the filter. In this way biases have to be shifted only once while

in the approach of FIG. 25A the shifts are repeated each time satellite MW biases are output.

[00161] However, note that unshifted and shifted WL ambiguities are not allowed to be used at

the same time in a single filter. This is e.g. important when WL ambiguities are forwarded to the

25   orbit processor 330 for fixing IF ambiguities. If fixed IF ambiguities are reintroduced into a

single original filter (and no filter copy as in FIG. 24C is used), WL ambiguities of different

epochs come together in the filter. It has to be ensured that the WL ambiguities of different

epochs are the same. If this is not the case the corresponding IF ambiguity is reset.

30   **Part 7.11 MW Bias Process: Numerical Examples**

[00162] The behavior of daily solutions for MW satellite biases was monitored over a time period

of 61 days in June and July 2008 and the difference of each daily solution to the first day of this

period (June 1). PRN 16 was chosen as the reference satellite with bias value 0. All biases were mapped into the interval [0,1]. Drifts of different sizes in the satellite biases are clearly detectable. All the larger drifts occur for block IIA satellites. Individual satellites show drifts of about 0.2 WL cycles within a month. These values would motivate a satellite bias update of perhaps once

5 per day. However, for PRN 24 there is a sudden bias jump on June 26 of almost 0.2 WL cycles. The occurrence of such events demonstrates the importance of real-time estimation and transmission of MW satellite biases.

[00163] In another example the MW satellite biases for the time period from Oct. 02 to 14, 2008 were continuously processed in a Kalman filter. Again PRN 16 was chosen as the reference. The

10 result shows that each satellite has its own daily pattern with some kind of repetition already after 12 hours (the time a GPS satellite needs for one revolution). The variations of the satellite biases are up to about 0.16 WL cycles within 6 hours. The difference of the MW satellite biases to the values they had 24 hours before demonstrates that the day to day repeatability is usually below 0.03 WL cycles. However, this day to day repeatability does not well reflect the large inner day

15 variations of the MW satellite biases.

[00164] The filtered satellite WL biases are dependent on their process noise input. With a noise input variance between 10^{-6} and 10^{-7} squared WL cycles per hour the periodical behavior and the sudden bias level change on June 26 is well reflected. With less noise input these patterns are not detected. Due to this analysis a process noise input variance of $5 \cdot 10^{-7}$ squared WL cycles per

20 hour on satellite WL biases is recommended.

Part 7.12   MW Bias Process: References

[00165] References relating to the MW bias process include the following:
Bierman, G. J. (1977). *Factorization Methods for Discrete Sequential Estimation*. New

25 York: Academic Press, Inc.

Collins, P. (2008). Isolating and Estimating Undifferenced GPS Integer Ambiguities. *Proceedings of ION-NTM-2008*, (pp. 720-732). San Diego, Calif.

Collins, P., Gao, Y., Lahaye, F., Héroux, P., MacLeod, K., & Chen, K. (2005). Accessing and Processing Real-Time GPS Corrections for Precise Point Positioning - Some User

30 Considerations. *Proceedings of ION-GNSS-2005*, (pp. 1483-1491). Long Beach, Calif.

Collins, P., Lahaye, F., Héroux, P., & Bisnath, S. (2008). Precise Point Positioning with Ambiguity Resolution using the Decoupled Clock Model. *Proceedings of ION-GNSS-2008*. Savannah, Georgia.

Cormen, T. H., Leiserson, C. E., Rivest, R. L., & Stein, C. (2001). Chapter 23: Minimum Spanning Trees. In *Introduction to Algorithms* (Second Edition ed., pp. 561-579). MIT Press and McGraw-Hill.

Datta-Barua, S., Walter, T., Blanch, J., & Enge, P. (2007). Bounding Higher Order Ionosphere Errors for the Dual Frequency GPS User. *Radio Sci., 43, RS5010,* doi:10.1029/2007RS003772.

Ge, M., Gendt, G., Rothacher, M., Shi, C., & Liu, J. (2008). Resolution of GPS carrier-phase ambiguities in Precise Point Positioning (PPP) with daily observations. *Journal of Geodesy, Vol. 82,* pp. 389-399.

Grewal, M. S., & Andrews, A. P. (2001). *Kalman Filtering: Theory and Practice Using MATLAB.* New York: Wiley-Interscience.

Héroux, P., & Kouba, J. (2001). GPS Precise Point Positioning Using IGS Orbit Products. *Phys. Chem. Earth (A), Vol. 26* (No. 6-8), pp. 572-578.

Laurichesse, D., & Mercier, F. (2007). Integer ambiguity resolution on undifferenced GPS phase measurements and its application to PPP. *Proceedings of ION-GNSS-2007,* (pp. 839-448). Fort Worth, Texas.

Laurichesse, D., Mercier, F., Berthias, J., & Bijac, J. (2008). Real Time Zero-difference Ambiguities Fixing and Absolute RTK. *Proceedings of ION-NTM-2008,* (pp. 747-755). San Diego, Calif.

Melbourne, W. (1985). The case for ranging in GPS-based geodetic systems. *Proceedings of the First International Symposium on Precise Positioning with the Global Positioning System. Vol. 1,* pp. 373-386. Rockville, Maryland: US Dept. of Commerce.

Mervart, L., Lukes, Z., Rocken, C., & Iwabuchi, T. (2008). Precise Point Positioning With Ambiguity Resolution In Real-Time. *Proceedings of ION-GNSS-2008.* Savannah, Georgia.

Morton, Y., van Graas, F., Zhou, Q., & Herdtner, J. (2008). Assessment of the Higher Order Ionosphere Error on Position Solutions. *ION GNSS 21st International Meeting of the Satellite Division.* Savannah, GA, USA.

Press, W. H., Teukolsky, S. A., Vetterling, W. T., & Flannery, B. P. (1996). F-Distribution Probability Function. In *Numerical Recipes in C* (p. 229). Cambridge University Press.

Schaer, S. (2000, May 09). *IGSMAIL-2827: Monitoring (P1-C1) code biases.* Retrieved from http://igscb.jpl.nasa.gov/mail/igsmail/2000/msg00166.html.

Teunissen, P. (1995). The least-squares ambiguity decorrelation adjustment: a method for fast GPS integer ambiguity estimation. *Journal of Geodesy, Vol. 70, No. 1-2,* pp. 65-82.

Wübbena, G. (1985). Software Developments for Geodetic Positioning with GPS using

TI 4100 code and carrier measurements. *Proceedings of the First International Symposium on*

Precise Positioning with the Global Positioning System. Vol. 1, pp. 403-412. Rockville,

Maryland: US Dept. of Commerce.

5   Zumberge, J., Heflin, M., Jefferson, D., Watkins, M., & Webb, F. (1997). Precise point

positioning for the efficient and robust analysis of GPS data from large networks. *Journal of*

Geophysical Research , Vol. 102 (No. B3), pp. 5005-5018.

Part 8: Orbit Processor

10   [00166] Precise (cm-accurate) orbits allow precise satellite clock estimation and precise

positioning. Orbit accuracy has a direct influence on the final position accuracy of the rover

using precise satellite orbits and clocks data a described herein.

Part 8.1   Option 1: Use IGS-published ultra-rapid orbits

15   [00167] The International GNSS Service (IGS) provides predicted satellite orbits which can be

downloaded via the Internet. A description of these orbits can be found in J. KOUBA, A GUIDE TO

USING INTERNATIONAL GPS SERVICE (IGS) PRODUCTS, Geodetic Survey Division, Natural

Resources Canada, February 2003, 31 pages and at

http://igscb.jpl.nasa.gov/components/prods.html.

20   [00168] The IGS Ultra-rapid (predicted) orbits, also called IGU orbits, are generated and

published four times a day at 3, 9, 15, 21 hours of the UTC day. IGS claims a 5 cm orbit standard

deviation, though our analyses have shown that individual satellite orbit errors can go up to 60

cm. In one case we have seen a 2 meter error.

[00169] Market requirements for commercial positioning service demand precise orbits with

25   errors less than 3 cm and with high reliability and availability. The currently available IGU orbits

do no meet these requirements. Nevertheless, they are useful either for positioning applications

where the requirements are less demanding, or as a countercheck to detect gross errors in orbits

estimated as described below.

30   **Part 8.2   Option 2: Determine Satellite Orbits in Real Time**

[00170] Referring to FIG. 1, observation data is streamed in real time from globally distributed

GNSS reference stations, such as reference stations 105, 110, 115, to network processor 140. In

some embodiments, the network processor estimates the satellite orbits in real time using a

Kalman-filter approach in a numerically stable UD-Filter implementation as described in G.

Bierman, *Factorization Methods for Discrete Sequential Estimation*, Academic Press, Inc., New York, 1977. Hereafter the term real time refers to processing immediately after observation data is available, typically in less than one second. The time-dependent filter state $x(t)$ is set up in the following way

5	$x_{cr}(t)$	receiver clock errors
	$x_{cs}(t)$	satellite clock errors
	$x_{qs}(t)$	satellite dependent orbit parameters
	$x(t) = x_r(t)$	receiver positions
	$x_{ZDT}(t)$	zenith tropospheric delays for each station
10	$x_{EOP}(t)$	earth orientation parameters
	(EOP: x_p, y_p,	$UT1 - UTC$ or length of day)
	x_{AMB}	carrier-phase ambiguities
	$x_{if-bias}$	iono-free biases

where

15     $x_{cr}(t)$ is the vector with all receiver clock errors in the network. Each station has at least one clock offset but may have also drift and drift rates, depending on the type and stability of the station clock. The receiver clocks are modeled, for example, as white noise processes or as stochastic processes (e.g., random walk, Gauss Markov) depending on the type and stability of the station clock.

20     $x_{cs}(t)$ is the vector with the satellite clocks. The vector contains a clock offset and a drift but may have drift and drift rates depending on the type and stability of the satellite clock (Rubidium, Cesium or Hydrogen maser). The satellite clocks are modeled, for example, as white noise processes or as stochastic processes depending on the type and stability of the satellite clock.

    $x_{qs}(t)$ is the vector with the satellite dependent dynamic orbit parameters. This includes the

25   satellite positions and velocities and additional force model parameters, which are

$$x_{qs}(t) = \begin{bmatrix} x_s(t) \\ \dot{x}_s(t) \\ x_{slr}(t) \\ x_{harm}(t) \end{bmatrix} \tag{47}$$

where

$x_s(t)$ is the satellite position vector (one per satellite) in the inertial reference frame (X,Y,Z).

$\dot{x}_s(t)$ is the satellite velocity vector (one per satellite) in the inertial reference frame (X,Y,Z).

$x_{slr}(t)$ is the vector with the solar radiation pressure parameters. It consists of a component in the sun-satellite direction, a second component in the direction of the solar radiation panel axis and a third component perpendicular on the first 2 axes. All three components are modeled for example as stochastic processes.

$x_{harm}(t)$ is the vector with harmonic coefficients for the orbit components along-track, radial and cross-track or in a satellite body fixed coordinate system. They are modeled for example as stochastic processes.

$x_r(t)$ is the station position vector in the Earth centered / Earth fixed reference frame. Stations can be either fixed or unknown in the estimation process.

$x_{ZTD}(t)$ is the vector with the tropospheric zenith delays estimated for each station. Tropospheric gradients are optionally also estimated. These parameters are modeled for example as stochastic processes.

$x_{EOP}(t)$ are earth orientation parameters (EOPs) estimated routinely in real time. The vector consists of the offsets to the conventional pole (x_p, y_p) and the difference between UT1 and UTC time scales ($UT1 - UTC$ or length of day). The precisely-known EOP parameters are used to transition between the inertial and the earth-fixed reference frames. All three parameters are estimated for example as stochastic processes.

x_{AMB} each satellite-station link has an individual carrier phase ambiguity in the filter state. These parameters are modeled for example as constants.

$x_{if-bias}$ ionospheric-free code-carrier biases, one bias per receiver-satellite pair. Code and carrier have biases, which are different from receiver to receiver and satellite to satellite and might vary with time These parameters are modeled for example via stochastic processes.

[00171] The ionospheric-free dual-frequency combinations of code and carrier observations have different biases, which vary with time. While these parameters can be estimated as additional unknowns in the orbit processor Kalman filter, they are optionally estimated in a separate processor (e.g. in standard clock processor 320 as ionospheric-free code-carrier biases 372, shown in FIG. 3) and applied to the pseudorange observations used in the orbit processor.

[00172] For linearization purposes, some embodiments have the filter set up to estimate differences to a reference trajectory and to initial force model parameters. In these embodiments the state vector for each satellite is

$$x_{qs}(t_k) = \begin{bmatrix} r(t_k) - r_0(t_k) \\ p(t_k) - p_0(t_k) \\ y - y_0 \end{bmatrix} = \begin{bmatrix} \Delta r(t_k) \\ \Delta p(t_k) \\ \Delta y \end{bmatrix} \tag{48}$$

where

$x_{qs}(t_k)$ is the satellite state vector at time t_k

$r(t_k)$ is the satellite position and velocity in the inertial reference frame

$r_0(t_k)$ represents the reference trajectory created by a numerical orbit integrator

$p(t_k)$ is the vector with stochastic force model parameters

$p_0(t_k)$ is the vector with approximate initial stochastic force model parameters

y is the vector with constant force model parameters

y_0 is the vector with approximate constant force model parameters

and where

$$r(t_k) = \begin{bmatrix} x_x(t_k) \\ \dot{x}_x(t_k) \end{bmatrix} \tag{49}$$

[00173] The prediction in the filter model for the satellite dependent part is done via the following relation

$$\begin{bmatrix} \Delta r(t_{k+1}) \\ \Delta p(t_{k+1}) \\ \Delta y \end{bmatrix} = \begin{bmatrix} \Phi_{rr}(t_{k+1},t_k) & \Phi_{rp}(t_{k+1},t_k) & \Phi_{ry}(t_{k+1},t_k) \\ 0 & M_k & 0 \\ 0 & 0 & 1 \end{bmatrix} \begin{bmatrix} \Delta r(t_k) \\ \Delta p(t_k) \\ \Delta y \end{bmatrix} + \begin{bmatrix} 0 \\ w_k \\ 0 \end{bmatrix} \tag{50}$$

with

$$\Phi_{rr}(t_{k+1},t_k) = \left[\frac{\partial r(t_{k+1})}{\partial r(t_k)} \right], r(t) = r_0(t) \tag{51}$$

$$\Phi_{rp}(t_{k+1},t_k) = \left[\frac{\partial r(t_{k+1})}{\partial p(t_k)} \right], r(t) = r_0(t), p(t) = p_0(t) \tag{52}$$

$$\Phi_{ry}(t_{k+1},t_k) = \left[\frac{\partial r(t_{k+1})}{\partial y} \right], r(t) = r_0(t), y = y_0 \tag{53}$$

[00174] These matrices are computed for example by integration of the variational equations as described in the section below on numerical orbit integration.

M_k is the matrix describing the stochastic noise modeling

w_k is the noise input

5

Part 8.3 Numerical orbit integration

[00175] The satellite motion in orbit can be described by a second order differential equation system

$$\ddot{x} = \ddot{x}(x, \dot{x}, q) \tag{54}$$

10   with

$\ddot{x}$ acceleration in the inertial reference frame

x position in the inertial reference frame

$\dot{x}$ velocity in the inertial reference frame

q vector of satellite dependent force model unknowns and initial position/velocity

15   [00176] The vector q is defined as

$$q = \begin{bmatrix} r(t_0) \\ a \end{bmatrix} \tag{55}$$

where

$r(t_0)$ are the initial position and velocity in inertial reference frame

a is the vector with dynamic force model parameters

20   [00177] Satellite position $x(t)$ and velocity $\dot{x}(t)$ at time t are derived from satellite position $x(t_0)$ and velocity $\dot{x}(t_0)$ at time t_0 using, for example, a numerical integration (a predictor-corrector method of higher order).

$$\dot{x}(t) = \dot{x}(t_0) + \int \ddot{x}(t)dt \tag{56}$$

$$x(t) = x(t_0) + \int \dot{x}(t)dt \tag{57}$$

25   [00178] The real-time filter uses the partial derivatives of the accelerations $\ddot{x}(t)$ with respect to the unknown parameters q

$$\left[\frac{\partial \ddot{x}}{\partial q}\right] = \left[\frac{\partial \ddot{x}}{\partial x}\right]\left[\frac{\partial x}{\partial q}\right] \tag{58}$$

[00179] The equation of this example ignores derivatives with respect to satellite velocity since there are no relevant velocity-dependent forces acting on GNSS satellites in medium earth orbit.

[00180] The following matrix is computed for epoch t_i :

$$\Phi_{rq}(t_i,t_0) = \begin{bmatrix} \dfrac{\partial x}{\partial q(t_i,t_0)} \\[2mm] \dfrac{\partial \dot{x}}{\partial q(t_i,t_0)} \end{bmatrix} \tag{59}$$

[00181] The matrix for the next epoch t_{i+1} can then be computed via the chain rule

$$\Phi_{rq}(t_{i+1},t_0) = \Phi_{rq}(t_{i+1},t_i)\Phi_{rq}(t_i,t_0) \tag{60}$$

[00182] The partial derivatives of the observations with respect to the unknowns q can again be derived via chain rule

$$\frac{\partial l}{\partial q} = \frac{\partial l}{\partial r}\Phi_{rq} \tag{61}$$

These partials are used in the observation update of the filter.

[00183] The following models are used to compute the accelerations $\ddot{x}$ acting on the satellite; some embodiments use these for the integration process:

1. The Earth's gravity field is modeled by available models such as the EIGEN-CG01C or the EGM96 model. These are spherical harmonic expansions with very high resolution. Some embodiments use up to degree and order 12 for orbit integration.

2. Gravitational forces due to the attraction by sun, moon and planets.

3. The gravitational forces of sun and moon acting on the Earth's figure will deform the Earth. This effect also changes the gravity field; it is called "Solid Earth Tide" effect. Some embodiments follow the recommendations of the IERS Conventions 2003.

4. Some embodiments account for the Solid Earth Pole Tide, caused by the centrifugal effect of polar motion. This tide must not be confused with Solid Earth Tides. Some embodiments follow the recommendations of the IERS Conventions 2003.

5. The gravitational forces of sun and moon acting on the oceans will change the gravity field; this is called the "Ocean Tide" effect. Some embodiments use the CSR3.0 model recommended by the IERS Conventions 2003.

6. Some embodiments also consider the relativistic acceleration, which depends upon position and velocity of the satellite.

7. The solar radiation pressure, the acceleration acting on GNSS satellites, is most difficult to model. Some embodiments consider three components: a first component in the sun-satellite

direction, a second component in the direction of the solar radiation panel axis (y-bias) and a third component perpendicular to the first two axes.

8. Some embodiments also model residual errors mainly induced by the insufficient knowledge of the force models via harmonic functions as described in the following.

[00184] GNSS satellites like GPS, GLONASS, GALILEO and COMPASS satellites are in mid earth orbits (MEO) of approximately 26000 km. The following table shows the accelerations acting on GNSS satellites and their effects after a one-day orbit integration.

Perturbation	Acceleration [m/s^2]	Orbit prediction error after one day [m]
Earth's gravitation	0.59	330000000
Earth's oblateness	$5 \cdot 10^{-5}$	24000
Lunar direct tides	$5 \cdot 10^{-6}$	2000
Solar direct tides	$2 \cdot 10^{-6}$	900
Higher degree terms in geopotential	$3 \cdot 10^{-7}$	300
Direct solar radiation pressure	$9 \cdot 10^{-8}$	100
Radiation pressure along solar panel axis	$5 \cdot 10^{-10}$	6
Earth albedo (solar radiation due to reflection by earth)	$3 \cdot 10^{-9}$	2
Solid Earth tides	$1 \cdot 10^{-9}$	0.3
Ocean tides	$1 \cdot 10^{-10}$	0.06
General relativity	$3 \cdot 10^{-10}$	0.3
Venus in lower conjunction	$2 \cdot 10^{-10}$	0.08

Part 8.4 Harmonic Force Modeling

[00185] Some embodiments handle residual errors by introducing a harmonic model having a cosine term and a sine term in each of the along-track, radial and cross-track directions. As the residuals have a period of about one revolution of the satellite about the Earth, the harmonics depend on the argument of latitude of the satellite:

$$\ddot{x}_{residual} = \begin{pmatrix} A_1 \cos u + A_2 \sin u \\ A_3 \cos u + A_4 \sin u \\ A_5 \cos u + A_6 \sin u \end{pmatrix} = \begin{pmatrix} A_1 & A_2 \\ A_3 & A_4 \\ A_5 & A_6 \end{pmatrix} \begin{pmatrix} \cos u \\ \sin u \end{pmatrix} \qquad (62)$$

with

A_1, A_2 ... amplitudes to be estimated for along-track

A_3, A_4 ... amplitudes to be estimated for cross-track

A_5, A_6 ... amplitudes to be estimated for radial component

u ... argument of latitude of the satellite

[00186]   Alternatively to the use of along track, cross track and radial components, the satellite related system (sun-satellite direction, solar panel direction and the normal to both) can be used, to model solar radiation pressure.

Part 8.5 Transformation from Inertial to Earth-Fixed Reference Frame

[00187] Some embodiments transform from Inertial to the Earth-fixed reference frame using the IAU 2000A precession/nutation formulas, which follow the IERS Conventions 2003.

Part 8.6 Earth orientation parameters

[00188]   Some embodiments take Earth orientation parameters (EOPs) from the IERS rapid files GPSRAPID.DAILY. These files are provided by IERS on a daily basis and are based on the combination of the most recently available observed and modeled data (including VLBI 24-hour and intensive, GPS, and AAM (Atmospheric Angular Momentum)). The combination process involves applying systematic corrections and slightly smoothing to remove the high frequency noise. GPSRAPID.DAILY contains the values for the last 90 days from Bulletin A for x/y pole, UT1-UTC, dPsi, dEps, and their errors and predictions for next 15 days at daily intervals.

[00189] After the interpolation, UT1 is corrected for diurnal and/or semidiurnal variations due to Ocean Tides. The polar motion angles are corrected for diurnal variations due to tidal gravitation for a non-rigid Earth, as well as for diurnal and/or semidiurnal variations due to Ocean Tides. Corrections are computed according to:

$$\Delta A = \sum_f B_{Af} \sin\theta_f + C_{Af} \cos\theta_f, \quad A \in \{UT1, x_P, y_P\} \tag{63}$$

[00190] Amplitudes B_{Af}, C_{Af} for 41 diurnal and 30 semi-diurnal Ocean Tidal constituents are listed in tables 8.2 and 8.3 in the IERS Conventions (2003). The EOPs from the GPSRAPID.DAILY are introduced as approximate values for the real-time estimation process, keeping linearization errors at a minimum.

Part 8.7 Startup of the Real-Time System

[00191] When starting the system for the first time or after interruptions of more than a day, some embodiments derive initial values for satellite position velocity and force model parameters using satellite broadcast ephemerides or IGU orbits. Some embodiments use a least-squares fit to adapt a numerically integrated orbit to the broadcast elements from the satellite navigation message or to the IGU orbit for the satellite. The adapted orbit initial state is then integrated for a time period of up to two days into the future. The satellite positions, velocities and partials are stored in a "partials" file for use by the real-time system.

[00192] FIG. 26A shows an embodiment of the startup process 2600 for the real-time orbit processor. An orbit integrator 2605 predicts the orbital states (position and velocity) of each satellite into the future starting from an approximate orbit vector 2615, an initial state taken for example from the broadcast satellite ephemeris or the IGS ultra-rapid orbit IGU by using numerical integration and modeling all relevant forces acting on the satellites, e.g., predicted Earth orientation parameters from IERS. During this process an orbit prediction 2620 is generated, which holds all predicted orbital states and the partial derivatives. In a next step an adaptation process fits the predicted orbit to the broadcast orbit or IGU orbit via a least squares batch process. This process is iterated until the initial orbital states for the satellites are no longer changing. Then the partials file 2620 is forwarded to the real-time real-time orbit process 2630 of FIG. 26B.

[00193] FIG. 26B shows an embodiment of a real-time orbit process 2630. Process 2630 obtains values for an initial start vector 2635 from partials file 2635; these values are used to construct predicted observations for an iterative filter 2640 on a regular basis, e.g., every 150 seconds. Iterative filter 2640 is, for example, a classical Kalman filter or a UD factorized filter or a Square Root Information Filter (SRIF} The orbit start vector 2635 contains the partial derivatives of the current orbit state and force model parameters with respect to the start vector and EOPs and are used to map the partials of the observations to the start vector and force model unknowns. Kalman filter 2640 receives iono-free linear combinations 2645 of observation data from the reference stations in real time, e.g., each epoch, such as once per second, and predicted Earth orientation parameters (EOP) 2610. With each observation update, Kalman filter 2640 provides improved values for the state vector parameters: receiver clocks 2655 (one per station), zenith tropospheric delays 2660 (one per station), satellite clocks 2665 (one per satellite), optional satellite clock rates 2670 (one per satellite), and orbit start vectors 2680 (one orbit start vector per satellite). In the embodiment of FIG. 26B, orbit state vector 2680 is supplied from time to time

(e.g., each epoch, such as once per second) and mapped via the orbit mapper 2682 to the current-epoch orbit position/velocity vector 350.

[00194] Orbit mapper 2682 uses the partial derivatives from the partials file and the following relationship to derive satellite position and velocity at the current epoch t_i from the state vector at

5   epoch t_0 (Fig 26C).

$$r(t_i) = r_0(t_i) + \Phi_{rq}(t_i, t_0) x_{qs}(t_0) = r_0(t_i) + \begin{bmatrix} \dfrac{\partial r(t_i)}{\partial r(t_0)} & \dfrac{\partial r(t_i)}{\partial p(t_0)} & \dfrac{\partial r(t_i)}{\partial y} \end{bmatrix} \begin{bmatrix} \Delta r(t_0) \\ \Delta p(t_0) \\ \Delta y \end{bmatrix} \quad (64)$$

with

$r_0(t_i)$ ... reference trajectory (position and velocity) created by a numerical

orbit integrator

10    $\Phi_{rq}(t_i, t_0)$ ... partials of the position and velocity at t_i with respect to the start vector

$x_{qs}(t_0)$ ... at t_i estimated difference of the start vector (state vector) at t_0

Next $r(t_i)$ which is given in the inertial reference frame is transformed into the Earth centered / Earth fixed reference frame.

[00195] The current-epoch orbit position/velocity vector 350 in the Earth centered / Earth fixed

15   reference frame is forwarded to the standard clock processor 320, to the phase clock processor 335 and to the scheduler 355 of FIG. 3.

[00196] Some embodiments of process 2630 avoid linearization errors by restarting the numerical integration in an orbit integrator 2685 from time to time, such as every 6 or 12 or 24 hours. Orbit mapper 2684 uses the partial derivatives from the partials file and the following relationship to

20   derive a new orbit state vector 2690 in the inertial reference frame at time $t_0 + x$ *hours* from the start vector at epoch t_0 (Fig 26D).

$$r(t_i) = r_0(t_i) + \Phi_{rq}(t_i, t_0) x_{qs}(t_0) = r_0(t_i) + \begin{bmatrix} \dfrac{\partial r(t_i)}{\partial r(t_0)} & \dfrac{\partial r(t_i)}{\partial p(t_0)} & \dfrac{\partial r(t_i)}{\partial y} \end{bmatrix} \begin{bmatrix} \Delta r(t_0) \\ \Delta p(t_0) \\ \Delta y \end{bmatrix} \quad (65)$$

with

$r_0(t_i)$ ... reference trajectory (position and velocity) created by a numerical

25   orbit integrator

$\Phi_{rq}(t_i, t_0)$ ... partials of the position and velocity at t_i with respect to the start vector

$x_{qs}(t_0)$ ... at t_i estimated difference of the start vector (state vector) at t_0

[00197] Predicted EOPs 2610 (e.g., from IERS) and estimated EOPs together with updated new orbit start vector 2690 are used as inputs to orbit integrator 2685 to transform coordinates between the inertial frame and the earth-fixed frame, e.g., following the IERS Conventions.

[00198] This numerical integration runs in the background and generates a new partials file 2635

5   which is used to update the predicted observations of Kalman filter 2640. The start vector for the numerical integration of orbit integrator 2675 is for example the latest best estimate of the real-time system, orbit start vector 2690.

Part 8.8 Fixing ambiguities in Real-Time Orbit Determination

10   [00199] Kalman filter 2640 uses the ionospheric-free dual-frequency combinations 2645 of the L1 and the L2 GNSS observations. The ionospheric-free combination usually leads to a very small wavelength

$$\lambda_{IF} N_{IF} \quad := \quad \frac{f_1^2 \lambda_1 N_1 - f_2^2 \lambda_2 N_2}{f_1^2 - f_2^2}$$

$$= \quad \underbrace{\lambda_1 \frac{F_1}{F_1^2 - F_2^2}}_{=:\lambda_{IF}} \underbrace{(F_1 N_1 - F_2 N_2)}_{:=N_{IF}} \quad \text{with} \quad \begin{array}{l} f_1 =: F_1 \, \mathrm{gcd}(f_1, f_2) \\ f_2 =: F_2 \, \mathrm{gcd}(f_1, f_2) \end{array} \quad (66)$$

[00200] The factors F_1 and F_2 are given in Table 3. For example, for GPS L1 and L2 frequencies

15   with $F_1 = 77, F_2 = 60$ and $\lambda_1 = 0.1903m$ the resulting iono-free wavelength is

$$\lambda_{IF} = \lambda_1 \frac{F_1}{F_1^2 - F_2^2} \approx 6mm \; .$$ This is below the noise level of the phase observations so that there is

no possibility to directly fix the iono-free ambiguity to the correct integer value. Notice that for the iono-free combination between L2 and L5 the iono-free wavelength is with $\lambda_{IF} \approx 12.47cm$ large enough for reliable ambiguity resolution.

20   [00201] To make use of the integer nature of the L1 and L2 ambiguities one could try to solve for the L1 and L2 ambiguities, which is difficult due to the unknown ionospheric contribution to the L1 and L2 carrier phase observations at the stations. A preferred approach is to solve for carrier-phase ambiguities by fixing the widelane ambiguities $N_{WL} := N_1 - N_2$ in a first step. .

·   Substituting N_2 in (64) by $N_2 = N_1 - N_{WL}$ results in

$$\lambda_{IF} N_{IF} \quad = \quad \lambda_{NL} N_1 + \frac{1}{2} (\lambda_{WL} - \lambda_{NL}) N_{WL}$$

$$(67)$$

25

with $\lambda_{WL} := \dfrac{c}{f_1 - f_2}$ and $\lambda_{NL} := \dfrac{c}{f_1 + f_2}$. Thus, once N_{WL} is known, (65) can be solved for

N_1 by using the float value from the filter for $\lambda_{IF} N_{IF}$. After fixing the N_1 ambiguity vector to

integer or to a weighted average of integer values it can be reinserted into (65) to get a fixed value

for $\lambda_{IF} N_{IF}$.

5   [00202] In some embodiments the widelane ambiguities N_{WL} are computed in the widelane bias

processor 325 and are transferred to the orbit processor 2630 for example every epoch. For

embodiments in which the orbit processor 2630 processes ionospheric-free observations, the

ambiguities estimated are ionospheric-free ambiguities $\lambda_{IF} N_{IF}$.

[00203] For embodiments in which the widelane ambiguities N_{WL} are provided by the MW bias

10   processor 325, equation (65) can also be used to reformulate the Kalman filter equations (by

subtracting $\dfrac{1}{2}(\lambda_{WL} - \lambda_{NL})N_{WL}$ from the observations) and estimate the N_1 ambiguities directly.

[00204] As an alternative to resolving the N_1 ambiguity with a given integer widelane ambiguity,

the equations above can be formulated such that N_2 or narrowlane ambiguities are estimated

instead; the approaches are equivalent because all these ambiguities are linearly related.

15   [00205] Some embodiments of ambiguity "fixing" mechanism 2695 employ any suitable

techniques known in the art, such as Simple rounding, , Bootstrapping , Integer Least Squares

based on the Lambda Method, or Best Integer Equivariant (Verhagen, 2005, Teunissen and

Verhagen, 2007)

[00206] The term "fixing" as used here is intended to include not only fixing of ambiguities to

20   integer values using techniques such as rounding, bootstrapping and Lambda search, but also to

include forming a weighted average of integer candidates to preserve the integer nature of the

ambiguities if not fixing them to integer values. The weighted average approach is described in

detail in international patent applications PCT/US2009/004476, PCT/US2009/004472,

PCT/US2009/004474, PCT/US2009/004473, and PCT/US2009/004471 which are incorporated

25   herein by this reference.

[00207] Analyses have shown that the orbit quality is significantly improved by "fixing" the

ambiguities, either as integer values or as weighted averages of integer candidates.

Part 8.9 Orbit Processing at IGS Analysis Centers

[00208] GNSS orbit determination is done by a variety of IGS Analysis Centers. To our knowledge none of these Centers provides real-time orbit estimation as proposed here.

[00209] The CODE Analysis Center (AC) uses a batch least squares approach as described in Dach et al. (2007) and not a sequential filter implementation as described here. Details on the modeling are also described in Beutler et al. (1994). The CODE AC participates in the generation of the IGS Ultra-rapid orbits (IGU). Orbit positions correspond to the estimates for the last 24 hours of a 3-day long-arc analysis plus predictions for the following 24 hours. This is done every 6 hours while the processing and prediction time span is shifted by 6 hours in each step.

[00210] The Geoforschungszentrum GFZ estimates orbits and computes a contribution to the IGS Ultra-rapid orbits. The approach is documented by Ge et al. (2005, 2006). Their processing and that of the CODE process is based on a batch least squares approach. GFZ does ambiguity resolution, but only in post-processing mode. No attempt is documented on real-time efforts involving a sequential filter.

[00211] The European Space Operation Centre ESOC of ESA also contributes to the IGS Ultra-rapid orbit computation. The approach is documented by Romero et al. (2001) and Dow et al. (1999). The approach is also based only on a prediction of satellite orbits. No true real-time processing is done.

[00212] The Jet Propulsion Laboratory JPL, USA, determines GPS satellite orbits with their system based on the GIPSY-OASIS II software package developed for the US Global Positioning System, general satellite tracking, orbit determination and trajectory studies. Details are published in US Patent 5,963,167 of Lichten et al. The JPL system allows a fully automatic operation and delivery of validated daily solutions for orbits, clocks, station locations and other information with no human intervention. This data contributes to the orbits published by the IGS including the Ultra-rapid orbit service providing IGU orbits. US Patent 5,828,336 of Yunck et al. describes the implementation of a real-time sequential filter.

[00213] The approach of embodiments of the present invention differs from that of US Patent 5,828,336 in at least these ways: (1) the approach described in US Patent 5,828,336 appears to use smoothed pseudo-ranges only; an example observation update rate given is 5 minutes, (2) the JPL system described in US Patent 5,828,336 does not appear to fix carrier-phase ambiguities, and (3) the approach of US Patent 5,828,336 uses an ionospheric model

Part 8.10 References

[00214] Some references related to orbit processing include the following:

Beutler, G., E. Brockmann, W. Gurtner, U. Hugentobler, L. Mervart, and M. Rothacher (1994), *Extended Orbit Modeling Techniques at the CODE Processing Center of the International GPS Service for Geodynamics (IGS):Theory and Initial Results*, Manuscripta Geodaetica, 19, 367-386, April 1994.

5   Bierman, Gerald J. (1977): *Factorization Methods for Discrete Sequential Estimation*, Academic Press, Inc., New York

Dach, R., U. Hugentobler, P. Fridez, M. Meindl (eds.) (2007), *Documentation of the Bernese GPS Software Version 5.0*, January 2007

Dow, J., Martin-Mur, T.J., *ESA/ESOC Processing Strategy Summary*, IGS Central Bureau
10   web site, igscb.jpl.nasa.gov/igscb/center/analysis/esa.acn, 1999

Ge, M., G. Gendt, G.Dick and F.P. Zhang (2005), *Improving carrier-phase ambiguity resolution in global GPS*, Journal of Geodesy, Volume 80, Number 4, July 2006, DOI: 10.1007/s00190-005-0447-0

Ge, M., G. Gendt, G.Dick, F.P. Zhang and M. Rothacher (2006), *A new data processing*
15   *strategy for huge GNSS global networks*, Journal of Geodesy, Volume 79, number 1-3, June 2005, DOI: 10.1007/s00190-006-0044-x

Landau, Herbert (1988): *Zur Nutzung des Global Positioning Systems in Geodäsie und Geodynamik: Modellbildung, Software-Entwicklung und Analyse*, Heft 36 der Schriftenreihe des Studiengangs Vermessungswesen der Universität der Bundeswehr München, Dezember 1988

20   Lichten, S., Yoaz Bar-Sever, Winy Bertiger, Michael Heflin, Kenneth Hurst, Ronald J. Muellerschoen, Sien-Chong Wu, Thomas Yunck, James Zumberge (1995) *GIPSY-OASIS II: A HIGH PRECISION GPS DATA PROCESSING SYSTEM AND GENERAL SATELLITE ORBIT ANALYSIS TOOL*, Proceedings of NASA Technology Transfer Conference, Oct 24-26, 1995, Chicago, Ill.

25   Lichten, Stephen M., Wu Sien-Chong, Hurst Kenneth, Blewitt Geoff, Yunck Thomas, Bar-Sever Yoaz, Zumberge James, Bertiger William I., Muellerschoen Ronald J., Thornton Catherine, Heflin Michael (1999), *Analyzing system for global positioning system and general satellite tracking*, United States Patent 5963167, October 5, 1999.

McCarthy, Dennis D. and Gérard Petit (2003), *IERS CONVENTIONS, IERS (International*
30   *Earth Rotation Service) Technical Note 32*, October 2003

Romero, I., C. Garcia Martinez, J.M. Dow, R. Zandbergen (2001), *Moving GPS Precise Orbit Determination Towards Real-Time*, Proceedings GNSS 2001, Seville, Spain, May 2001.

Yunck, Thomas P., William I. Bertiger, Stephen M. Lichten, Anthony J. Mannucci, Ronald J. Muellerschoen, Sien-Chong Wu, (1998), *Robust real-time wide-area differential GPS navigation*, US Patent 5828336, October 27, 1998.

Teunissen, P.J.G, S. Verhagen (2009); *GNSS Carrier Phase Ambiguity Resolution:*
Challenges and Open Problems, In M.G. Sideris (ed.); Observing our Changing Earth, International Association of Geodesy Symposia 133, Spinger Verlag Berlin-Heidelberg 2009.

Verhagen, Sandra (2995): *The GNSS integer ambiguities: estimation and validation*, Publications on Geodesy 58, Delft, 2005. 194 pages., ISBN-13: 978 90 6132 290 0. ISBN-10: 90 6132 290 1.

Part 9: Phase-Leveled Clock Processor

[00215] Referring to FIG. 3, the phase clock processor 335 receives as input MW biases b_{MW}^j 345 (one per satellite) and/or widelane ambiguities $N_{i,WL}^j$ 340 (one per satellite-receiver pair), precise orbit information 350 (one current orbit position/velocity per satellite), troposphere information 370 (one troposphere zenith delay per station), low-rate code leveled clocks 365 (one low-rate code-leveled clock error per satellite) and the reference-station GNSS observation data 305 or 315. The phase clock processor 335 generates from these inputs the computed high-rate code-leveled clocks 375 (one high-rate code-leveled clock error per satellite) and the high-rate phase-leveled clocks 370 (one high-rate phase-leveled clock error per satellite), and forwards the MW biases 345 (one per satellite).

Part 9.1 Determining WL Ambiguities from MW Biases

[00216] Neglecting multipath, a useful characteristic of the Melbourne-Wübbena (MW) linear combination $\Phi_{i,WL}^j - P_{i,NL}^j$ is that, aside from some remaining noise $\varepsilon_{i,MW}^j$, only the satellite MW biases b_{MW}^j and the receiver MW biases $b_{i,MW}$ and the widelane ambiguity term $\lambda_{WL} N_{i,WL}^j$ remain:

$$\Phi_{i,WL}^j - P_{i,NL}^j = b_{i,MW} - b_{MW}^j + \lambda_{WL} N_{i,WL}^j + \varepsilon_{i,MW}^j \tag{68}$$

[00217] To get rid of the noise $\varepsilon_{i,MW}^j$, the Melbourne-Wübbena linear combination for each satellite is in some embodiments reduced by the satellite MW bias b_{MW}^j for that satellite and smoothed (e.g., averaged) over time. Single-differencing between satellites then cancels out the receiver MW bias $b_{i,MW}$, leaving only a single-differenced widelane ambiguity term per

satellite-receiver-satellite connection. The single-differenced widelane ambiguities are computed using the (constant) widelane wavelength λ_{WL} . Since only single-differenced widelane ambiguities are used in the phase clock processor, this method is in some embodiments used as a substitute for using the widelane ambiguities 340 from the MW bias processor 325 and/or for a

5   quality check on the widelane ambiguities 340 received from the MW bias processor 325.

Part 9.2 Single-Differenced Phase-Leveled Clocks

[00218] The location of each reference station is precisely known. The precise location of each satellite at each epoch is given by the current orbit position/velocity data 350 from orbit processor

10   330. The geometric range ρ_i^j between a satellite j and a reference station i at each epoch is calculated from their known locations. The tropospheric delay T_i^j for each reference station is received from the code clock processor 320.

[00219] The ionospheric-free linear combination

$$\Phi_{i,IF}^j = \rho_i^j + c\Delta t_{\Phi,i} - c\Delta t_\Phi^j + T_i^j + \lambda_{IF} N_{i,IF}^j + \varepsilon_{\Phi,i,IF}^j \tag{69}$$

is reduced by the (known) geometric range ρ_i^j and the (known) troposphere delay T_i^j , leaving as

15   unknowns only the ionospheric-free ambiguity term $\lambda_{IF} N_{i,IF}^j = \lambda_{NL} N_{i,1}^j + \frac{1}{2}\left(\lambda_{WL} - \lambda_{NL}\right)N_{i,WL}^j$,

the satellite phase clock error term $c\Delta t_\Phi^j := c\Delta t + b_{\Phi,IF}^j$ and the receiver phase clock error term

$c\Delta t_{\Phi,i} := c\Delta t + b_{\Phi,i,IF}$.

[00220] Single-differencing the observations of two satellites at the same receiver cancels out the receiver clock error.

20   [00221] Reducing this single difference by the according single difference widelane ambiguity leads to the single difference phase clock together with a single difference N_1 ambiguity (often also called narrowlane ambiguity in this context since its corresponding wavelength here is λ_{NL}).

$$\Phi_{i,IF}^{j_1,j_2} - \rho_i^{j_1,j_2} - T_i^{j_1,j_2} - \frac{1}{2}\left(\lambda_{WL} - \lambda_{NL}\right)N_{i,WL}^{j_1,j_2} = -c\Delta t_\Phi^{j_1,j_2} + \lambda_{NL} N_{i1}^{j_1,j_2} + \varepsilon_{\Phi,i,IF}^{j_1,j_2} \tag{70}$$

[00222] This is computed for each station observing the same pair of satellites. At this point it is impossible to distinguish between the single difference satellite clock error and the single

25   difference narrowlane ambiguity term, which is an integer multiple of the narrowlane wavelength.
[00223] If the single difference ambiguity is set to zero a single difference phase clock

$$c\Delta \tilde{t}_{\Phi,i}^{j_1 j_2} := -\left(\Phi_{i,IF}^{j_1 j_2} - \rho_i^{j_1,j_2} - T_i^{j_1 j_2} - \frac{1}{2}\left(\lambda_{WL} - \lambda_{NL} \right) N_{i,WL}^{j_1 j_2} \right) \tag{71}$$

shifted by an integer number of narrowlane cycles is achieved. This phase clock has a non fixed narrowlane status. The difference of two of those single difference clocks $c\Delta \tilde{t}_{\Phi,i_1}^{j_1 j_2}$ and $c\Delta \tilde{t}_{\Phi,i_2}^{j_1 j_2}$ is an integer number of narrowlane cycles.

5   **Part 9.3 Smoothed Single-Differenced Phase Clocks**

[00224] For each pair of satellites, the single-differenced phase clock errors observed from different stations shifted to a common level using fixed narrowlane ambiguities is averaged to get a more precise clock error:

$$c\Delta \bar{t}_{\Phi}^{j_1 j_2} = \frac{1}{n} \sum_{i=1}^{n} (c\Delta \tilde{t}_{\Phi,i}^{j_1 j_2} + \lambda_{NL} N_{i1}^{j_1 j_2}) \tag{72}$$

10   **Part 9.4 Phase-Leveled Clock Estimation**

         Part 9.4.1 Spanning-Tree-Based Phase Clocks

[00225] Some embodiments use a spanning-tree approach to estimate phase-leveled clocks. To compute a single-differenced clock error between any arbitrary pair of satellites, a set of single difference-phase clocks is needed for the satellite-to-satellite links such that there is a unique path

15   to reach each satellite via satellite-to-satellite links starting from a dedicated reference satellite. If all satellites are nodes of a graph, such a path is called spanning tree. If each edge of the graph is equipped with a weight, a minimum spanning tree is a spanning tree with a minimal sum of edge weights. Some embodiments use a discrete category based weighting scheme for an edge between two satellites and assign the following phase clock values to the edge:

20   i. Several edges connecting satellites j_1 and j_2 have a fixed N_1 ambiguity: (Weighted) averaged single-differenced clock $c\overline{\Delta t}_{\Phi}^{j_1 j_2}$,

ii, Only a single edge connecting satellites j_1 and j_2 has a fixed N_1 ambiguity:

$c\Delta \tilde{t}_{\Phi,i}^{j_1 j_2} + \lambda_{NL} N_{i1}^{j_1 j_2}$,

iii. No edge connecting satellites j_1 and j_2 has a fixed N_1 ambiguity: $c\Delta \tilde{t}_{\Phi,i}^{j_1 j_2}$ for receiver i with

25   min(elevation(j1,j2) is maximal,

iv. No WL ambiguity available for edge connecting satellites j_1 and j_2:   Don't use such an edge; thus no phase clock has to be defined;

[00226] Each edge of category (i) has a lower weight than an edge of category (ii), each edge of

category (ii) has a lower weight than an edge of category (iii) etc. Edges within each category have a continuous weight that is in some embodiments derived in category (i) from the variance of the average and in category (ii) and (iii) from the elevations under which the satellites in the single difference are seen at the corresponding station.

5 [00227] If the minimum spanning tree uses an edge without a fixed narrowlane status, the narrowlane ambiguity $N_{i1}^{j_1 j_2}$ is set to zero and achieves fixed status. Choosing a reference satellite with phase clock error $c\Delta t_\Phi^{j_{ref}}$ set to zero, single-differenced phase clock errors $c\Delta t_\Phi^{j_{ref} j_2}$ to all other satellites are computed solving a linear system. The satellite's phase clock error is then defined as $c\Delta t_\Phi^{j_2} := c\Delta t_\Phi^{j_{ref} j_2}$

10

Part 9.4.2 Filter Estimation of Phase-Leveled Clocks

[00228] Some embodiments use a filter approach to estimate phase-leveled clocks. A filter is set up with all satellite phase clock errors as states. The state of the reference satellite's clock error $c\Delta t_\Phi^{j_{ref}}$ is set to zero. In some embodiments all links from the spanning tree and in addition all

15 links with fixed narrowlanes are added to the filter to estimate more precise single-differenced phase clock errors.

Part 9.5 Narrowlane Filter Bank

[00229] Once a set of single-differenced phase clock errors is estimated, e.g., as in Part 9.4, all

20 observations for shifted single-differenced phase clocks in Part 9.2 are reduced by the clock errors estimated in Part 9.4:

$$N_{i1}^{j_1 j_2} \approx \frac{1}{\lambda_{NL}} \left(c\Delta \bar{t}_\Phi^{j_1 j_2} - c\Delta \tilde{t}_{\Phi,i}^{j_1 j_2} \right) \tag{73}$$

[00230] What remains is an observable for the integer narrowlane offset. For each station a narrowlane filter with a narrowlane ambiguity state per satellite is updated with those observations.

25

Part 9.6 High-Rate Single-Differenced Code-Leveled Clocks

[00231] The phase clock processor 335 also computes high-rate code-leveled clocks.

Part 9.6.1 Buffering Low-Rate Code-Leveled Clocks

[00232] GNSS observations (reference station data 305 or 315) for a time (e.g., an epoch) t_1 are buffered for use when the low-rate information with the same time tag (t_1) arrives from the code-leveled clock processor 360; this information comprises two of: clock errors 365, tropospheric delays 370, and ionospheric-free float ambiguities 374. Thus, GNSS observations matched in

5   time with the low-rate clock processor information are always available from an observation buffer. When a set of low-rate code leveled clocks 365 arrive they are combined with the GNSS observations and with the tropospheric delays 370 and with time-matched satellite position/velocity information 350 to compute the carrier ambiguities.

[00233] FIG. 27 shows at 2700 the flow of data for the case where the satellite clocks (clock

10   errors) 365 and the tropospheric delays 370 are used. GNSS observations arrive over time at the phase clock processor 335 with (e.g. epoch) time tags t_0, t_1, t_2, t_3, etc. Low-rate code leveled clocks $c\Delta t_P^j$ and tropospheric delays T arrive asynchronously over time with time tags t_0, t_1, t_2, t_3, etc. An observation buffer 2705 holds the observations. These are combined for each time t_i in a combiner 2710 with satellite position/velocity data, with the low-rate code-leveled

15   clocks $c\Delta t_P^j$ and with the tropospheric delays T to produce the ionospheric-free float ambiguity terms $\lambda N_i^j := \lambda_{IF} N_{i,IF}^j + b_{\Phi,i,IF} - b_{P,i;IF} - \left(b_{\Phi,IF}^j - b_{P,IF}^j \right)$. A process 2715 computes the single-differenced code-leveled clocks 2720.

[00234] If the low rate processor sends the float ambiguities, the buffering of observations is not needed. The float ambiguities can directly be used for future observations.

20

Part 9.6.2 Computing Iono-Free Float Ambiguities in the Phase Clock Processor

[00235] The data combiner (2710) forms an ionospheric-free linear combination of the carrier-phase observation, and reduces this by the geometric range ρ_i^j (computed using the receiver and satellite positions), the tropospheric delay T_i^j and the low-rate code-leveled satellite clock error

25     $c\Delta t_P^j$ (e.g., clocks 365). After this reduction the receiver clock error and a float ambiguity remains. If this is done using between-satellite single-differenced observations, the receiver clock is eliminated and thus only the single-differenced ionospheric-free ambiguity term remains:

$$\Phi_{i,IF}^{j_1 j_2}(t_1) - \rho_i^{j_1,j_2}(t_1) - T_i^{j_1 j_2}(t_1) + c\Delta t_P^{j_1 j_2}(t_1) = \lambda N_i^{j_1 j_2}(t_1) + \varepsilon_{\Phi,i,IF}^{j_1 j_2}(t_1) \quad (74)$$

with $c\Delta t_P^{j_1 j_2} := c\Delta t^{j_1 j_2} + b_{P,IF}^{j_1 j_2}$ and float ambiguity $\lambda N_i^{j_1 j_2} := \lambda_{IF} N_{i,IF}^{j_1 j_2} - \left(b_{\Phi,IF}^{j_1 j_2} - b_{P,IF}^{j_1 j_2} \right)$ which is a constant value and is kept to be used until the next update of low rate clocks.

[00236] As an alternative to computing the ionospheric-free ambiguities in the phase clock processor 335, the ionospheric-free float ambiguities are obtained from a previous processor, such as ionospheric-free float ambiguities 374 from the low-rate code clock processor 320.

5   **Part 9.6.3 Using Iono-Free Float Ambiguities to Compute High Rate Code Clocks**

[00237] Once iono-free ambiguities are known for time t_1, single-differenced ionospheric-free linear combinations at any time in the future (e.g. t_2) can be used for each pair of satellites along with tropospheric delay and current geometric range:

$$\Phi_{i,IF}^{j_1 j_2}(t_2) - \rho_i^{j_1,j_2}(t_2) - T_i^{j_1 j_2}(t_1) - \lambda N_i^{j_1 j_2}(t_1) = -c\Delta t_P^{j_1 j_2}(t_2) + \varepsilon_{\Phi,i,IF}^{j_1 j_2}(t_2) + \varepsilon_{\Phi,i,IF}^{j_1 j_2}(t_1) \quad (75)$$

10   The result of this computation is the single-differenced code-leveled satellite clock error $c\Delta t_P^{j_1 j_2}$.

With this it is possible to estimate high-rate single-differenced code-leveled clock errors $c\Delta t_P^{j_{ref} j_2}$ between a given satellite j_2 and a chosen reference satellite j_{ref}. If only the between-satellite single-differenced clock errors are of interest, the reference satellite clock error $c\Delta t_P^{j_{ref}}$ is set to zero, otherwise the reference clock can be steered to the corresponding broadcast or low rate

15   clock to shift the clocks to an absolute level. For simplicity FIG. 28A to FIG. 28C do not include this shift.

[00238] FIG. 28A shows a first embodiment 2800 for preparing the high-rate code-leveled satellite clocks 375. Precise satellite orbit information, e.g., satellite position/velocity data 350 or 360, and GNSS observations, e.g., reference station data 305 or 315, are supplied as inputs to a

20   first process 2805 and as inputs to a second process 2810. The first process 2805 estimates a set of ionospheric-free float ambiguities 2815. These are supplied to the second process 2810 which estimates the high-rate code-leveled satellite clocks (clock errors) 375.

[00239] FIG. 28B shows a second embodiment 2820 for preparing the high-rate code-leveled satellite clocks 375. Precise satellite orbit information, e.g., satellite position/velocity data 350 or

25   360, and GNSS observations, e.g., reference station data 305 or 315, are supplied as inputs to a low-rate code-leveled clock processor 2825, e.g., code clock processor 320, and as inputs to a high-rate code-leveled clock processor 2830. The low-rate code-leveled clock processor 2825 prepares ionospheric-free float ambiguities 2835, e.g., ionospheric-free float ambiguities 374, and tropospheric delays 2840, e.g., tropospheric delays 370. The ionospheric-free float ambiguities

30   2835 and the tropospheric delays 2840 are supplied to the high-rate code-leveled clock processor 2830, e.g., forming a part of phase clock processor 335. The high-rate code-leveled clock processor 2830 uses the inputs at 2845 to compute single-differenced high-rate code-leveled

satellite clocks 2850 per station. A filter 2855 uses these to estimate qualitatively improved code-leveled satellite clocks (clock errors) 2860, e.g., high-rate code-leveled satellite clocks 375.

[00240] FIG. 28C shows a third embodiment 2865 for preparing the high-rate code-leveled satellite clocks 375. Precise satellite orbit information, e.g., satellite position/velocity data 350 or 360, and GNSS observations, e.g., reference station data 305 or 315, are supplied as inputs to a low-rate code-leveled clock processor 2870, e.g., code clock processor 320, and as inputs to a high-rate code-leveled clock processor 2875. The low-rate code-leveled clock processor 2870 prepares low-rate code-leveled clocks 2880, e.g., low-rate code-leveled satellite clocks 365, and tropospheric delays 2882, e.g., tropospheric delays 370. The low-rate code-leveled satellite clocks 2880 and the tropospheric delays 2882 are supplied to the high-rate code-leveled clock processor 2875, e.g., forming a part of phase clock processor 335. The high-rate code-leveled clock processor 2884 uses the inputs at 2884 to compute ionospheric-free float ambiguities 2886 which are used at 2888 to compute single-differenced high-rate code-leveled satellite clocks 2890. A filter 2892 uses these to estimate qualitatively improved high-rate code-leveled satellite clocks (clock errors) 2894, e.g., high-rate code-leveled satellite clocks 375.

Part 9.6.4 Clock Shifter

[00241] Single-differenced phase-leveled clock errors $c\Delta t_\Phi^{j_{ref}j_2}$ and single-differenced code-leveled clock errors $c\Delta t_P^{j_{ref}j_2}$ are estimated as in the course of estimating phase-leveled satellite clocks and high-rate single-differenced code-leveled satellite clocks. The single-differenced high-rate code-leveled satellite clocks have the same accuracy as single differences of the low-rate code-leveled satellite clocks. The phase-leveled satellite clocks are constructed to preserve the integer nature of the narrowlane ambiguity if used for single-differenced ionospheric-free carrier-phase observations together with the precise satellite orbits and the widelane ambiguities, derived from the MW biases, used in the clock estimation. Thus the quality of a single-differenced phase-leveled clock error is not changed if this clock error is shifted by an integer number of narrowlane cycles. Since the phase-leveled satellite clock errors will always be used in a single difference, such a shift which is applied to all satellite clock errors will cancel out again in the single-differencing operation. In accordance with some embodiments the following shift is applied to the phase-leveled satellite clock errors to keep their values close to the low-rate code-leveled satellite clock errors and reduce their noise.

[00242] Thus in some embodiments an integer number of narrowlane cycles

$$s_{NL}^{j_{ref}j_2} = \text{Round}(c\Delta t_P^{j_{ref}j_2} - c\Delta t_\Phi^{j_{ref}j_2})\qquad(76)$$

is added to each of the phase-leveled satellite clock errors to minimize the distance to the high-rate code-leveled satellite clocks.

[00243] In some embodiments the low-rate code-leveled clock errors are approximated with a continuous steered clock $c\Delta t^{j}_{P,steered}$. The value of the steered clock of the reference satellite

$$S_{ref} = c\Delta t^{j_{ref}}_{P,steered} \tag{77}$$

is then added to all high-rate clocks. Doing so, all clocks are close to the code-leveled low-rate clocks, but the reference clock is smooth.

[00244] In some embodiments the mean of the difference between the high-rate phase-leveled satellite clocks and their corresponding steered low-rate clock is computed and added to all shifted phase-leveled satellite clock errors. The same is done for the high-rate code-leveled satellite clocks. This procedure pushes some noise into the reference clock. If the number of clocks used to compute this mean changes, the computed mean can be discontinuous. To handle those jumps one can simply send a jump message or smooth the mean, e.g., by steering to the current value or using a moving average, etc.

$$\begin{aligned}
S_{P,noise} &= \frac{1}{n}\sum_{j=1}^{n}\left(c\Delta t^{j_{ref}\,j_2}_{P} - c\Delta t^{j_{ref}\,j_2}_{P,steered}\right) \\
S_{\Phi,noise} &= \frac{1}{n}\sum_{j=1}^{n}\left(c\Delta t^{j_{ref}\,j_2}_{\Phi} - c\Delta t^{j_{ref}\,j_2}_{P,steered} + s^{j_{ref}\,j_2}_{NL}\right)
\end{aligned} \tag{78}$$

[00245] The shifted clock errors read as

$$\begin{aligned}
c\Delta t^{j_2}_{P} &= c\Delta t^{j_{ref}j_2}_{P} + S_{P,noise} + S_{ref} \\
c\Delta t^{j_2}_{\Phi} &= c\Delta t^{j_{ref}j_2}_{\Phi} + S_{\Phi,noise} + S_{ref} + s^{j_{ref}j_2}_{NL}
\end{aligned} \tag{79}$$

[00246] The shifting is mainly done to keep the phase-leveled satellite clock errors near GPS time and therefore make certain transmission methods applicable. In addition the clock bias

$$b^{j}_{\Delta t} = c\Delta t^{j}_{P} - c\Delta t^{j}_{\Phi}, \tag{80}$$

which is the difference between the phase-leveled satellite clocks and code-leveled satellite clocks, can be kept within a certain range.

Part 9.6.5 Jump messages

[00247] If the clock bias leaves its range or if the phase-leveled clocks' satellite-to-satellite links have been estimated without using fixed narrowlane ambiguities, the shift will change and a jump message is sent. This also means that the phase-leveled satellite clock error changes its level.

Part 9.7 Phase Clock Processor Embodiments

[00248] FIG. 29 shows an architecture 2900 of a phase clock processor 335 in accordance with some embodiments of the invention. The inputs to the phase clock processor are: MW biases and/or fixed WL ambiguities 2095 (e.g., MW biases 345 and/or fixed WL ambiguities 340), low-

5   rate (LR) code-leveled clocks 2910 (one per satellite, e.g., low-rate code-leveled satellite clocks 365), satellite orbit information (e.g., precise satellite orbit position/velocities 350 and/or IGU orbit data 360), tropospheric delays 2920 (one per reference station, e.g., tropospheric delays 370), and GNSS observations 2925 (of multiple satellites at multiple reference stations, e.g, reference station data 305). The choice of MW biases or fixed WL ambiguities gives two

10   options. A first option is to use the low-rate MW biases together with the low-rate orbit information 2915 and the GNSS observations 2925 in an optional fixer bank 2930 to fix the WL ambiguities. These are then provided at a high rate (HR) as single-differenced fixed WL ambiguities 2935 to a computation process 2940. A second option is use the low-rate fixed WL ambiguities directly to supply single-differenced (SD) fixed WL ambiguities to the process 2940.

15   By high-rate is meant that the single-differenced fixed WL ambiguities used in the high-rate process 2940 remain the same from epoch to epoch in process 2940 between low-rate updates.

[00249] The low-rate code-leveled clocks 2910 are used in process 2945 to compute low-rate single-differenced ionospheric-free float ambiguities 2950. These are used with the low-rate orbit data 2915 and the low-rate tropospheric delays 2920 and the high-rate GNSS observations 2925

20   in a process 2955 to compute single-differenced high-rate code-leveled clocks 2960 (one per satellite, such as high-rate code-leveled satellite clocks 375).

[00250] The high-rate single-differenced fixed WL ambiguities 2935 are used with the low-rate orbit data 2915 and the low-rate tropospheric delays 2920 and the GNSS observations 2925 in a process 2940 which computes high-rate phase-leveled clocks 2945 (one per satellite, such as

25   high-rate phase-leveled satellite clocks 375). The high-rate phase-leveled clocks 2945 are used together with the orbit data 2915 and the tropospheric delays 2920 and the GNSS observations 2925 in an ambiguity fixer bank 2975 which attempts to fix single-differenced ambiguities, e.g., L1 ambiguities. The single-diffierenced fixed ambiguities 2980 are pushed into the process 2965 to aid the computation of high-rate phase-leveled clocks 2970.

30   [00251] The MW biases and/or fixed WL ambiguities 2905 and the low-rate code-leveled clocks 2910 and the single-differenced high-rate code-leveled clocks 2960 and high-rate phase-leveled clocks 2970 are fed into a process 2985 which shifts and combines these to deliver a high rate data flow 2990 containing (at least) high-rate phase-leveled satellite clocks, high-rate code-

leveled clocks and high-rate MW biases. Data 2990 is supplied to scheduler 355 as described in FIG. 3.

[00252] FIG. 30A shows an embodiment 3000 of a process for estimating high-rate phase-leveled satellite clocks. Precise satellite orbit information, e.g., satellite position/velocity data 350 or

5   360, and GNSS observations, e.g., reference station data 305 or 315, are supplied at low rate as inputs to a first process 3015 and at high rate as inputs to a second process 3020. The first process 3015 estimates ambiguities 3025, one set of ambiguities per receiver. Each ambiguity corresponds to one of a receiver-satellite link and a satellite-receiver-satellite link. These ambiguities are supplied at low rate to the second process 3020 which estimates the high-rate

10   phase-leveled clocks 3030.

[00253] In general a linear combination of carrier phase observations has receiver-dependent parameters p_r like receiver position, receiver clock error or receiver biases, satellite-dependent parameters p^s like the satellite position, and receiver-satellite-link dependent parameters p_r^s like the tropospheric or the ionospheric delay. Let $\Omega_{rk}^s, k \in L$ be linear combinations of code

15   and carrier phase observations with wavelength λ_k and ambiguity N_{rk}^s. A code and carrier phase combination as assumed here can be written as

$$\hat{\Omega}_r^s := \sum_{k \in \hat{L}} a_k \Omega_{rk}^s = f(p_r; p^s, p_r^s) + c\Delta t^s + \sum_{k \in \hat{L}} a_k (b_k^s + \lambda_k N_{rk}^s) + \varepsilon_r^s, \tag{81}$$

with $\hat{L} \subseteq L, \hat{L}$ not empty and real factors $a_k \in \Re$.

[00254] Note that $f : \Re^{n_p} \to \Re$ is linear in most of the parameters. If a mapping exists to convert between a receiver-satellite link dependent parameter and a receiver dependent

20   parameter, it can be used to reduce the number of unknowns. As an example the troposphere delay can be modeled as a delay at zenith, which is mapped to line of sight. Thus instead of having one parameter per receiver-satellite link, only one parameter per receiver is needed.

[00255] Using special linear combinations such as an ionospheric-free combination, parameters can be canceled out. Each additional input of at least one of the parameters contained in p_r, p^s

25   and p_r^s simplifies and accelerates the estimation process. In satellite-receiver-satellite single differences the parameters p_r cancel out. In the following all can be done in single or zero difference, but this will not be mentioned explicitly in each step.

[00256] If all parameters p_r, p^s, p_r^s and $c\Delta t^s$ are known and the noise is neglected, the

remaining part $\sum_{k \in L} a_k (b_k^s + \lambda_k N_{rk}^s)$ is not unique without additional information. Setting the

ambiguities for a specific satellite-receiver combination to zero will shift the biases accordingly.
If the ambiguities are known, the level of the bias is defined; if the bias is known, the level of

5   ambiguities is defined.

[00257] In some linear combinations Ω_{rk}^s of code and carrier-phase observations the parameter

p_r, p^s, p_r^s and $c\Delta t^s$ cancel out, as do the receiver biases b_{rk}. This allows estimating the

biases b_k^s, b_{rk} and the ambiguities N_{rk}^s separated from the other parameter.

[00258] Not all satellite biases can be estimated separately from the satellite clock error $c\Delta t^s$. In

10   this case the sum of the real satellite clock and the biases are estimated together and the result is
just referred as the satellite clock error. In this case shifting a bias is equivalent with shifting a
clock.

[00259] In the following a distinction is made between ambiguities belonging to biases and
ambiguities belonging to clock errors. The clock ensemble and also the biases ensemble

15   estimated from GNSS observations are underdetermined. Thus one of the satellite or receiver
clock errors/biases or any combination of them can be set to any arbitrary value or function to
make the system solvable. In some embodiments one of the clocks/biases is set to zero, or
additional measurements or constraints for one of the clock errors/biases or a linear combination
of clock errors/biases are added. The examples given here always have a reference clock/bias set

20   to zero, for purposes of illustration, but this is not a requirement and another approach can be
used.

[00260] **Process I (3015):** In a first step all other input parameters are used to reduce the linear
combination of carrier phase observations. Depending on the linear combination used, there are
small differences in how to estimate phase-leveled satellite clock errors. One option is to use a

25   single, big filter: In this case, all remaining unknown parameters of p_r, p^s and p_r^s, the satellite

clock errors, including biases, and all ambiguities of $\hat{\Omega}_r^s$ are modeled as states in one filter, e.g. a

Kalman filter. As an example the filter used for orbit determination in Part 8 (Orbit Processor),
the one used for code-leveled clocks in Part 6 (Code-Leveled Clock Processor) (except the integer
nature of ambiguities) or the Melbourne-Wübbena bias processor in Part 7 (MW Bias Processor)

30   can be used. Another option is to perform a hierarchical estimation.

[00261] In some embodiments using linear combinations Ω_{rk}^s of code and carrier-phase

observations in which the parameters p_r, p^s, p_r^s and $c\Delta t^s$ cancel out, the biases and ambiguities

of Ω_{rk}^s estimated in an auxiliary filter and can be used to simplify the main filter.

[00262] Another option is to use a bank of filters rather than a single filter or rather than a main

filter with auxiliary filter. If all parameter beside the ambiguities are known, in at least one of the

5   code and carrier-phase combinations $\hat{\Omega}_r^s$ or $\Omega_{rk}^s, k \in \hat{L}$ the ambiguities can be estimated in a

filter bank with one filter for each ambiguity or one filter for each receiver. This is done for

single-differenced observations in the phase clock processor to estimate the widelane ambiguities

using the Melbourne-Wübbena linear combination and Melbourne-Wübbena biases as input.

[00263] A further option is to use a combination of a main filter with a bank of filters. In some

10   embodiments the results of the filter banks are used to reduce the carrier-phase combinations $\hat{\Phi}_r^s$

in the main filter used to estimate the remaining unknowns.

[00264] At least one set of fixed ambiguities is sent from process I (3015) to process II (3020),

but all the estimated parameters could be sent in addition.

[00265] **Process II (3025):** In process II the linear combination $\hat{\Omega}_r^s$ is reduced by all input

15   parameters from process I or additional sources. If no fixed ambiguities are available for the

ambiguities from process I that belong to the clock error, a subset of those ambiguities defined

e.g. by a spanning tree is in some embodiments set to any arbitrary integer number and used like

fixed ambiguities as discussed above. If this subset changes or is replaced by fixed ambiguities

of process I, the resulting satellite phase clock errors may change their level. All remaining

20   unknowns are modeled as states in a filter, e.g. a Kalman filter.

[00266] As in FIG. 30A, some embodiments estimate the ambiguities at a first rate and estimate a

phase-leveled clock per satellite at a second rate higher than the first rate. The ambiguities

estimated in process I (3005) are constant as long the receiver has no cycle slip. Thus an

estimated ambiguity can be used for a long time. Also some of the other states like the

25   troposphere estimated in process I (3005) vary slowly and can be assumed to be constant for a

while. If the observations of process II (3020) are reduced by those constant and slowly varying

parameters, the filter used to estimate clock errors has only a view unknowns left and is therefore

quite fast. In general, processor II can work at a higher update rate than process I.

[00267] FIG. 31 shows an embodiment 3100 in which estimating a phase-leveled clocks per

30   satellite comprises using at least the satellite orbit information, the ambiguities and the GNSS

signal data to estimate a set of phase-leveled clocks per receiver, each phase-leveled clock

corresponding to one of a receiver-satellite link and a satellite-receiver-satellite link; and using a

plurality of the phase-leveled clocks to estimate one phase-leveled clock per satellite. The satellite orbit information 3105 (e.g, 350 or 360) and the GNSS observations 3110 (e.g., 305 or 315) are used in a first process 3115 to determine the ambiguities 3120. The ambiguities 3120 are used with the satellite orbit information 3105 and the GNSS observations 3110 in a second

5   process 3125 to estimate the set of phase leveled clocks 3130, each phase-leveled clock corresponding to one of a receiver-satellite link and a satellite-receiver-satellite link. These are used in a third process 3135 to estimate satellite clocks 3140, one per satellite.

[00268] This means, instead of having a big filter in the second process, the problem can be decoupled using a small filter for each satellite-to-satellite link to estimate clock errors per

10   receiver-satellite link or in single difference case per satellite-receiver-satellite link. Afterwards those clock errors per link can be combined either using only links defined by a spanning tree (e.g., as at 3058) or using a filter with one clock error state per satellite.

[00269] In some embodiments, the ambiguities are estimated using at least one previously-estimated phase-leveled clock per satellite. As mentioned above, the known fixed ambiguities

15   define the clock error level, and (vice versa) a known clock error leads to ambiguities fitting this clock error. Thus the feedback of clock error estimates to process I allows to estimate ambiguities without having a dedicated clock error state. Since process II can already produce clock error estimates before having all ambiguities fixed, this feedback is advantageous in such a scenario to fix ambiguities belonging to clock errors. FIG. 32 shows one such embodiment 3200.

20   The satellite orbit information 3205 (e.g., 350 or 360) and the GNSS observations 3210 (e.g., 305 or 315) are used in a first process 3215 to determine the ambiguities 3220. The ambiguities 3220 are used with the satellite orbit information 3205 and the GNSS observations 3210 in a second process 3225 to estimate the set of phase leveled clocks 3230. These are fed back to the first process 3215 where they are used in estimating the ambiguities 3220.

25   [00270] Two more detailed realizations of this process are illustrated in FIG. 30B and FIG. 30C.

[00271] FIG. 30B is a simplified schematic diagram of an alternate phase clock processor embodiment 3035 with WL ambiguities input as in option 2 of FIG. 29 (compare with process 2965). Satellite orbit data 3005 (e.g., 350 or 360), GNSS observations 3010 (e.g., 305 or 315), tropospheric delays 3040 (e.g., 370) and fixed WL ambiguities 3045 (e.g., 340) are supplied to a

30   filter bank 3050 of process I (3015). Filter bank 3050 estimates single-differenced free narrowlane ambiguities 3055. The SD free NL ambiguities 3055 and the fixed WL ambiguities 3045 are combined in a process 3060 with the satellite orbit data 3005, the GNSS observations 3010, and the tropospheric delays 3040 to compute single-differenced satellite clocks 3062. These are applied to a narrowlane filter bank 3064 to estimate single-differenced- satellite clocks

3066. A spanning tree process 3068 (e.g. MST) is applied to these to produce a set of single-differenced satellite clocks 3070. These are fed back to the filter bank 3050 of process I (3015) to improve the estimation of the single-differenced free narrowlane ambiguities 3055.

[00272] FIG. 30C is a simplified schematic diagram of an alternate phase clock processor embodiment 3075 with MW biases input as in option 1 of FIG. 29 (compare with process 2965). Satellite orbit data 3005 (e.g., 350 or 360), GNSS observations 3010 (e.g., 305 or 315), tropospheric delays 3040 (e.g., 370) and fixed WL ambiguities 3045 (e.g., 340) are supplied to a filter bank 3078 of process I (3015). Filter bank 3078 estimates single-differenced free narrowlane ambiguities 3088. A filter bank 3082 uses the MW satellite biases 3045 to estimate WL ambiguities 3084. As in FIG. 30B, the SD free NL ambiguities 3055 and the fixed WL ambiguities 3084 are combined in a process 3060 with the satellite orbit data 3005, the GNSS observations 3010, and the tropospheric delays 3040 to compute single-differenced satellite clocks 3062. These are applied to a narrowlane filter bank 3064 to estimate single-differenced-satellite clocks 3066. A spanning tree process 3068 (e.g. MST) is applied to these to produce a set of single-differenced satellite clocks 3070. These are fed back to the filter bank 3078 of process I (3015) to improve the estimation of the single-differenced free narrowlane ambiguities 3080.

[00273] Using clock error estimates from a second phase clock processor as input to process I allows to estimate ambiguities fitting those clocks and finally to estimate satellite clock errors at the same level as the other processor's clock errors. For this embodiment it is advantageous to have a secondary clock processor as a back up which is available to immediately provide clock error estimates without level change in case of a failure of the primary clock processor.

[00274] In some embodiments at least one additional phase-leveled clock per satellite estimated from an external source is obtained and used to estimate the ambiguities. FIG. 33 shows one such embodiment 3300. In part 3335, the satellite orbit information 3305 (e.g., 350 or 360) and the GNSS observations 3310 (e.g., 305 or 315) are used in a first process 3315 to determine the ambiguities 3320. The ambiguities 3320 are used with the satellite orbit information 3305 and the GNSS observations 3310 in a second process 3325 to estimate the set of phase leveled clocks 3330. In part 3385, the satellite orbit information 3355 (e.g, 350 or 360) and the GNSS observations 3360 (e.g., 305 or 315) are used with one or more of satellite clocks 3330 in a first process 3365 to estimate the ambiguities 3370. In this embodiment part 3335 is an external source of the satellite clocks 3330 with respect to part 3385. The ambiguities 3370 are used with the satellite orbit information 3355 and the GNSS observations 3360 in a second process 3375 to estimate the set of phase leveled clocks 3380.

[00275] In some embodiments, at least one set of ambiguities per receiver is determined for additional receivers, each ambiguity corresponding to one of a receiver-satellite link and a satellite-receiver-satellite link. After determining the ambiguities for the additional receivers, at least the precise orbit information, the ambiguities for the additional receivers and the GNSS signal data are used to estimate the at least one additional phase-leveled clock per satellite.

[00276] FIG. 34 shows one such embodiment 3400. In part 3455, the satellite orbit information 3405 (e.g, 350 or 360) and the GNSS observations 3310 (e.g., 305 or 315) are used in a first process 3415 to determine the ambiguities 3420. The ambiguities 3420 are used with the satellite orbit information 3405 and the GNSS observations 3410 in a second process 3425 to estimate the set of phase leveled clocks 3430. In part 3485, the satellite orbit information 3455 (e.g, 350 or 360, but optionally from a different orbit processor associated with a different network of reference stations) and the GNSS observations 3410 (e.g., 305 or 315, but optionally from a different network of reference stations) are used with one or more of satellite clocks 3430 in a first process 3465 to estimate the ambiguities 3470. The ambiguities 3470 are used with the satellite orbit information 3455 and the GNSS observations 3460 in a second process 3475 to estimate the set of phase leveled clocks 3480.

[00277] The primary and secondary clock processors can also be of different kind. This option can be used to estimate the ambiguities close to the level of clock errors based on a different linear combination (e.g. code clock error or different phase combination). Using those ambiguities in process II will lead to clock errors close to clock errors input in process I.

Part 10: Scheduler & Message Encoder

[00278] The scheduler 355 and message encoder 385 can be implemented as desired. Methods and apparatus for encoding and transmitting satellite information are described for example in Patent Application Publications US 2009/0179792 A1, US2009/0179793 A1, US2010/0085248 A1, US2010/0085249 A1 and/or US2010/0214166 A1.

Part 11: Rover Processing with Synthesized Reference Station Data
Part 11.1 Introduction

[00279] Existing RTK rover positioning engines are typically designed to process differenced data; the rover data is differenced with base station data and the filters operate on the differenced data. The GNSS observations are contaminated with a number of errors such as satellite clock error, receiver clock error, troposphere delay error, and ionospheric delay error. The satellite-dependent errors (e.g. satellite clock error) can be eliminated if the difference between the

observations of two receivers observing the same satellite is used. If those receivers are located close enough to each other (e.g. a few kilometers under normal conditions) then the atmosphere-related errors can also be eliminated. In case of VRS (Virtual Reference Station) the difference is done not between two stations, but between the rover station and a virtual station, whose data is generated using observations from a network of receivers. From this network it is possible to create knowledge of how errors behave over the region of the network, allowing differential positioning over longer distances.

[00280] Prior approaches for Precise Point Positioning (PPP) and PPP with ambiguity resolution (PPP/RTK) remove modeled errors by applying them as corrections (subtracting the errors) to the rover data. Though this works, using a rover receiver configured to process differenced data requires a change in data preparation in that single-differencing has to be replaced by rover-data-only error correction before the data can be processed.

[00281] This implies two different modes of operation inside the rover's positioning engine. In practice this results in separate processors for PPP and RTK. This consumes a lot of software development resource, and occupies more of the rover's CPU memory for the additional modules and data.

Part 11.2 Global Virtual Reference Station Positioning

[00282] Some embodiments of the invention are based on a substantially different approach, in which a Synthesized Base Station (SBS) data stream is generated for any position on or near the Earth's surface using precise satellite information (e.g., precise orbits and clocks). This data stream is equivalent to having a real reference station near the rover.

[00283] For processing at the rover, a Real-Time Kinematic (RTK) positioning engine is used that is adapted to the different error characteristics of PPP as compared to traditional Virtual Reference Station (VRS) processing. Unlike traditional VRS processing, some embodiments of the invention use a processing approach which does not rely on small ionospheric residuals. And in contrast with traditional VRS processing, some embodiments of the invention optionally process different pseudorange observables.

[00284] PPP and PPP/RTK functionality are retained, with comparatively low software development and few changes in the rover positioning engine, while retaining the advantage of well-proven RTK engines that had been developed and perfected with many man-years of development time. Examples of such functionality include processing of data collected under canopy and dealing with delays in the reference data/corrections (low-latency positioning).

[00285] PPP-RTK studies using the SBS technique have proven the high performance of such a system. A positioning accuracy of 10 cm horizontal (95%) was achieved after about 600 seconds (mean) when processing a test data set. Convergence to the typical long baseline and VRS survey accuracy of 2.54 cm horizontal (95%) was achieved after 900 seconds (mean). This suggests that

5   SBS techniques described here can provide sub-inch horizontal-positioning performance.

Part 11.3 Generating SBS Data

[00286] The SBS technique enables the generation of virtual GNSS data (data from a virtual GNSS reference/base station) for any position on or near the Earth's surface using precise

10   satellite information (e.g., orbits, clocks). The core of the processing is done inside a module which responsible for the generation of the virtual data. The aim of such data generation is to make it possible to use GNSS satellite precise information in a GNSS receiver running a conventional real-time kinematic (RTK) process as is typically used with reference receiver data of a physical base station or virtual reference station. In the SBS technique the receiver's antenna

15   position is computed by the RTK engine with differential GNSS data processing (i.e., difference between observations of a reference receiver and a rover receiver) using the SBS data as coming from the (virtual) reference receiver, and the rover receiver data. The technique therefore allows that a differential GNSS processor is used to compute positions anywhere without the explicit need of a nearby reference station.

20   [00287] The SBS module uses at least one of the following:

Phase-leveled clocks: These are the satellite clock offsets computed as described in Part 9 (Phase-Leveled Clock Processor).

Code-leveled clocks: These are the satellites clock offsets computed as described in Part 6 (Code-Leveled Clock Processor).

25   Melbourne-Wübbena bias: These are the satellite biases for the Melbourne-Wübbena phase and code combination computed as described in Part 7 (MW Bias Processor).

Jump messages: These messages can indicate whether or not the satellite phase clock had a change of level in the recent past (e.g. 10 minutes). The reasons for a level change are pointed out in Part 9 (Phase-Leveled Clock Processor). Whenever a jump (level change) occurs in the

30   satellite phase clock offset, some action has to be taken on the rover. This action might be the reset of the satellite's ambiguity/ambiguities in the RTK engine.

Approximate rover position: This is the position for which the virtual base data will be generated. The approximate position of the rover can be used for example so that geometric-dependent components (e.g. satellite position) are the same as for the rover data.

Time tag: This is the time (epoch) for which the virtual data is generated. The virtual data is created for certain instants of time (epochs) that depend on the rover observation time tags, so that it can be used in the differential data processing together with the rover data.

[00288] Given one or more items of the list above as input, the SBS module generates as output a set of GNSS virtual observations. These observations may comprise and are not restricted to: L1 code, L2 code, L1 phase, L2 phase, L1 cycle slip information, L2 cycle slip information, and/or exact virtual base position. Once the virtual reference station dataset is available it can be delivered to the RTK engine for differential processing with the rover's own GNSS observation data and optionally using the precise satellite data. The RTK engine can then apply conventional RTK processing to compute the rover coordinates.

Part 11.4 Moving Base

[00289] The best corrections for kinematic rovers are obtained when the SBS position and the synthesized reference station data for the SBS position are updated frequently, e.g., for every epoch of rover observations a new set of SBS data is generated. Some embodiments use as the SBS position a first estimate of the rover position, derived for example from a simple navigation solution using the rover observations.

[00290] In the case of prior-art Virtual Reference Station (VRS) processing, a moving rover can result in a significant separation between the rover position and the VRS location for which the VRS data is synthesized. Some implementations mitigate this by changing the VRS position when this distance exceeds a certain threshold. This can lead to resets of the RTK engine in most implementations.

[00291] For attitude determination (heading, blade control etc.), typical RTK processing engines are usually capable of processing data from a moving base station; frequent updating of the SBS position and the synthesized reference station data for the SBS position do not require modification of these rover processing engines.

Part 11.5 SBS Embodiments

[00292] FIG. 38 shows an embodiment 3800 of SBS processing in accordance with the invention. Rover receiver 3805 receives GNSS signals from multiple GNSS satellites, of which three are shown at 3810, 3815 and 3820. Receiver 3805 derives GNSS data 3825 from code observations and carrier-phase observations of the GNSS signal over multiple epochs.

[00293] Precise satellite data 3830 for the GNSS satellites are received, such as via a correction message 390 broadcast by a communications satellite 3835 or by other means, and decoded by a

message decoder 3832. A SBS module 3835 receives the precise satellite data 3830 and also receives information which it can use as a virtual base location, such as an approximate rover position with time tag 3842 generated by an optional navigation processor 3845. The approximate rover position is optionally obtained from other sources as described below.

[00294] SBS module 3835 uses the precise satellite data 3830 and the approximate rover position with time tag 3842 to synthesize base station data 3850 for the virtual base location. The base station data 3850 comprises, for example, synthesized observations of L1 code, L2 code, L1 carrier-phase and L2 carrier-phase, and optionally includes information on L1 cycle slip, L2 cycle slip, and the virtual base location. The SBSD module 3835 is triggered by an event or arrival of information which indicates that a new epoch of synthesized base station data is to be generated. In some embodiments the trigger is the availability of a rover observation epoch data set. In some embodiments the trigger is the current rover time tag, In some embodiments one epoch of synthesized base station data 3850 is generated for each epoch of GNSS data observations 3825. In some embodiments the trigger is the availability of an updated set of precise satellite data 3830.

[00295] In some embodiments a differential processor 3855, such as a typical RTK positioning engine of an integrated GNSS receiver system 3700, receives the precise satellite data 3830, the synthesized base station data 3850, and the GNSS data 3825 of rover receiver 3805, and uses these to determine a precise rover position 3860. Synthesized base station data 3850 is substituted for base station data in such processing.

[00296] FIG. 39 shows clock prediction between an observation time Obs 0 and a subsequent observation time OBs 1.

[00297] FIG. 40 is a schematic block diagram of the SBS module 3835.

[00298] The SBS module 3835 uses at least one of the following:

Phase-leveled clocks 370: These are the satellite clock offsets computed as described in Part 9: Phase Clock Processor.

Code-leveled clocks 365: These are the satellite clock offsets computed as described in Part 6: Standard Clock Processor;.

Melbourne-Wübbena biases 345: These are the satellite biases for the Melbourne-Wübbena phase and code combination computed as described in Part 8: Widelane Bias Processor;.

Jump messages (e.g., from correction message 390): Jump messages indicate when the satellite phase clock has had a change of level in the recent past (e.g. 10 minutes). The reasons for a level change are pointed out in Part 9: Phase Clock Processor. When a jump (level change)

in the satellite phase clock offset is indicated, action is taken at the rover such as reset of the satellite's ambiguity(ies) in the RTK engine.

Approximate rover position 3840: This is the position for which the virtual base data will be generated. The approximate position of the rover can be used so geometric-dependent components (e.g. satellite position) are the same as for the rover data.

Time tag 3842: This is the time for which the virtual data is to be generated. The synthesized base station data 3850 is created for certain instants of time that depend on the rover observation time tags, so that it can be used in the differential data processing together with the rover data.

[00299] Given one or more of these items as input the SBS module 3850 generates as output 3850 a set of GNSS virtual observations. These observations comprise and are not restricted to: L1 code, L2 code, L1 phase, L2 phase, L1 cycle slip information, L2 cycle slip information, and exact virtual base position. The virtual base station is delivered to the differential processor 3855 as is the rover's GNSS data 3825 and, optionally, the precise satellite data 3830. The differential processor 3855 computes the coordinates of the precise rover position 3860, e.g., using a conventional RTK receiver processing approach (see, for example, P. Misra et al., Global Positioning System: Signals, Measurements, and Performance, 2d Edition (2006), pp. 239-241, and US Patent 5,610,614 issued 11 March 1997 to Talbot *et al.*).

[00300] At any instant the SBS module 3835 may receive one or more of the following: approximate rover position 3840, precise satellite data 3830, and/or a time tag 3842. The approximate rover position 3840 is stored at 4005 as an updated current virtual base position. The precise satellite data 3840 is saved at 4010. The time tag 3842 is saved at 4015. Any of these items, or an optional external trigger 4020, can be used as a trigger event at decision point 4025 begin the generation of a new set of synthesized base station data 3850.

[00301] The satellite data for the current time tag is evaluated at 4030. This means that the satellite position and clock error that are stored are converted to the correct transmission time of the signal, so they can be consistently used with the rover observations. This is done because the stored satellite position and clock errors do not necessarily match the time tag of each requested epoch of the SBS module. The precise satellite data set for the current time tag 4035 is used at 4040 to synthesize a base station data set for the current time tag. At 4040, the satellite position and satellite velocity are computed for the current time tag. The geometric range between the virtual base station i and the satellite j is computed for example as:

$$\rho_i^j = \sqrt{\left(\left(X^j - X_i \right)^2 + \left(Y^j - Y_i \right)^2 + \left(Z^j - Z_i \right)^2 \right)} \qquad (82)$$

where X^j, Y^j, Z^j is the satellite position at the time of the current time tag, and

X_i, Y_i, Z_i is the virtual base station location at the time of the current time tag.

[00302] The neutral atmosphere (or, troposphere) delay T_i^j is computed for example using a prediction model. E For examples of prediction models see [Leandro 2009], [Leandro et al. 2006a], or [Leandro et al. 2006b].

[00303] The ionospheric delay I_i^j for L1 frequency is computed for example using an ionosphere model. This can be a prediction model, such as the GPS broadcast ionosphere model [ICD-GPS], or something more sophisticated. Optionally the ionospheric delay can be set to zero.

[00304] The uncorrected synthesized base station data set for the time of the time tag is then computed for example as:

$$\Phi_{i,1}^j{'} = \rho_i^j - c\Delta t_\Phi^j + T_i^j - I_i^j \tag{83}$$

$$\Phi_{i,2}^j{'} = \rho_i^j - c\Delta t_\Phi^j + T_i^j - \frac{f_1^2}{f_2^2} I_i^j \tag{84}$$

$$P_{i,1}^j{'} = \rho_i^j - c\Delta t_P^j + T_i^j + I_i^j + \frac{f_2}{f_1}\left(\lambda_{WL} \cdot b_{MW}^j - c\Delta t_\Phi^j + c\Delta t_P^j\right) \tag{85}$$

$$P_{i,2}^j{'} = \rho_i^j - c\Delta t_P^j + T_i^j + \frac{f_1^2}{f_2^2} I_i^j + \frac{f_1}{f_2}\left(\lambda_{WL} \cdot b_{MW}^j - c\Delta t_\Phi^j + c\Delta t_P^j\right) \tag{86}$$

where $\Phi_{i,1}^j{'}$ is the synthesized L1 carrier observation for the virtual base location,

$\Phi_{i,2}^j{'}$ is the synthesized L2 carrier observation for the virtual base location,

$P_{i,1}^j{'}$ is the synthesized L1 code observation for the virtual base location, and

$P_{i,2}^j{'}$ is the synthesized L2 code observation for the virtual base location.

[00305] The uncorrected synthesized base station data set 4045 is corrected at 4050 to create a synthesized base station data set 3850 for the current time tag. The corrections includes one or more of the effects described in Part 3: Observation Data Corrector, such as solid earth tides, phase wind-up, and antenna phase center variation. The corrected synthesized base station data set is:

$$\Phi_{i,1}^j = \Phi_{i,1}^j{'} - C_{i,1}^j \tag{87}$$

$$\Phi_{i,2}^j = \Phi_{i,2}^j{'} - C_{i,2}^j \tag{88}$$

$$P_{i,1}^j = P_{i,1}^j{}' - C_{i,1}^j \tag{89}$$

$$P_{i,2}^j = P_{i,2}^j{}' - C_{i,2}^j \tag{90}$$

The synthesized base station data set generation is then complete for the current time tag and is delivered to the differential processor 3855.

[00306] In some embodiments the differential processor 3855 uses the broadcast ephemeris to determine the satellite position and clock error, as in this mode of positioning only approximate quantities are needed for the satellite. This is also true when the differential processor is using SBS data, however in some embodiments the processor optionally uses the available precise satellite data.

[00307] FIG. 42 shows an alternate embodiment 4200 which is a variant of the processing 3800 of FIG. 38. In this embodiment the precise satellite data 3830 and rover observation data 3825 are sent to a PPP (Precise Point Positioning) engine 4210 rather or in addition to the differential processor 3855. The PPP engine 4210 delivers the rover coordinates in place of or in addition to those from the differential processor 3855.

[00308] FIG. 43 is a simplified view of the embodiment of FIG. 38. The synthesized GNSS data 3850 is created for a given location using precise satellite data 3830. The synthesized data 3850 is forwarded to the differential processor 3855 which, also using the rover GNSS data 3825, computes the rover position 3860.

[00309] FIG. 44 is a timing diagram of a low-latency version of the processing of FIG. 38, FIG. 42 or FIG. 44. In this variant, the arrival an epoch of rover observation data (e.g., 3825) or an epoch time tag (e.g., 3842) is used as a trigger for the generation of synthesized base station data (e.g., 3850). For example, a set of synthesized base station data (e.g., 3850) is generated for each epoch of rover observation data (e.g., 3825). The virtual base location (e.g., approximate rover position 3840) is updated from time to time as indicated by timing marks 4402 - 4408. Precise satellite data (e.g., precise satellite data 3830) is received from time to time as indicated by timing marks 4410 – 4424. Rover data (e.g., rover observations 3825) are received from time to time as indicated by timing marks 4426 – 4454. The arrivals of virtual base locations, the precise satellite data and the rover data are asynchronous. Each arrival of an epoch of rover data (indicated by a respective one of timing marks 4426 – 4454) results in the generation of a corresponding set of virtual base station data (indicated by a respective one of timing marks 4456 – 4484). In each case it is preferred to use the latest virtual base station location and the latest precise satellite data when processing an epoch of rover observation data with the corresponding virtual base station data. Each pairing of rover data and virtual base station data, e.g., of timing mark pair 4424 and

4456, results in the generation of a corresponding rover position, e.g, of timing mark 4485. Generated rover positions are indicated by timing marks 4485 – 4499.

[00310] In some embodiments a new SBS data epoch is created at each time a new rover data epoch is observed. FIG. 45 is a timing diagram of a high-accuracy version of the processing of

5   FIG. 38, FIG. 42 or FIG. 43. In this variant, the arrival of a set of precise satellite data (e.g., 3830) is used as a trigger for the generation of synthesized base station data (e.g., 3850). For example, a set of synthesized base station data (e.g., 3850) is generated for each set of precise satellite data (e.g., 3850). The virtual base location 3840 (e.g., approximate rover position) is updated from time to time as indicated by timing marks 4502 - 4508. Precise satellite data (e.g.,

10 precise satellite data 3830) are received from time to time as indicated by timing marks 4510 – 4524. Synthesized base station data (e.g., 3850) are generated for example from each new set of precise satellite data, as indicated by timing marks 4526 – 4540. Rover data (e.g., rover observations 3825) are received from time to time as indicated by timing marks 4542 – 4570. The arrivals of virtual base locations, the precise satellite data and the rover data are

15 asynchronous, but in this variant the synthesized base station data sets are synchronized (have the same time tags) as with precise satellite data sets, e.g., indicated by timing marks 4510 and 4526, 4512 and 4528, etc. Each new epoch of rover data is processed using the most recent synthesized base station data set. For example the rover data epochs arriving at timing marks 4544 and 4536 are processed using synthesized base station data prepared at timing mark 4526, etc.

20 [00311] In some embodiments a new SBS data epoch is created each time a new precise satellite data set is obtained. FIG. 46 shows a variant 4600 of the process of FIG. 38, FIG. 42 or FIG. 43 in which the virtual base location 4605 is taken from any of a variety of sources. Some embodiments take as the virtual base location 4605 (a) the autonomous position 4610 of the rover as determined for example by the rover's navigation engine 3845 using rover data 3825. Some

25 embodiments take as the virtual base station location 4605 (b) a previous precise rover position 4615 for example a precise rover position 4220 determined for a prior epoch by differential processor 3855 or by PPP engine 4210. Some embodiments take as the virtual base location 4605 (c) the autonomous position 4610 of the rover as determined for example by the SBS module 3835 using rover data 3825. Some embodiments take as the virtual base location 4605 (d) the

30 autonomous position 4610 of the rover as determined for example by the SBS module 3835 using rover data 3825 and precise satellite data 3830. Some embodiments take as the virtual base station location 4605 an approximate rover location obtained from one or more alternate position sources 4620, such as a rover position determined by an inertial navigation system (INS) 4625 collocated with the rover, the position of a mobile phone (cell) tower 4630 in proximity to a rover

collocated with a mobile telephone communicating with the tower, user input 4635 such as a location entered manually by a user for example with the aid of keyboard 3755 or other user input device, or any other desired source 4640 of a virtual base station location.

[00312] Regardless of the source, some embodiments update the virtual base station location 4605 or 3840 from time to time for use by SBS module 3835 as indicated by arrow 4645. The virtual base station location 4605 can be updated for example:

      (a) never,

      (b) for each epoch of rover data,

      (c) for each nth epoch of rover data,

      (d) after a predetermined time interval,

      (e) when the distance between the approximate rover antenna position (e.g., 3840) or autonomous rover antenna position (e.g., 4610) and the virtual base station location (e.g., 4605) exceeds a predetermined threshold,

      (f) when the distance between the approximate rover antenna position (e.g., 3840) or autonomous rover antenna position (e.g., 4610) and the precise rover antenna position (e.g., 4220) exceeds a predetermined threshold,

      (g) for each update of the approximate rover antenna position (e.g., 3840),

      (h) for each update of the precise rover antenna position (e.g., 4220).

[00313] For case (a), the first virtual base station location (e.g., 4605) that is provided to SBS module 3835 is used for the whole period during which the data processing is done. For case (b), the virtual base station location (e.g., 4605) is updated every time a new epoch of the rover data 3825 is collected, as this new epoch can be used to update the rover approximate position 3840 which can be used as the virtual base station location 4805. For cases (b) and (c) the virtual base station location 4605 is updated every time a certain number (e.g., 1 to 10) of epochs of rover data 3825 is collected. In case (d) the virtual base station location 4605 is updated at a certain time interval (e.g., every 10 seconds). Case (e) can be viewed as a mixture of cases (a) and (b), where the current virtual base station location 4605 is kept as long as the distance between the current virtual base station location and the approximate rover antenna position is less than a limiting distance (e.g., 100 m). Case (f) is similar to case (e), except that the distance between the virtual base station location and a recent precise rover position is used. For case (g) the virtual base station location is updated each time the approximate rover antenna position changes. For case (h) the virtual base station location is updated each time the precise rover antenna position changes.

[00314] In some embodiments the virtual base station location 3840 used for the generation of the SBS data comes from the autonomous position solution of the rover receiver, e.g., approximate rover position 3840. In some embodiments the virtual base station location 3840 is not the same position as the autonomous position solution, but somewhere close to it.

Some embodiments use as the virtual base station location 3840 a source such as: an autonomously determined position of the rover antenna, a previously determined one of said rover antenna positions, a synthesized base station data generating module (e.g., 3835), a precise rover position (e.g., 4220), a position determined by a PPP engine (e.g., 4210), a position determined by an inertial navigation system (e.g., 4625), a mobile telephone tower location (e.g., 4630), information provided by a user (e.g., 4635), or any other selected source (e.g., 4540).

[00315] In some embodiments the virtual base station location 3840 is not kept constant throughout the rover observation period but is updated if certain conditions are met such as: never, for each epoch of rover data, when the distance between an approximate rover antenna position and the virtual base station location exceeds a predetermined threshold, for each update of the rover antenna positions, and for a specific GNSS time interval. In some embodiments a change of the virtual base station location 3840 location is used to trigger the generation of a new SBS epoch of data.

[00316] In some embodiments the SBS data is used for any kind of between-station differential GNSS processor, no matter what type data modeling is involved, such as processors using: aided inertial navigation (INS), integrated INS and GNSS processing, normal real-time kinematic (RTK), Instant RTK (IRTK, e.g., using L1/L2 for fast on-the-fly ambiguity resolution), Differential GPS (DGPS) float-solution processing, and/or triple-differenced processing. In some embodiments the SBS data is used in post-processing of rover data. In some embodiments the SBS data is used in real time (i.e., as soon as the rover observation is available and a SBS record can be generated for it). In some embodiments the time tag of the rover matches the time tag of the SBS data within a few milliseconds.

Part 11. 5 SBS References

[00317] Some references relevant to rover processing include:

Leandro R.F., Santos, M.C. and Langley R.B., (2006a). "UNB Neutral Atmosphere Models: Development and Performance". Proceedings of ION NTM 2006, Monterey, California, January, 2006.

Leandro R.F., Santos, M.C. and Langley R.B., (2006b). "Wide Area Neutral Atmosphere Models for GNSS Applications". Proceedings of ION GNSS 2006, Fort Worth, Texas, September, 2006.

Leandro, R. F. (2009). Precise Point Positioning with GPS: A New Approach for Positioning, Atmospheric Studies, and Signal Analysis. Ph.D. dissertation, Department of Geodesy and Geomatics Engineering, Technical Report No. 267, University of New Brunswick, Fredericton, New Brunswick, Canada, 232 pp.

Part 12: Rover Processing with Ambiguity Fixing

Part 12.1 Ambiguity Fixing Introduction

[00318] The common high accuracy absolute positioning solution (also called Precise Point Positioning, or PPP) makes use of precise satellite orbit and clock error information. This solution also uses iono-free observations because there is no information available about the behavior of the ionosphere for the location of the rover receiver (few cm). High accuracy absolute positioning solutions in this scenario have always been based on float estimates of carrier-phase ambiguities, as it was not possible to maintain the integer nature of those parameters using un-differenced iono-free observations. Another issue concerning the integer nature of un-differenced ambiguities is the presence of non-integer phase biases in the measurements. These biases have to be also present in the correction data (e.g. clocks), otherwise the obtained ambiguities from the positioning filter will not be of integer nature.

[00319] Typical observation models used in prior-art processing are:

$$\phi = R + dT - dt + T + N_{if} \qquad (91)$$

$$P = R + dT - dt + T \qquad (92)$$

where

ϕ is the phase observation at the rover of a satellite signal (measured data),

P is the code observation at the rover of a satellite signal (measured data),

R is the range from satellite to rover at the transmission time of the observed signals,

dT is the receiver clock (also called herein a code-leveled receiver clock or receiver code clock or standard receiver clock),

dt is the satellite clock (also called herein a code-leveled satellite clock or satellite code clock or standard satellite clock),

T is the tropospheric delay of the satellite to rover signal path, and

N_{if} is the iono-free ambiguity.

[00320] Typical prior-art PPP processing uses the ionospheric-free phase ϕ and code P observations (measurements) of the signals of multiple satellites along with externally-provided

satellite clock information dt in an attempt to estimate values for the receiver position

(X^r, Y^r, and Z^r), receiver clock dT, tropospheric delay T and the iono-free float ambiguities

N_{if}^{Float}. The state vector of parameters to be estimated in a Kalman-filter implementation, for

each satellite j observed at the rover is thus:

5
$$\left\{ \begin{array}{l} X^r \\ Y^r \\ Z^r \\ dT \\ T \\ N_{if}^{j\ Float} \end{array} \right\} \tag{93}$$

[00321] Some embodiments of the invention provide for absolute positioning which takes into account the integer nature of the carrier-frequency ambiguities in real time processing at the rover. By real time processing is meant that the observation data is processed as soon as: (a) the data is collected; and (b) the necessary information (e.g. satellite corrections) are available for

10 doing so. Novel procedures use special satellite clock information so that carrier-phase (also called phase) ambiguity integrity is maintained in the ambiguity state values computed at the rover. The rover's processing engine handles the satellite clock error and a combination of satellite biases that are applied to the receiver observations.

[00322] Prior-art PPP engines are not able to use phase-leveled clocks, or at least are not able to

15 take advantage of the integer nature of these clocks. Some embodiments of the invention make use of this new information, e.g., in a modified position engine at the rover.

[00323] One goal of using phase-leveled satellite clocks and bias information is to obtain supposed integer ambiguities, which are used to obtain an enhanced position solution which takes advantage of the integer nature of the ambiguities. This improves the position solution (4710) as

20 compared with a position solution (4705) in which the ambiguities are considered to be float numbers, as shown in Figure 47.

[00324] The result of such prior-art PPP processing does not allow the integer nature iono-free ambiguities N_{if} to be reliably determined, but instead only enables estimation of iono-free float

ambiguities N_{if}^{Float}. The iono-free float ambiguities N_{if}^{Float} can be viewed as including

25 additional effects that can be interpreted as an error e such that:

$$N_{if}^{Float} = [\alpha N_{WL}^{Integer} + \beta N_1^{Integer}] + e \tag{94}$$

$$N_{if}^{Float} = N_{if}^{PL} + e \qquad\qquad (95)$$

where

N_{if}^{Float} is an iono-free float ambiguity representing a combination of an iono-free

         integer ambiguity $N_{if}^{Integer}$ and an error e

$N_{WL}^{Integer}$ is a Widelane integer ambiguity

α is an Widelane ambiguity coefficient

$N_1^{Integer}$ is an L1 integer ambiguity

β is an L1 ambiguity coefficient

N_{if}^{PL} is a phase-leveled iono-free ambiguity

[00325] In some particular cases it is possible to consider $N_{if}^{Float} \cong N_{if}^{integer}$ in a practical way.

Therefore there are cases where the formulation of the float ambiguity N_{if}^{Float} as a composition

of other two integer-nature ambiguity (as in $N_{if}^{Float} = [\alpha N_{WL}^{Integer} + \beta N_1^{Integer}] + e$) is not

necessary.

Part 12.2   Determining iono-free phase-leveled ambiguities N_{if}^{PL} : Option 1

[00326] Some embodiments of the invention are based on eliminating the un-wanted effects, or in
other words the iono-free float ambiguity error e to allow determination of iono-free phase-
leveled ambiguities N_{if}^{PL} . To eliminate the error e, the phase observation model is redefined:

$$\phi = R + dT_p - dt_p + T + N_{if}^{PL} \qquad\qquad (96)$$

where

     dT_p is a phase-leveled receiver clock (also called a receiver phase clock),

     dt_p is a phase-leveled satellite clock (also called a satellite phase clock), and

     N_{if}^{PL} is a phase-leveled iono-free ambiguity.

[00327] Satellite phase clock dt_p in (96) is phase-based and has integer nature and, in contrast to

Eq. (94), it can provide phase-leveled ambiguities free of error e, so that:

$$N_{if}^{PL} = [\alpha N_{WL}^{Integer} + \beta N_1^{Integer}] \qquad\qquad (97)$$

[00328] The phase-leveled iono-free ambiguity N_{if}^{PL} is not an integer but yet has an integer

nature; the phase-leveled iono-free ambiguity N_{if}^{PL} can be interpreted as a combination of two

integer ambiguities. One way of doing so is assuming that it is a combination of a widelane

integer ambiguity $N_{WL}^{Integer}$ and an L1 integer ambiguity $N_1^{Integer}$ in which the widelane

5   ambiguity coefficient α and the L1 ambiguity coefficient are not necessarily integers.

[00329] The phase-leveled clock dt_p can be quite different from a standard (code-leveled)

satellite clock dt . To avoid confusion, the term dt_p is used herein to denote the phase-leveled

satellite clock and the term dt_c is used herein to denote the standard (code-leveled) satellite

clock, i.e., $dt_c = dt$.

10   [00330] The introduction of the phase-leveled satellite clock term dt_p in (96) means that the

corresponding receiver clock term dT_p is also phase leveled. The term dT_p is used herein to

denote the phase-leveled receiver clock and the term dT_c is used to denote the standard (code-

leveled) receiver clock, i.e., $dT_c = dT$. In a positioning engine where phase and code

measurements are used simultaneously two clock states are therefore modelled for the receiver; in

15   this formulation these are the phase-leveled receiver clock dT_p and the standard (code-leveled)

receiver clock dT_c .

[00331] As mentioned above, typical prior-art PPP processing attempts to estimate values for four

parameters for each observed satellite: receiver coordinates X^r, Y^r, and Z^r, receiver clock dT ,

tropospheric delay T and the iono-free float ambiguities N_{if}^{Float} . The introduction of phase-

20   leveled clock terms adds one further parameter to be estimated in the rover engine: phase-leveled

receiver clock dT_p . The restated observation models are therefore as shown in equations (91)

and (92), respectively and reproduced here:

$$\phi = R + dT_p - dt_p + T + N_{if}^{PL} \qquad (98)$$

$$P = R + dT_c - dt_c + T \qquad (99)$$

25   [00332] In this formulation each observation type (phase ϕ or code P) is corrected with its own

clock type (phase-leveled satellite clock dt_p or code-leveled satellite clock dt_c). Some

embodiments of the invention therefore use the phase ϕ and code P observations

(measurements) of the signals of multiple satellites observed at a rover along with externally-provided code-leveled (standard) satellite clock information dt_c and phase-leveled satellite clock information dt_p to estimate values for range R, code-leveled receiver clock dT_c, phase-leveled receiver clock dT_p, tropospheric delay T and the iono-free phase-leveled ambiguities N_{if}^{PL}.

5   The state vector of parameters to be estimated in a Kalman-filter implementation, for each satellite j observed at the rover is thus:

$$\begin{Bmatrix} X^r \\ Y^r \\ Z^r \\ dT_c \\ dT_p \\ T \\ N_{if}^{j\,PL} \end{Bmatrix} \qquad . \qquad\qquad (100)$$

Part 12.3   Determining iono-free phase-leveled ambiguities N_{if}^{PL} : Option 2

10   [00333] A second formulation for handling the phase-leveled information is to substitute for the code-leveled receiver clock dT_c an offset δdT_p representing the difference between the code-leveled receiver clock dT_c and the phase-leveled receiver clock dT_p:

$$\delta dT_p = dT_c - dT_p \qquad\qquad (101)$$

so that equations (91) and (92) become, respectively:

15    $$\phi = R + dT_p - dt_p + T + N_{if}^{PL} \qquad\qquad (102)$$

$$P = R + dT_p + \delta dT_p - dt_c + T \qquad\qquad (103)$$

[00334] Accordingly, some embodiments of the invention use the phase ϕ and code P observations (measurements) of the signals of multiple satellites observed at a rover along with externally-provided code-leveled (standard) satellite clock information dt_c and phase-leveled

20   satellite clock information dt_p to estimate values for range R, phase-leveled receiver clock dT_p, receiver-clock offset δdT_p, tropospheric delay T and the iono-free phase-leveled ambiguities N_{if}^{PL}. The state vector of parameters to be estimated in a Kalman-filter implementation, for each satellite j observed at the rover is thus:

$$\begin{Bmatrix} X^r \\ Y^r \\ Z^r \\ dT_p \\ \delta dT_p \\ T \\ N_{if}^{j\,PL} \end{Bmatrix} \qquad\qquad (104)$$

[00335] This second formulation still has five types of parameters to be estimated, but because δdT_p is an offset there is less process noise in the Kalman filter than for state vector (100). The advantage of such model as compared to option 1 is that the stochastic model can be setup differently, meaning that the noise level assigned to a clock bias state (e.g. δdT_p) can be different from a clock state (e.g. dT_c). Assuming that phase- and code-leveled clocks behave in a similar way, the noise level needed for modelling a bias state should be less than for modelling a clock state.

Part 12.4   Determining iono-free phase-leveled ambiguities N_{if}^{PL} : Option 3

[00336] A third formulation for handling the phase-leveled information is to substitute for the phase-leveled receiver clock dT_p an offset $-\delta dT_p$ representing the difference between the phase-leveled receiver clock dT_p and the code-leveled receiver clock dT_c:

$$- \delta dT_p = dT_p - dT_c \qquad\qquad (105)$$

so that equations (91) and (92) become, respectively:

$$\phi = R - dT_p + dT_c - dt_p + T + N_{if}^{PL} \qquad\qquad (106)$$

$$P = R + dT_c + \delta dT_c - dt_c + T \qquad\qquad (107)$$

[00337] Accordingly, some embodiments of the invention use the phase ϕ and code P observations (measurements) of the signals of multiple satellites observed at a rover along with externally-provided code-leveled (standard) satellite clock information dt_c and phase-leveled satellite clock information dt_p to estimate values for range R, code-leveled receiver clock dT_c, receiver-clock offset $-\delta dT_p$, tropospheric delay T and the iono-free phase-leveled ambiguities

N_{if}^{PL} . The state vector of parameters to be estimated in a Kalman-filter implementation, for

each satellite j observed at the rover is thus:

$$\begin{Bmatrix} X^r \\ Y^r \\ Z^r \\ dT_c \\ -\delta dT_p \\ T \\ N_{if}^{j~PL} \end{Bmatrix} \tag{108}$$

This third formulation still has five types of parameters to be estimated, but because $-\delta dT_p$ is an

5   offset there is less process noise in the Kalman filter than for state vector (100).

Part 12.5   Determining iono-free phase-leveled ambiguities N_{if}^{PL} : Option 4

[00338] A fourth formulation for handling the phase-leveled information first estimates the iono-

free float ambiguities $N_{if}^{j~Float}$ using code-leveled (standard) satellite clocks dt_c for phase

10   observations ϕ and for code observations P as in (95), and shifts the iono-free float ambiguities

$N_{if}^{j~Float}$ afterward using the phase-leveled clock information to obtain the iono-free phase-

leveled ambiguities N_{if}^{PL} .

[00339] The starting point for this formulation is:

$$\phi = R + dT_c - dt_c + T + N_{if}^{Float} \tag{109}$$

15      $$P = R + dT_c - dt_c + T \tag{110}$$

Note that (109) and (110) are identical to (91) and (92), since $dT_c = dT$ and $dt_c = dt$.

[00340] This fourth formulation, as in the typical prior-art PPP processing discussed above, uses

the phase ϕ and code P observations (measurements) of the signals of multiple satellites

observed at a rover along with externally-provided code-leveled (standard) satellite clock

20   information dt_c to estimate values for range R , code-leveled receiver clock dT_c , tropospheric

delay T and the iono-free float ambiguities N_{if}^{Float} . The state vector of parameters to be

estimated in a Kalman-filter implementation, for each satellite j observed at the rover is thus:

$$\begin{Bmatrix} X^r \\ Y^r \\ Z^r \\ dT_c \\ T \\ N_{if}^{j\ Float} \end{Bmatrix} \qquad (111)$$

[00341] As with the prior-art PPP processing, the estimation of parameter values of state vector (111) does not allow the iono-free float ambiguities $N_{if}^{j\ Float}$ to be reliably determined as iono-free phase-leveled ambiguities N_{if}^{PL} :

$$N_{if}^{Float} = N_{if}^{PL} + e = [\alpha N_{WL}^{Integer} + \beta N_1^{Integer}] + e \qquad (112)$$

where

N_{if}^{Float} is an iono-free float ambiguity representing a combination of a iono-free phase-leveled ambiguity N_{if}^{PL} and an error e,

$N_{WL}^{Integer}$ is a Widelane integer ambiguity,

α is a Widelane ambiguity coefficient,

$N_1^{Integer}$ is an L1 integer ambiguity, and

β is an L1 ambiguity coefficient.

[00342] This fourth formulation assumes that error e represents the difference between the code-leveled (standard) satellite clock dt_c and the phase-leveled satellite clock dt_p :

$$e = dt_c - dt_p \qquad (113)$$

so that

$$N_{if}^{PL} = N_{if}^{Float} - (dt_c - dt_p) \qquad (114)$$

$$N_{if}^{PL} = [\alpha N_{WL}^{Integer} + \beta N_1^{Integer}] + e - e \qquad (115)$$

$$N_{if}^{PL} = [\alpha N_{WL}^{Integer} + \beta N_1^{Integer}] \qquad (116)$$

[00343] To summarize, this fourth formulation obtains iono-free float ambiguities N_{if}^{Float} from (109) and then shifts each of these by the difference between the standard (code-leveled) satellite

clock dt_c^j and the phase-leveled clock dt_p^j for the respective satellite j to obtain the iono-free

phase-leveled ambiguities N_{if}^{PL} as shown in (114).

[00344] For this purpose, the rover can be provided with (1) the standard (code-leveled) satellite

clock dt_c^j and the phase-leveled clock dt_p^j for each satellite j observed at the rover, or (2) the

5   standard (code-leveled) satellite clock dt_c^j and a clock bias δt_c representing the difference

between the standard (code-leveled) satellite clock dt_c^j and the phase-leveled clock dt_p^j, or (3)

the phase-leveled clock dt_p^j and a clock bias δt_p representing the difference between the phase-

leveled clock dt_p^j and the standard (code-leveled) satellite clock dt_c^j. These are equivalent for

processing purposes as can be seen from (114).

10   [00345] This fourth formulation has advantages and disadvantages. A disadvantage is that it

assumes the behavior of the standard (code-leveled) satellite clock dt_c^j and the phase-leveled

clock dt_p^j for each satellite j observed at the rover is substantially the same over the period of

time for the ambiguity was computed. An advantage is that jumps (integer cycle slips) which

might occur in the phase clock estimations can be more easily handled in processing at the rover.

15

Part 12.6   Determining position using Melbourne-Wübbena biases b_{WL}^j :

[00346] After the iono-free phase-leveled ambiguities N_{if}^{jPL} are determined for a given epoch,

they can be single-differenced as $\nabla^{ab} N_{if}^{PL}$, single-differenced integer (fixed) widelane

ambiguities $\nabla^{ab} N_{WL}^{Integer}$ can be removed from them to obtain single-differenced L1 float

20   ambiguities $\nabla^{ab} N_1^{Float}$, and the single-differenced L1 float ambiguities $\nabla^{ab} N_1^{Float}$ can be fixed

as single-differenced L1 integer ambiguities $\nabla^{ab} N_1^{Integer}$.

[00347] Single-differenced widelane integer ambiguities $\nabla^{ab} N_{WL}^{Integer}$ are estimated in a

widelane-ambiguity filter which runs in parallel with the geometry filter of the rover's processing

engine. The rover receiver is provided with a Melbourne-Wübbena bias b_{MW}^j for each of the j

25   satellites in view, e.g., from an external source of data corrections - see Part 7 (MW Bias

Processor). Melbourne-Wübbena bias b_{MW}^j can be computed as:

$$\frac{\phi_{WL}^{j} - P_{NL}^{j}}{\lambda_{WL}} = N_{WL}^{j \ Integer} + b_{MW}^{j} - b_{MW}^{R} \tag{117}$$

where

ϕ_{WL}^{j} is the widelane carrier-phase combination of rover observations of satellite j

P_{NL}^{j} is the narrowlane code combination of rover observations of satellite j

5   λ_{WL} is the widelane wavelength

$N_{WL}^{j \ Integer}$ is the widelane integer ambiguity for satellite j

b_{MW}^{R} is the Melbourne-Wübbena bias for the rover R.

[00348] The widelane ambiguity filter eliminates the rover's Melbourne-Wübbena bias b_{WL}^{R} by

differencing (115) for each pairing of satellites "a" and "b" to obtain the single-differenced

10   widelane integer ambiguities $\nabla^{ab} N_{WL}^{\cdot \ Integer}$:

$$\nabla^{ab} N_{WL}^{Integer} = \nabla^{ab} \left(\overline{\frac{\phi_{WL} - P_{NL}}{\lambda_{WL}}} \right) - \nabla^{ab} b_{MW} \tag{118}$$

where

$$\nabla^{ab} b_{MW} = b_{MW}^{a} - b_{MW}^{b} \tag{119}$$

[00349] Once the single-differenced widelane integer ambiguities $\nabla^{ab} N_{WL}^{Integer}$ are known, they

15   are removed from the single-differenced iono-free phase-leveled ambiguities $\nabla^{ab} N_{if}^{PL}$ to obtain

the single-differenced L1 float ambiguities $\nabla^{ab} N_{1}^{Float}$.

[00350] The float Kalman filter used to estimate the iono-free phase-leveled ambiguities

N_{if}^{PL} (or the iono-free float ambiguities $N_{if}^{j \ Float}$ in the third alternate formulation discussed

above) also gives $C_{N_{if}}$, the covariance matrix of the iono-free phase-leveled ambiguities N_{if}^{PL} .

20   Because the widelane ambiguities are integer (fixed) values after their values are found, $C_{N_{if}}$ is

the same for N_{if}^{PL} as for $N_{if}^{j \ Float}$.

[00351] From (95) it is known that:

$$\nabla N_{if}^{ab \ PL} = \alpha \nabla N_{WL}^{ab \ Integer} + \beta \nabla N_{1}^{ab \ Float} \tag{120}$$

where

$\nabla N_{if}^{ab\,PL}$ is the single-difference phase-leveled iono-free ambiguity (differenced

between satellites "a" and "b")

$\nabla N_{WL}^{ab\,Integer}$ is the single-difference widelane integer ambiguity (differenced between

satellites "a" and "b')

$\nabla N_1^{ab\,Float}$ is the single-difference L1 float ambiguity (differenced between satellites

"a" and "b")

[00352] Therefore

$$\nabla N_1^{ab\,Float} = \frac{\nabla N_{if}^{ab\,PL} - \alpha \nabla N_{WL}^{ab\,Integer}}{\beta} \tag{121}$$

[00353] Because $\nabla N_{WL}^{ab\,Integer}$ are fixed (integer) values, it is assumed that the respective

covariance matrices of the L1 float ambiguities $N_1^{ab\,Float}$ and the iono-free phase-leveled

ambiguities $N_{if}^{j\,PL}$ are related by:

$$C_{N_1^{Float}} = C_{Nif^{PL}} \cdot F^2 \tag{122}$$

where

$C_{N_1^{Float}}$ is the covariance matrix of the L1 float ambiguities $N_1^{j\,Float}$

$C_{Nif^{PL}}$ is the covariance matrix of the iono-free phase-leveled ambiguities $N_{if}^{j\,PL}$

F is a factor to convert the units of the variances from iono-free cycles to L1 cycles.

[00354] The desired "fixed" (integer-nature) single-differenced L1 float ambiguities

$\nabla N_1^{ab\,Integer}$ can be determined from the single-differenced L1 float ambiguities $\nabla N_1^{ab\,Float}$ and the

covariance matrix $C_{N_1^{Float}}$ of the L1 float ambiguities $N_1^{ab\,Float}$ using well-known techniques,

such as Lambda (Jonge et al. 1994), modified Lambda (Chan et al. 2005), weighted averaging of

candidate sets, or others.

[00355] Having determined the single-differenced integer widelane ambiguities $\nabla N_{WL}^{ab\,Integer}$ and

the single-differenced integer L1 ambiguities, integer-nature iono-free ambiguities $\nabla N_{if}^{ab\,Integer}$ are

determined from:

$$\nabla N_{if}^{ab\,Integer} = \alpha \nabla N_{WL}^{ab\,Integer} + \beta \nabla N_1^{ab\,Integer} \tag{123}$$

[00356] The integer-nature iono-free ambiguities $\nabla N_{if}^{ab\,Integer}$ are introduced ("pushed") as a

pseudo-observation into the Kalman float filter (or optionally a copy of it) to determine a rover

position based on integer-nature ambiguities. The state vector of the float filter copy is thus:

$$\left\{ \begin{array}{c} X^r \\ Y^r \\ Z^r \\ dT_c \\ T \end{array} \right\} \qquad\qquad (124)$$

5   [00357] The rover position can then be determined with an accuracy (and precision) substantially

better than for the typical prior-art PPP processing in which the ambiguities are considered to be

float numbers, as shown in FIG. 47.

[00358] FIG. 48 shows a block diagram of a positioning scheme 4800 using ambiguity fixing in

accordance with some embodiments of the invention. In this example, after satellite clock (clock

10   and orbit) corrections 4802 and MW bias corrections 4804 are received, e.g., via a link such as

communications satellite 4806, they are used along with GNSS data 4808 collected by the rover

receiver 4810, e.g., from observations of GNSS satellites 4812, 4814, 4816. Processing is

performed in two filters: a first filter 4818 with a geometric, ionospheric-free model (Part 12.5,

Equations 107-108), and a second filter 4820 with a geometry- and ionospheric-free model (Part

15   12.6, Equation 116). From the first filter 4818 phase-levelled ionospheric-free ambiguities 4822

with corresponding covariance matrix 4824 are obtained. From the second filter 4820 integer

wide-lane ambiguities 4826 are obtained. At 4828, single-differenced integer-nature float

ambiguities 4830 are determined from the phase-leveled ionospheric-free ambiguities 4822 and

the wide-lane ambiguities 4826. The single-differenced integer-nature float ambiguities 4830 are

20   re-processed at 4832 using an integer-least-squares-based approach (to "fix" them as that term is

defined herein to mean fixing as integers or forming weighted averages) to obtain single-

differenced, integer-nature L1 ambiguities 4834. These ambiguities 4834 are then re-combined at

4836 with the integer nature wide-lane ambiguities 4826 to yield single-differenced integer-

nature ionospheric-free ambiguities 4840. These ambiguities 4840 are then applied in a third filter

25   4842 which estimates rover receiver clock 4844, and satellite-rover ranges 4846 from which the

receiver position is determined.

[00359] FIG. 49 shows a block diagram of a positioning scheme 4900 using ambiguity fixing in

accordance with some embodiments of the invention. In this example, satellite clock corrections

4902 received, e.g., via a link such as communications satellite 4904, are used along with GNSS

data 4906 collected by the rover receiver 4908, e.g., from observations of GNSS satellites 4910, 4912, 4814, in a first filter 4916. Filter 4916 estimates float values for carrier ambiguities 4918 with corresponding covariances 4920. At 4922, integer-nature carrier-phase ambiguities 4924 are determined using float ambiguities 4918 and the respective covariance matrix 4920 provided by

5   first filter 4916. The integer-nature carrier-phase ambiguities 4924 and satellite clock corrections 4902 and GNSS data 4906 are used in a second filter 4926 to determine the receiver position 4928.

[00360] FIG. 50 shows a block diagram of a positioning scheme 5000 using ambiguity fixing in accordance with some embodiments of the invention. In this example, satellite clock corrections

10 5002 received, e.g., via a link such as communications satellite 5004, are used along with GNSS data 5006 collected by the rover receiver 5008, e.g., from observations of GNSS satellites 5010, 5012, 5014, in a first filter 5016. Filter 5016 estimates values for carrier ambiguities 5018 with corresponding covariances 5020. At 5022, integer-nature single-differenced carrier-phase ambiguities 5024 are determined using float ambiguities 5018 and the respective covariance

15 matrix 5020 provided by first filter 5016. The integer-nature single-differenced carrier-phase ambiguities 5024 and satellite clock corrections 5002 and GNSS data 5006 are used in a second filter 5026 to determine the receiver position 5028.

[00361] FIG. 51 shows a block diagram of a positioning scheme 5100 using ambiguity fixing in accordance with some embodiments of the invention. In this example, satellite clock corrections

20 5102 and satellite MW biases 5104 received, e.g., via a link such as communications satellite 5106, are used along with GNSS data 5108 collected by the rover receiver 5110, e.g., from observations of GNSS satellites 5112, 5114, 5116 in a first filter 5118. Filter 5118 estimates values for carrier-phase ionospheric-free float ambiguities 5120 with corresponding covariances 5122. A third filter 5124 uses the satellite MW bias corrections 5104 and the GNSS data 5108 to

25 determine wide-lane carrier ambiguities 5126. At 5128, integer-nature carrier-phase ambiguities 5130 are determined using the float iono-free ambiguities 5120 and the respective covariance matrix 5122 provided by first filter 5118 and the wide-lane carrier ambiguities 5126 provided by third filter 5124. A second filter 5132 uses the integer-nature carrier-phase ambiguities 5130 with the GNSS data 5108 and the satellite clock corrections 5102 to determine receiver position 5134.

30 [00362] FIG. 52 shows a block diagram of a positioning scheme 5200 using ambiguity fixing in accordance with some embodiments of the invention. In this variant of the example of FIG. 51, satellite clock corrections 5202 and satellite MW biases 5204 are received, e.g., via a link such as communications satellite 5206. Satellite clock corrections 5202 are used along with GNSS data 5208 collected by the rover receiver 5210, e.g., from observations of GNSS satellites 5212, 5214,

5216 in a first filter 5218. First filter 5218 estimates values for float ambiguities 5220 with corresponding covariances 5222. A third filter 5224 uses the satellite MW bias corrections 5204 and the GNSS data 5208 to determine wide-lane carrier ambiguities 5228. At 5228, integer-nature ambiguities 5230 are determined from the carrier ambiguities 5220, the carrier ambiguities covariances 5222 and the widelane carrier ambiguities 5226, using a covariance matrix which is scaled with a certain factor (see, e.g., Equation 120). A second filter 5232 uses the integer-nature carrier-phase ambiguities 5230 with the GNSS data 5208 and the satellite clock corrections 5202 to determine receiver position 5234.

[00363] FIG. 53 shows a block diagram of a positioning scheme 5300 using ambiguity fixing in accordance with some embodiments of the invention. In this variant of the examples of FIG. 51 and FIG. 52, satellite clock corrections 5302 and satellite MW biases 5304 are received, e.g., via a link such as communications satellite 5306. Satellite clock corrections 5302 are used along with GNSS data 5308 collected by the rover receiver 5310, e.g., from observations of GNSS satellites 5312, 5314, 5316 in a first filter 5318. First filter 5318 estimates values for float ambiguities 5320 with corresponding covariances 5322. A third filter 5324 uses the satellite MW bias corrections 5304 and the GNSS data 5308 to determine single-differenced-between-satellites wide-lane carrier ambiguities 5326. At 5328, single-differenced-between-satellites integer-nature carrier-phase ambiguities 5330 are determined from the carrier-phase ambiguities 5320, the carrier ambiguities covariances 5322 and the widelane carrier ambiguities 5326, using a covariance matrix which is scaled with a certain factor (see, e.g., Equation 120). A second filter 5232 uses the integer-nature carrier-phase ambiguities 5330 with the GNSS data 5308 and the satellite clock corrections 5302 to determine receiver position 5334.

[00364] FIG. 54 shows a block diagram of a positioning scheme 5400 using ambiguity fixing in accordance with some embodiments of the invention. In this variant, satellite clock corrections 5402 and satellite MW biases 5404 are received, e.g., via a link such as communications satellite 5406. Satellite clock corrections 5402 are used along with GNSS data 5408 collected by the rover receiver 5410, e.g., from observations of GNSS satellites 5412, 5414, 5416 in a first filter 5418. First filter 5418 estimates values for float ambiguities 5420 with corresponding covariances 5422. A third filter 5424 uses the satellite MW bias corrections 5404 and the GNSS data 5408 to determine wide-lane carrier ambiguities 5426. At 5428, integer-nature iono-free ambiguities 5430 of two carrier frequencies (e.g., L1 and L2) are determined from the carrier ambiguities 5420, the carrier ambiguities covariances 5422 and the widelane carrier ambiguities 5426, using a covariance matrix which is scaled with a certain factor (see, e.g., Equation 120). A second filter 5432 uses the integer-nature carrier-phase ambiguities 5430 with the GNSS data

5408 and the satellite clock corrections 5402 to determine receiver position 5434. The integer-nature carrier ambiguities 5430 can be sets of L1 and L2 ambiguities, or sets of L2 and L5 ambiguities, or sets of any linear combination of two or more GNSS frequencies.

[00365] FIG. 55 shows a block diagram of a positioning scheme 5500 using ambiguity fixing in

5   accordance with some embodiments of the invention. In this variant, satellite clock corrections 5502 and ionospheric delay information 5504 and satellite MW biases 5506 are received, e.g., via a link such as communications satellite 5508. Satellite clock corrections 5502 and ionospheric delay information 5504 are used along with GNSS data 5510 collected by the rover receiver 5512, e.g., from observations of GNSS satellites 5514, 5516, 5518 in a first filter 5520. First

10   filter 5520 estimates values for float ambiguities 5522 with corresponding covariances 5524. A third filter 5526 uses the satellite MW bias corrections 5506 and the GNSS data 5510 to determine wide-lane carrier ambiguities 5528. At 5530, integer-nature L1 ambiguities 5532 are determined from the carrier ambiguities 5522, the carrier ambiguities covariances 5524 and the widelane carrier ambiguities 5528, using a covariance matrix which is scaled with a certain factor

15   (see, e.g., Equation 120). A second filter 5534 uses the integer-nature L1 carrier-phase ambiguities 5532 with the GNSS data 5510 and the satellite clock corrections 5502 and ionospheric delay information 5504 to determine receiver position 5536. In further variants of FIG. 55 the ionospheric delay information 5504 is used to feed one or more filters used in the data processing, and/or the determined integer-nature ambiguities 5532 used for determining the

20   receiver position 5536 can be sets of L1 ambiguities or L2 ambiguities or L5 ambiguities, or sets of ambiguities of any GNSS frequency.

[00366] FIG. 56 is the same as FIG. 54, in which the second filter 5632 is an independent filter from the first filter 5418 and third filter 5424.

[00367] FIG. 57 shows a variation 5700 of the embodiment of FIG. 56 in which the second filter

25   5732 is a copy of the first filter 5418.

[00368] FIG. 58 shows a variation 5800 of the embodiments of FIG. 56 and FIG. 57, in which the second filter 5632 of FIG. 56 and 5732 of FIG. 57 is replaced by the first filter 5418. This means that when the integer-nature ionospheric-free ambiguities 5430 are determined, they are fed back to the first filter 5418 which is then used to determine the receiver position 5434.

30   [00369] FIG. 59 is a detailed view of an embodiment of the first filter 5418, showing that the satellite clock corrections 5402 include code-leveled satellite clock corrections 5906 and phase-leveled satellite clock corrections 5908. The code-leveled satellite clock corrections 5906 are used at 5914 for modeling GNSS observations in an observation filter 5912. The resulting code-leveled float carrier ambiguities 5918 are adapted at 5920 to the level of the phase-leveled

satellite clocks 5908 by applying the difference between the code-leveled satellite clock 5906 and the phase-leveled satellite clock 5908 to obtain phase-leveled carrier ambiguities 5420. Observation filter 5912 also provides covariances 5422 of the carrier ambiguities.

[00370]   FIG. 60 is a detailed view of an embodiment of the first filter 5418 in which the code-

5   leveled satellite clock corrections 5906 are used in an observation filter 6012 for modeling code observations at 6014. The phase-leveled satellite clock 5908 is used at 6016 for modeling carrier-phase observations. The resulting ambiguities from the observation filter 6012 are the phase-leveled carrier ambiguities 5420. The observation filter 6012 also provides covariances 5422 of the carrier ambiguities.

10   [00371]   FIG. 61 shows a variant of previous FIGS. in which the integer-nature ambiguities are determined at 6128 using at least one of: rounding the float ambiguity to the nearest integer, choosing best integer candidates from a set of integer candidates generated using integer least squares, and computing float values using a set of integer candidates generated using integer least squares.

15   [00372]   FIG. 62 shows a variant of previous FIGS. in which at least one of the first filter 5418 and the second filter 5432 further estimates values 6202, 6252, respectively including at least one of values for: receiver phase-leveled clock states 6204, 6254, receiver code-leveled clock states 6606, 6256, tropospheric delay states 6208, 6258, receiver clock bias states 6210, 6260 representing a difference per satellite between code-leveled receiver clock and phase-leveled

20   receiver clock, and multipath states 6212, 6262.

Part 12.7   Ambiguity Fixing References

[00373]   Some references relevant to ambiguity fixing include:

Jonge de, P.J., and C.C.J.M. Tiberius (1994). A new GPS ambiguity estimation method

25   based on integer least squares. *Proceedings of the 3rd International Symposium on Differential Satellite Navigation Systems DSNS'94,* London, UK, April 18-22, Paper No. 73, 9 pp.

X.-W. Chang, X. Yang and T. Zhou (2005). MLAMBDA: a modified LAMBDA method for integer least-squares estimation. Journal of Geodesy, Springer Berlin / Heidelberg.

30   Volume 79, Number 9 / December, 2005, pp.552-565.

Part 13: Summary of Some of the Inventive Concepts

Section 13A: MW (Melbourne-Wübbena) Bias Processing (A-2565)

1.   [MW Processing] A method of processing a set of GNSS signal data derived from code
5   observations and carrier-phase observations at multiple receivers of GNSS signals of
     multiple satellites over multiple epochs, the GNSS signals having at least two carrier
     frequencies, comprising:

     a.   forming an MW (Melbourne-Wübbena) combination per receiver-satellite
     pairing at each epoch to obtain a MW data set per epoch, and

10   b.   estimating from the MW data set per epoch an MW bias per satellite which may
     vary from epoch to epoch, and a set of WL (widelane) ambiguities, each WL ambiguity
     corresponding to one of a receiver-satellite link and a satellite-receiver-satellite link,
     wherein the MW bias per satellite is modeled as one of (i) a single estimation parameter
     and (ii) an estimated offset plus harmonic variations with estimated amplitudes.

15   2.   The method of 1, further comprising applying corrections to the GNSS signal data.

     3.   The method of one of 1-2, further comprising smoothing at least one linear combination
     of GNSS signal data before estimating an MW bias per satellite.

     4.   The method of one of 1-3, further comprising applying at least one MW bias constraint.

     5.   The method of one of 1-4, further comprising applying at least one integer WL ambiguity
20   constraint

     6.   The method of one of 1-4, further comprising using a spanning tree (ST) over one of an
     observation graph and a filter graph for constraining the WL ambiguities.

     7.   The method of one of 1-4, further comprising using a minimum spanning tree (MST) on
     one of an observation graph and a filter graph for constraining the WL ambiguities.

25   8.   The method of 7, wherein the minimum spanning tree is based on edge weights, each
     edge weight derived from receiver-satellite geometry.

     9.   The method of 8, wherein the edge weight is defined with respect to one of (i) a
     geometric distance from receiver to satellite, (ii) a satellite elevation angle, and (iii) a
     geometric distance from satellite to receiver to satellite, and (iv) a combination of the
30   elevations under which the two satellites in a single differenced combination are seen at a
     station.

     10. The method of 7, wherein the minimum spanning tree is based on edge weights, with
     each edge weight based on WL ambiguity information, defined with respect to one of (i)

difference of a WL ambiguity to integer, (ii) WL ambiguity variance, and (iii) a combination of (i) and (ii).

11.   The method of one of 1-10, further comprising fixing at least one of the WL ambiguities as an integer value.

12.   The method of one of 1-10, further comprising determining candidate sets of WL integer ambiguity values, forming a weighted combination of the candidate sets, and fixing at least one of the WL ambiguities as a value taken from the weighted combination.

13.   The method of one of 11-12, wherein the estimating step comprises introducing fixed WL ambiguities so as to estimate MW biases which are compatible with fixed WL ambiguities.

14.   The method of 13, wherein the estimating step comprises applying an iterative filter to the MW data per epoch and wherein introducing fixed WL ambiguities comprises one of (i) putting the fixed WL ambiguities as observations into the filter, (ii) putting the fixed WL ambiguities as observations into a copy of the filter generated after each of a plurality of observation updates, and (iii) reducing the MW combinations by the fixed WL ambiguities and putting the resulting reduced MW combinations into a second filter without ambiguity states to estimate at least one MW bias per satellite.

15.   The method of one of 1-14, further comprising shifting at least one MW bias by an integer number of WL cycles.

16.   The method of one of 1-14, further comprising shifting at least one MW bias and its respective WL ambiguity by an integer number of WL cycles.

17.   The method of one of 1-16, wherein the navigation message comprises orbit information,

18.   Apparatus adapted to perform the method of one of 1 – 17.

19.   A computer program comprising instructions configured, when executed on a computer processing unit, to carry out a method according to one of 1 - 17.

20.   A computer-readable medium comprising a computer program according to 19.

Section 13B: Orbit Processing (A-2647)

1.   A method of processing a set of GNSS signal data derived from signals of GNSS satellites observed at reference station receivers, the data representing code observations and carrier observations on each of at least two carriers over multiple epochs, comprising:

a.   obtaining an orbit start vector (2635) comprising: a time sequence of predicted positions and predicted velocities for each satellite over a first interval and the partial

derivatives of the predicted positions and predicted velocities with respect to initial

positions, initial velocities, force model parameters and Earth orientation parameters,

b.   obtaining ionospheric-free linear combinations (2645) of the code observations

and the carrier observations for each satellite at multiple reference stations, and

5   c.   iteratively correcting the orbit start vector (2635) using at each epoch the

ionospheric-free linear combinations (2645) and predicted Earth orientation parameters

(2610), as soon as the ionospheric-free linear combinations of the epoch are available, to

obtain updated orbit start vector values (2680) comprising a time sequence of predicted

positions and predicted velocities for each satellite over a subsequent interval of epochs

10   and an estimate of Earth orientation parameters.

2.   [Startup] The method of 1, wherein obtaining an orbit start vector (2635) comprises:

        i.   obtaining an approximate orbit vector (2615) for the satellites,

        ii.   obtaining predicted Earth orbit parameters (2610),

        iii.   iteratively integrating the approximate orbit vector with the predicted Earth orbit

15   parameters to obtain an orbit prediction (2620) for an initial time interval and, with each

iteration, adapting the orbit prediction (2620) to the approximate orbit vector, and

        iv.   preparing from the orbit prediction (2620) an initial set of values for the orbit

start vector and partial derivatives (2635).

3.   The method of 2, wherein the approximate orbit vector (2615) is obtained from one of: a

20   broadcast satellite navigation message, IGS Ultra-rapid Orbits data, and another source of

predicted orbits.

4.   The method of one of 2 – 3, wherein adapting the orbit prediction (2620) to the

approximate orbit vector (2615) is performed using a least squares approach.

5.   The method of one of 2 – 4, wherein integrating the approximate orbit vector (2615) with

25   the predicted Earth orientation parameters (2610) to obtain an orbit prediction (2620) is

iterated until the orbit prediction remains substantially constant.

6.   The method of 1, wherein obtaining an orbit start vector (2635) comprises preparing the

orbit start vector (2635) from a set of the updated orbit start vector values (2680) which is

not older than a predetermined time interval.

30   7.   The method of 6, wherein the predetermined time interval is not more than a few hours.

8.   [Operation] The method of one of 6 - 7, wherein preparing the orbit start vector (2635)

comprises: mapping a new orbit start vector (2690) from the updated orbit start vector

(2680) and integrating the new orbit start vector (2690) to obtain new values for the orbit

start vector (2635).

9.   The method of 8, wherein integrating the new orbit start vector (2690) comprises integrating the new orbit start vector using Earth orientation parameters from the updated start vector values (2680).

10.   [Kalman] The method of one of 1 - 9, wherein correcting comprises applying an iterative filter comprising one of: a Kalman filter, a UD factorized filter, and a Square Root Information Filter.

11.   [Satellite parameters] The method of one of 1 - 10, wherein the updated orbit start vector (2680) further comprises additional parameters for each satellite, and wherein iteratively correcting the orbit start vector comprises correcting the additional parameters for each satellite.

12.   [Output] The method of one of 1 – 11, further comprising: mapping values from the updated orbit start vector 2680 to a current epoch to obtain a current-epoch orbit position and velocity for each satellite.

13.   [Fixing] The method of one of 1 - 6, wherein the orbit start vector further comprises an ionospheric-free ambiguity (2575) per receiver-satellite pair, wherein correcting the orbit start vector (2635) comprises estimating float values for the ionospheric-free ambiguities, and

wherein the method further comprises:

1.   obtaining a value for a widelane ambiguity (340) per receiver-satellite pair, the widelane ambiguity values having integer nature,

2.   determining integer-nature values for ambiguities linearly related to the widelane ambiguities and the ionospheric-free ambiguities from the values of the widelane ambiguities and the float values of the ionospheric-free ambiguities,

3.   fixing the values of the ionospheric-free ambiguities using the integer-nature values, and

4.   with the values of the ionospheric-free ambiguities fixed, iteratively correcting the orbit start vector (2635) using a time sequence of the ionospheric-free linear combinations (2645) and a set of Earth orbit parameters to obtain an updated orbit start vector (2680) comprising a time sequence of predicted positions and predicted velocities for each satellite over an interval of multiple epochs and an estimate of Earth orientation parameters.

14.   The method of 13, wherein the ambiguities linearly related to the widelane ambiguities and the ionospheric-free ambiguities comprise one of: narrowlane ambiguities, L1 ambiguities and L2 ambiguities.

15.   [Epoch] The method of one of 1 - 14, wherein the epochs occur at a rate of about 1 Hz.

16.   [Filter Update] The method of one of 1 – 15, wherein iteratively correcting the orbit start vector comprises estimating for each epoch the values of a satellite clock for each satellite and a satellite position for each satellite at each epoch.

17.   [Filter Update] The method of one of 1 – 15, wherein iteratively correcting the orbit start vector comprises estimating for each epoch the values of a satellite clock for each satellite, a satellite clock drift, a satellite clock drift rate, and a satellite position for each satellite at each epoch.

18.   [Orbit Estimate] The method of one of 1 - 17, wherein the predicted time sequence of approximate positions for each satellite for at least some of the epochs covers an interval of at least 150 seconds.

19.   [Worldwide network] The method of one of 1 - 18, wherein the reference stations are widely distributed about the Earth and the GNSS signal data from each reference station represents code observations and carrier observations of a subset of the GNSS satellites at each epoch.

20.   Apparatus adapted to perform the method of one of 1 – 19.

21.   A computer program comprising instructions configured, when executed on a computer processing unit, to carry out a method according to one of 1 - 19.

22.   A computer-readable medium comprising a computer program according to 21.

Section 13C: Phase Clock Processing (A-2585)

1.   [Network Processing – Estimating Phase Clocks] A method of processing a set of GNSS signal data derived from code observations and carrier-phase observations at multiple receivers of GNSS signals of multiple satellites over multiple epochs, the GNSS signals having at least two carrier frequencies and a navigation message containing orbit information, comprising:

    a. obtaining precise orbit information for each satellite,

    b. determining at least one set of ambiguities per receiver, each ambiguity corresponding to one of a receiver-satellite link and a satellite-receiver-satellite link, and

    c. using at least the precise orbit information, the ambiguities and the GNSS signal data to estimate a phase-leveled clock per satellite.

2.   The method of 1, wherein determining ambiguities is performed at a first rate and wherein estimating a phase-leveled clock per satellite is performed at a second rate higher than the first rate.

3.   The method of one of 1-2, wherein estimating the phase-leveled clock per satellite comprises:

    i.   using at least the precise orbit information, the ambiguities and the GNSS singal data to estimate a set of phase-leveled clocks per receiver, each phase-leveled clock corresponding to one of a receiver-satellite link and a satellite-receiver-satellite link, and

    ii.   using a plurality of the phase-leveled clocks to estimate one phase-leveled clock per satellite.

4.   The method of one of 1 – 3, wherein determining the ambiguities comprises using at least one phase-leveled clock per satellite previously estimated to estimate the ambiguities.

5.   The method of one of 1 - 4, further comprising obtaining at least one additional phase-leveled clock per satellite estimated from an external source, and wherein determining the ambiguities comprises using said at least one additional phase-leveled clock per satellite to estimate the ambiguities.

6.   The method of one of 1-5, further comprising

    1.   determining at least one set of ambiguities per receiver for additional receivers, each ambiguity corresponding to one of a receiver-satellite link and a satellite-receiver-satellite link,

    2.   after determining the ambiguities for the additional receivers, using at least the precise orbit information, the ambiguities for the additional receivers and the GNSS signal data to estimate the at least one additional phase-leveled clock per satellite

7.   The method of one of 1 – 6, wherein the at least two carrier frequencies comprise at least two of the GPS L1, GPS L2 and GPS L5 frequencies.

8.   The method of one of 1 – 7, wherein determining at least one set of ambiguities per receiver comprises at least one of: estimating float ambiguity values, estimating float ambiguity values and fixing the float ambiguity values to integer values, estimating float ambiguity values and forming at least one weighted average of integer value candidates, and constraining the ambiguity values in a sequential filter.

9.   The method of one of 1 – 8, wherein the ambiguities are undifferenced between satellites.

10.   The method of one of 1 – 8, wherein the ambiguities are single-differenced between satellites.

11.   Apparatus adapted to perform the method of one of 1-10.

12.   A computer program comprising instructions configured, when executed on a computer processing unit, to carry out a method according to one of 1 – 10.

13.   A computer-readable medium comprising a computer program according to 12.

Section 13D: Rover Processing with Synthesized Reference Station Data (A-2617)
[Abstract (FIG. 38)]

1.   [SBS Processing] A method of determining position of a rover antenna, comprising:

a.   obtaining rover GNSS data derived from code observations and carrier phase observations of GNSS signals of multiple satellites over multiple epochs,

b.   obtaining precise satellite data for the satellites,

c.   determining a virtual base station location,

d.   generating epochs of synthesized base station data using at least the precise satellite data and the virtual base station location, and

e.   applying a differential process to at least the rover GNSS data and the synthesized base station data to determine at least rover antenna positions.

2.   [Low Latency] The method of 1, wherein generating epochs of synthesized base station data comprises generating an epoch of virtual base station data for each epoch of GNSS rover data.

3.   [High Accuracy] The method of 1, wherein obtaining precise satellite data comprises obtaining precise satellite data in sets, wherein generating epochs of synthesized base station data comprises generating an epoch of synthesized base station data for each set of precise satellite data, and wherein applying a differential process comprises matching each set of GNSS rover data with an epoch of synthesized base station data.

4.   [Virtual Base Station Location] The method of one of 1 – 3, wherein determining a virtual base station location comprises determining the virtual base station location from at least one of: an autonomously determined position of the rover antenna, a previously determined one of said rover antenna positions, a synthesized base station data generating module, an inertial navigation system, a mobile telephone tower location, and information provided by a user.

5.   The method of one of 1 – 4, further comprising updating the virtual base station location on the occurrence of at least one of: never, for each epoch of rover data, when the distance between an approximate rover antenna position and the virtual base station location exceeds a predetermined threshold, and for each update of the rover antenna positions.

6. The method of one of 1 – 5, wherein each epoch of the synthesized base station data is generated for a corresponding virtual base station location.

7. The method of one of 1 – 5, wherein determining the virtual base station location comprises selecting a virtual base station location close to a current approximate rover antenna position.

8. The method of one of 1 – 7, wherein a new virtual base position is determined when one or more of the following criteria is met: each rover epoch, each nth rover epoch, after a time interval, after exceeding a distance between a current approximate rover position and a current virtual base station location.

9. The method of one of 1 – 8, wherein the virtual base station location is generated for a specific GNSS time interval

10. The method of one of 1 – 9, wherein applying a differential process to at least the rover GNSS data and the synthesized base station data to determine at least rover antenna positions comprises at least one of: aided inertial navigation (integrated inertial navigation and GNSS) processing, real-time kinematic (RTK) processing, irtk processing; differential GPS processing; float processing; triple differenced processing; post-processing and real-time processing.

11. The method of one of 1 – 10, further comprising matching each epoch of the rover GNSS data with an epoch of synthesized base station data within a few milliseconds.

12. The method of one of 1 – 11, wherein generating epochs of synthesized base station data comprises generating a set of synthesized base station observations for each of a plurality of discrete times, and wherein applying a differential process comprises processing each epoch of GNSS rover data with a set of synthesized base station observations for a discrete time which is within ten seconds of the epoch of the GNSS rover data being processed.

13. Apparatus adapted to perform the method of one of 1-12.

14. A computer program comprising instructions configured, when executed on a computer processing unit, to carry out a method according to one of 1 – 12.

15. A computer-readable medium comprising a computer program according to 14.

Section 13E: Rover Processing with Ambiguity Fixing (A-2599)

[Abstract (FIG. 49)]

1. A method of processing a set of GNSS signal data derived from signals of a set of satellites having carriers observed at a rover antenna, wherein the data includes a carrier observation and a code observation of each carrier of each satellite, comprising:

    a.   obtaining for each satellite clock corrections comprising at least two of: (i) a code-leveled satellite clock, (ii) a phase-leveled satellite clock, and (iii) a satellite clock bias representing a difference between a code-leveled satellite clock and a phase-leveled satellite clock,

    b.   running a first filter which uses at least the GNSS signal data and the satellite clock corrections to estimate values for parameters comprising at least one carrier ambiguity for each satellite, and a covariance matrix of the carrier ambiguities,

    c.   determining from each carrier ambiguity an integer-nature carrier ambiguity comprising one of: an integer value, and a combination of integer candidates,

    d.   inserting the integer-nature carrier ambiguities as pseudo-observations into a second filter, and applying the second filter to the GNSS signal data and the satellite clock corrections to obtain estimated values for parameters comprising at least the position of the receiver.

2. The method of 1, wherein the integer-nature carrier ambiguities are between-satellite single-differenced ambiguities.

3. The method of one of 1 – 2, further comprising

    a. obtaining a set of MW corrections,

    b. running a third filter using the GNSS signal data and at least the MW corrections to obtain at least a set of WL ambiguities,

    c. using the set of WL ambiguities to obtain the integer-nature carrier ambiguity.

4. The method of 3, wherein the WL ambiguities comprise at least one of: float values, integer values, and float values based on integer candidates.

5. The method of 4, wherein the covariance matrix of the ambiguities is scaled to reflect the change due to the use of the WL ambiguities.

6. The method of one of 1 – 5, wherein the WL ambiguties are between-satellite single-differenced ambiguities.

7. The method of one of 1 – 6, wherein the integer-nature ambiguities comprise at least one of: L1-L2 ionospheric-free ambiguities, L2-L5 ionospheric-free ambiguities, and carrier ambiguities of a linear combination of two or more GNSS frequencies.

8.   The method of one of 1 – 6, wherein ionospheric delay information is used to feed one or more of the filters and wherein the integer-nature ambiguity comprises at least one of: carrier ambiguity of L1 frequency, carrier ambiguity of L2 frequency, carrier ambiguity of L5 frequency, and carrier ambiguity of any GNSS frequency.

5   9.   The method of one of 1 – 8, wherein the second filter comprises one of: a new filter, a copy of the first filter, and the first filter.

10.   The method of one of 1 – 9, wherein the code-leveled satellite clock is used for modeling all GNSS observations, and the float ambiguity is adapted to the level of the phase-leveled clock by applying the difference between the code-leveled satellite clock and the

10   phase-leveled satellite clock.

11.   The method of one of 1 – 9, wherein the code-leveled satellite clock is used for modeling all GNSS code observations and the phase-leveled satellite clock is used for modeling all GNSS carrier observations.

12.   The method of one of 1 – 11, wherein determining the integer-nature carrier ambiguity

15   from a float ambiguity comprises at least one of: rounding the float ambiguity to the nearest integer, choosing best integer candidates from a set of integer candidates generated using integer least squares, and computing float values using a set of integer candidates generated using integer least squares.

13.   The method of one of 1 -12, wherein at least one of the first filter and second filter further

20   estimates at least one of: receiver phase-leveled clock, receiver code-leveled clock, tropospheric delay, receiver clock bias representing a difference between the code-leveled receiver clock and the phase-leveled receiver clock, and multipath states.

14.   The method of one of 1 -13, wherein at least one of the first filter, the second filter and the third filter is adapted to update the estimated values for each of a plurality of epochs

25   of GNSS signal data.

15.   Apparatus adapted to perform the method of one of 1-14.

16.   A computer program comprising instructions configured, when executed on a computer processing unit, to carry out a method according to one of 1 – 14.

17.   A computer-readable medium comprising a computer program according to 16.

Any plurality of the above described aspects of the invention may be combined to form further aspects and embodiments, with the aim of providing additional benefits notably in terms of surveying efficiency and/or system usability.

Above-described methods, apparatuses and their embodiments may be integrated into a
5   rover, a reference receiver or a network station, and/or the processing methods described can be carried out in a processor which is separate from and even remote from the receiver/s used to collect the observations (e.g., observation data collected by one or more receivers can be retrieved from storage for post-processing, or observations from multiple network reference stations can be transferred to a network processor for near-real-time processing to generate a correction data
10   stream and/or virtual-reference-station messages which can be transmitted to one or more rovers). Therefore, the invention also relates to a rover, a reference receiver or a network station including any one of the above apparatuses.

In some embodiments, the receiver of the apparatus of any one of the above-described embodiments is separate from the filter and the processing element. Post-processing and network
15   processing of the observations may notably be performed. That is, the constituent elements of the apparatus for processing of observations does not itself require a receiver. The receiver may be separate from and even owned/operated by a different person or entity than the entity which is performing the processing. For post-processing, the observations may be retrieved from a set of data which was previously collected and stored, and processed with reference-station data which
20   was previously collected and stored; the processing is conducted for example in an office computer long after the data collection and is thus not real-time. For network processing, multiple reference-station receivers collect observations of the signals from multiple satellites, and this data is supplied to a network processor which may for example generate a correction data stream or which may for example generate a "virtual reference station" correction which is supplied to a
25   rover so that the rover can perform differential processing. The data provided to the rover may be ambiguities determined in the network processor, which the rover may use to speed its position solution, or may be in the form of corrections which the rover applies to improve its position solution. The network is typically operated as a service to rover operators, while the network operator is typically a different entity than the rover operator.

30   Any of the above-described methods and their embodiments may be implemented by means of a computer program. The computer program may be loaded on an apparatus, a rover, a reference receiver or a network station as described above. Therefore, the invention also relates to a computer program, which, when carried out on an apparatus, a rover, a reference receiver or a

network station as described above, carries out any one of the above above-described methods and their embodiments.

The invention also relates to a computer-readable medium or a computer-program product including the above-mentioned computer program. The computer-readable medium or
5   computer-program product may for instance be a magnetic tape, an optical memory disk, a magnetic disk, a magneto-optical disk, a CD ROM, a DVD, a CD, a flash memory unit or the like, wherein the computer program is permanently or temporarily stored. The invention also relates to a computer-readable medium (or to a computer-program product) having computer-executable instructions for carrying out any one of the methods of the invention.

10   The invention also relates to a firmware update adapted to be installed on receivers already in the field, i.e. a computer program which is delivered to the field as a computer program product. This applies to each of the above-described methods and apparatuses.

GNSS receivers may include an antenna, configured to received the signals at the frequencies broadcasted by the satellites, processor units, one or more accurate clocks (such as crystal
15   oscillators), one or more computer processing units (CPU), one or more memory units (RAM, ROM, flash memory, or the like), and a display for displaying position information to a user.

Where the terms "receiver", "filter" and "processing element" are used herein as units of an apparatus, no restriction is made regarding how distributed the constituent parts of a unit may be. That is, the constituent parts of a unit may be distributed in different software or hardware
20   components or devices for bringing about the intended function. Furthermore, the units may be gathered together for performing their functions by means of a combined, single unit. For instance, the receiver, the filter and the processing element may be combined to form a single unit, to perform the combined functionalities of the units.

The above-mentioned units may be implemented using hardware, software, a
25   combination of hardware and software, pre-programmed ASICs (application-specific integrated circuit), etc. A unit may include a computer processing unit (CPU), a storage unit, input/output (I/O) units, network connection units, etc.

Although the present invention has been described on the basis of detailed examples, the detailed examples only serve to provide the skilled person with a better understanding, and are
30   not intended to limit the scope of the invention. The scope of the invention is much rather defined by the appended claims.

CLAIMS

1.   A method of processing a set of GNSS signal data derived from code observations and carrier-phase observations at multiple receivers of GNSS signals of multiple satellites over multiple epochs, the GNSS signals having at least two carrier frequencies, comprising:

forming an MW (Melbourne-Wübbena) combination per receiver-satellite pairing at each epoch to obtain a MW data set per epoch, and

estimating from the MW data set per epoch an MW bias per satellite which may vary from epoch to epoch, and a set of WL (widelane) ambiguities, each WL ambiguity corresponding to one of a receiver-satellite link and a satellite-receiver-satellite link, wherein the MW bias per satellite is modeled as one of (i) a single estimation parameter and (ii) an estimated offset plus harmonic variations with estimated amplitudes.

2.   The method of claim 1, further comprising applying corrections to the GNSS signal data.

3.   The method of claim 1, further comprising smoothing at least one linear combination of GNSS signal data before estimating an MW bias per satellite.

4.   The method of claim 1, further comprising applying at least one MW bias constraint.

5.   The method of claim 1, further comprising applying at least one integer WL ambiguity constraint

6.   The method of claim 1, further comprising using a spanning tree (ST) over one of an observation graph and a filter graph for constraining the WL ambiguities.

7.   The method of claim 1, further comprising using a minimum spanning tree (MST) on one of an observation graph and a filter graph for constraining the WL ambiguities.

8.   The method of claim 7, wherein the minimum spanning tree is based on edge weights, each edge weight derived from receiver-satellite geometry.

9.   The method of claim 8, wherein the edge weight is defined with respect to one of (i) a geometric distance from receiver to satellite, (ii) a satellite elevation angle, and (iii) a geometric distance from satellite to receiver to satellite, and (iv) a combination of the elevations under which the two satellites in a single differenced combination are seen at a station.

10.   The method of claim 7, wherein the minimum spanning tree is based on edge weights, with each edge weight based on WL ambiguity information, defined with respect to one of (i) difference of a WL ambiguity to integer, (ii) WL ambiguity variance, and (iii) a combination of (i) and (ii).

11.   The method of claim 1, further comprising fixing at least one of the WL ambiguities as an integer value.

12.   The method of claim 1, further comprising determining candidate sets of WL integer ambiguity values, forming a weighted combination of the candidate sets, and fixing at least one of the WL ambiguities as a value taken from the weighted combination.

13.   The method of claim 11, wherein the estimating step comprises introducing fixed WL ambiguities so as to estimate MW biases which are compatible with fixed WL ambiguities.

14.   The method of claim 13, wherein the estimating step comprises applying an iterative filter to the MW data per epoch and wherein introducing fixed WL ambiguities comprises one of (i) putting the fixed WL ambiguities as observations into the filter, (ii) putting the fixed WL ambiguities as observations into a copy of the filter generated after each of a plurality of observation updates, and (iii) reducing the MW combinations by the fixed WL ambiguities and putting the resulting reduced MW combinations into a second filter without ambiguity states to estimate at least one MW bias per satellite.

15.   The method of claim 1, further comprising shifting at least one MW bias by an integer number of WL cycles.

16.   The method of claim 1, further comprising shifting at least one MW bias and its respective WL ambiguity by an integer number of WL cycles.

17.   The method of claim 1, wherein the navigation message comprises orbit information,

18.   Apparatus for performing the method of one of claims 1 – 17.

19.   Apparatus for processing a set of GNSS signal data derived from code observations and carrier-phase observations at multiple receivers of GNSS signals of multiple satellites over multiple epochs, the GNSS signals having at least two carrier frequencies, comprising:

        an element adapted to form an MW (Melbourne-Wübbena) combination per receiver-satellite pairing at each epoch to obtain a MW data set per epoch, and

        an element adapted to estimate from the MW data set per epoch an MW bias per satellite which may vary from epoch to epoch, and a set of WL (widelane)

ambiguities, each WL ambiguity corresponding to one of a receiver-satellite link and

a satellite-receiver-satellite link, wherein the MW bias per satellite is modeled as one

of (i) a single estimation parameter and (ii) an estimated offset plus harmonic

variations with estimated amplitudes.

20.   The apparatus of claim 19, further comprising an element adapted to apply

corrections to the GNSS signal data.

21.   The apparatus of claim 19, further comprising an element adapted to smooth at least

one linear combination of GNSS signal data before an MW bias per satellite is

estimated.

22.   The apparatus of claim 19, further comprising an element adapted to apply at least

one MW bias constraint.

23.   The apparatus of claim 19, further comprising an element adapted to apply at least

one integer WL ambiguity constraint

24.   The apparatus of claim 19, further comprising an element adapted to use a spanning

tree (ST) over one of an observation graph and a filter graph to constrain the WL

ambiguities.

25.   The apparatus of claim 19, further comprising an element adapted to use a minimum

spanning tree (MST) on one of an observation graph and a filter graph to constrain

the WL ambiguities.

26.   The apparatus of claim 25, wherein the minimum spanning tree is based on edge

weights, each edge weight derived from receiver-satellite geometry.

27.   The apparatus of claim 26, wherein the edge weight is defined with respect to one of

(i) a geometric distance from receiver to satellite, (ii) a satellite elevation angle, and

(iii) a geometric distance from satellite to receiver to satellite, and (iv) a combination

of the elevations under which the two satellites in a single differenced combination

are seen at a station.

28.   The apparatus of claim 25, wherein the minimum spanning tree is based on edge

weights, with each edge weight based on WL ambiguity information, defined with

respect to one of (i) difference of a WL ambiguity to integer, (ii) WL ambiguity

variance, and (iii) a combination of (i) and (ii).

29.   The apparatus of claim 19, further comprising an element adapted to fix at least one

of the WL ambiguities as an integer value.

30.   The apparatus of claim 19, further comprising an element adapted to determine

candidate sets of WL integer ambiguity values, form a weighted combination of the

candidate sets, and fix at least one of the WL ambiguities as a value taken from the weighted combination.

31.   The apparatus of claim 29, wherein the element adapted to estimate is further adapted to introduce fixed WL ambiguities so as to estimate MW biases which are compatible with fixed WL ambiguities.

32.   The apparatus of claim 31, wherein the element adapted to estimate is further adapted to apply an iterative filter to the MW data per epoch and to introduce fixed WL ambiguities as one of (i) fixed WL ambiguities as observations in the filter, (ii) fixed WL ambiguities as observations in a copy of the filter generated after each of a plurality of observation updates, and (iii) MW combinations reduced by the fixed WL ambiguities and in a second filter without ambiguity states to estimate at least one MW bias per satellite.

33.   The apparatus of claim 19, further comprising an element adapted to shift at least one MW bias by an integer number of WL cycles.

34.   The apparatus of claim 19, further comprising an element adapted to shift at least one MW bias and its respective WL ambiguity by an integer number of WL cycles.

35.   The apparatus of claim 19, wherein the navigation message comprises orbit information,

36.   A computer program comprising instructions configured, when executed on a computer processing unit, to carry out a method according to claim 1.

37.   A computer-readable medium comprising a computer program according to claim 36.

FIG. 1

FIG. 2

FIG. 3

FIG. 4

FIG. 5

	Functional Model	Stochastic Model
Dynamic Model	$x_K = \Phi_{K-1} x_{K-1} + w_{K-1}$	$Q_K = E[w_K w_K^T]$
Measurement Model (Observation Model)	$H_K x_K = z_K + v_K$	$R_K = E[v_K v_K^T]$

Prediction (Time Update)

$$\hat{x}_K^- = \Phi_{K-1}\hat{x}_{K-1}$$

$$P_K^- = \Phi_{K-1}P_{K-1}\Phi_{K-1}^T + Q_{K-1}$$

Correction (Measurement Update)

$$K_K = P_K^- H_K^T [H_K P_K^- H_K^T + R_K]^{-1}$$

$$\hat{x}_K = \hat{x}_K^- + K_K(z_K - H_K \hat{x}_K^-)$$

$$P_K = (1 - K_K H_K)P_K^-$$

$\hat{x}_0, P_0$

FIG. 6

7/71
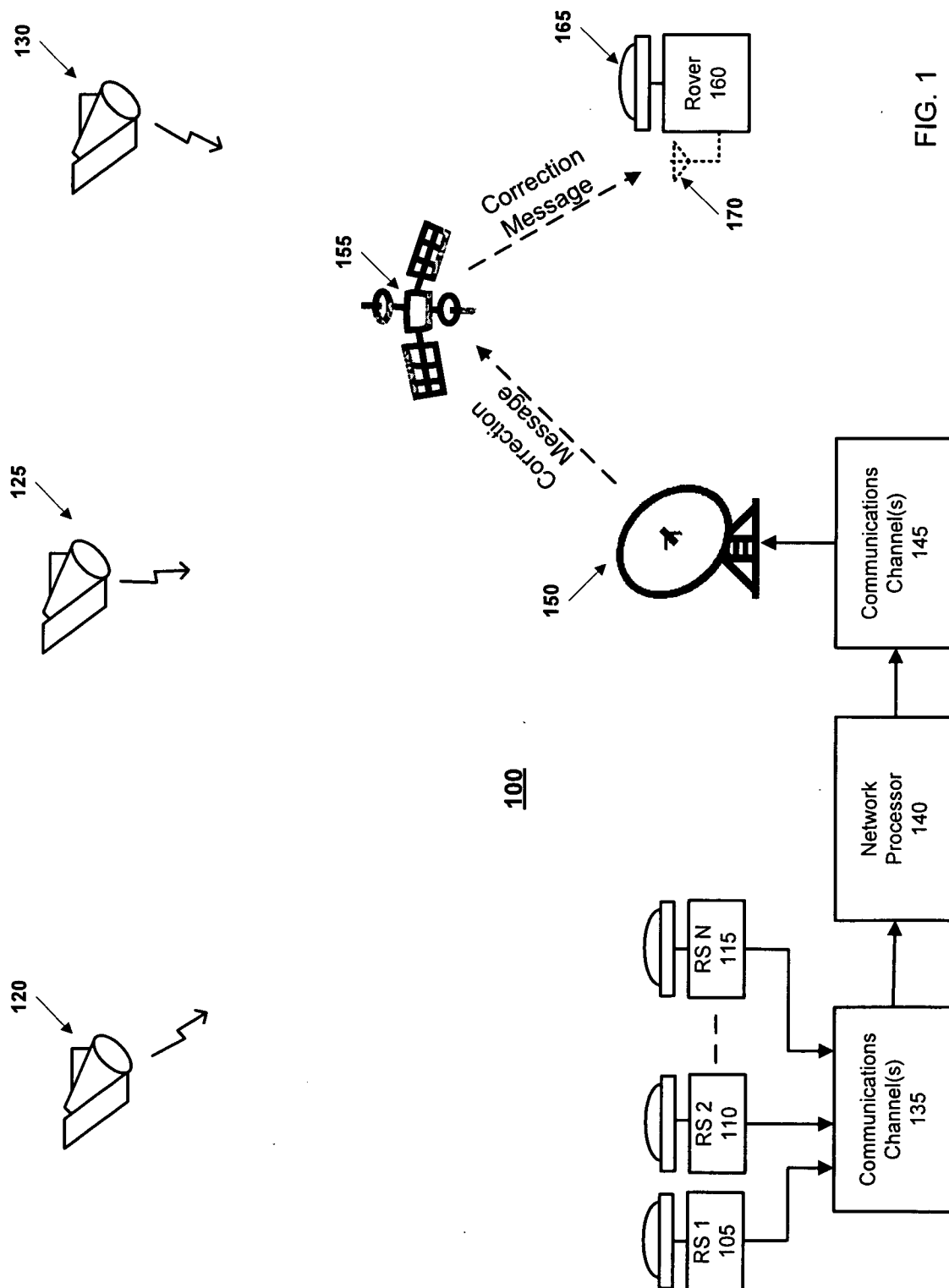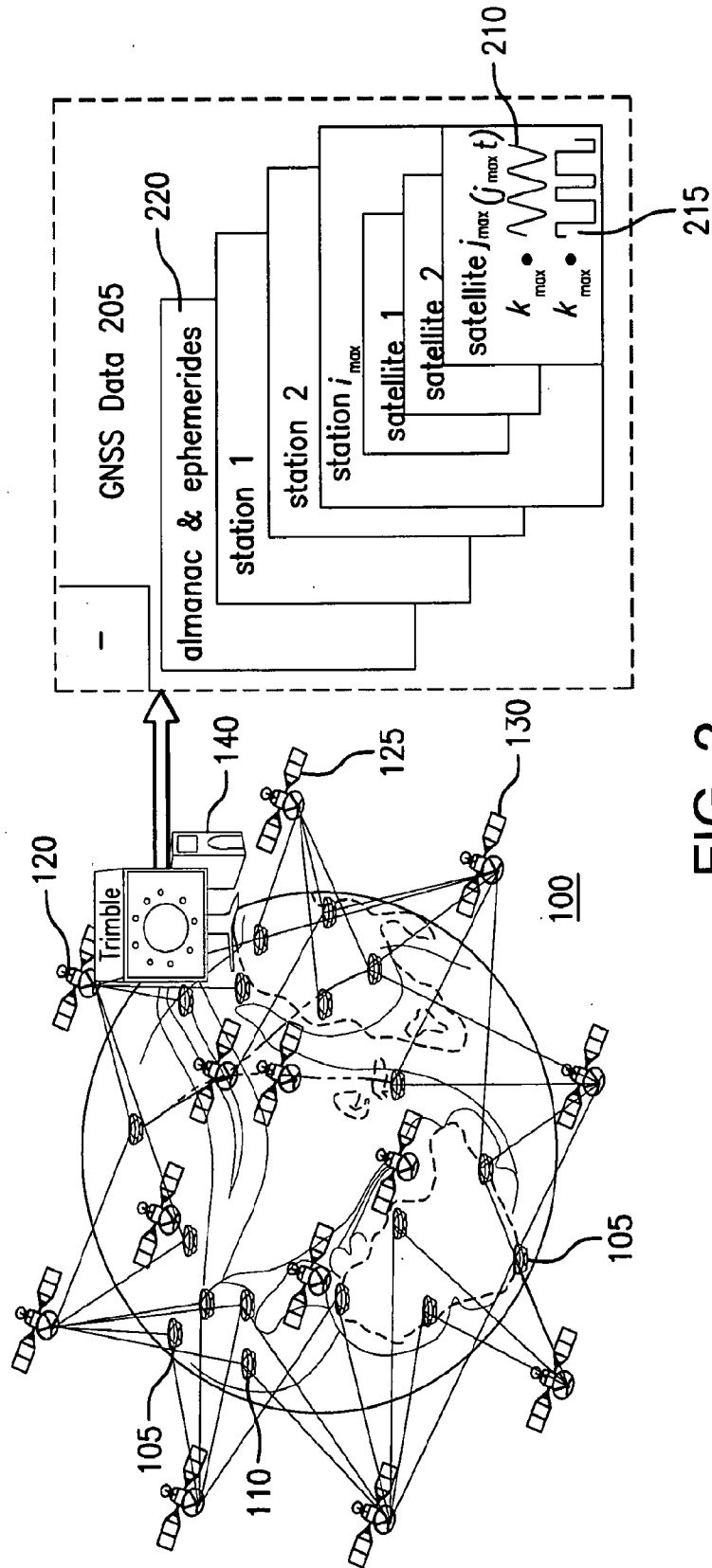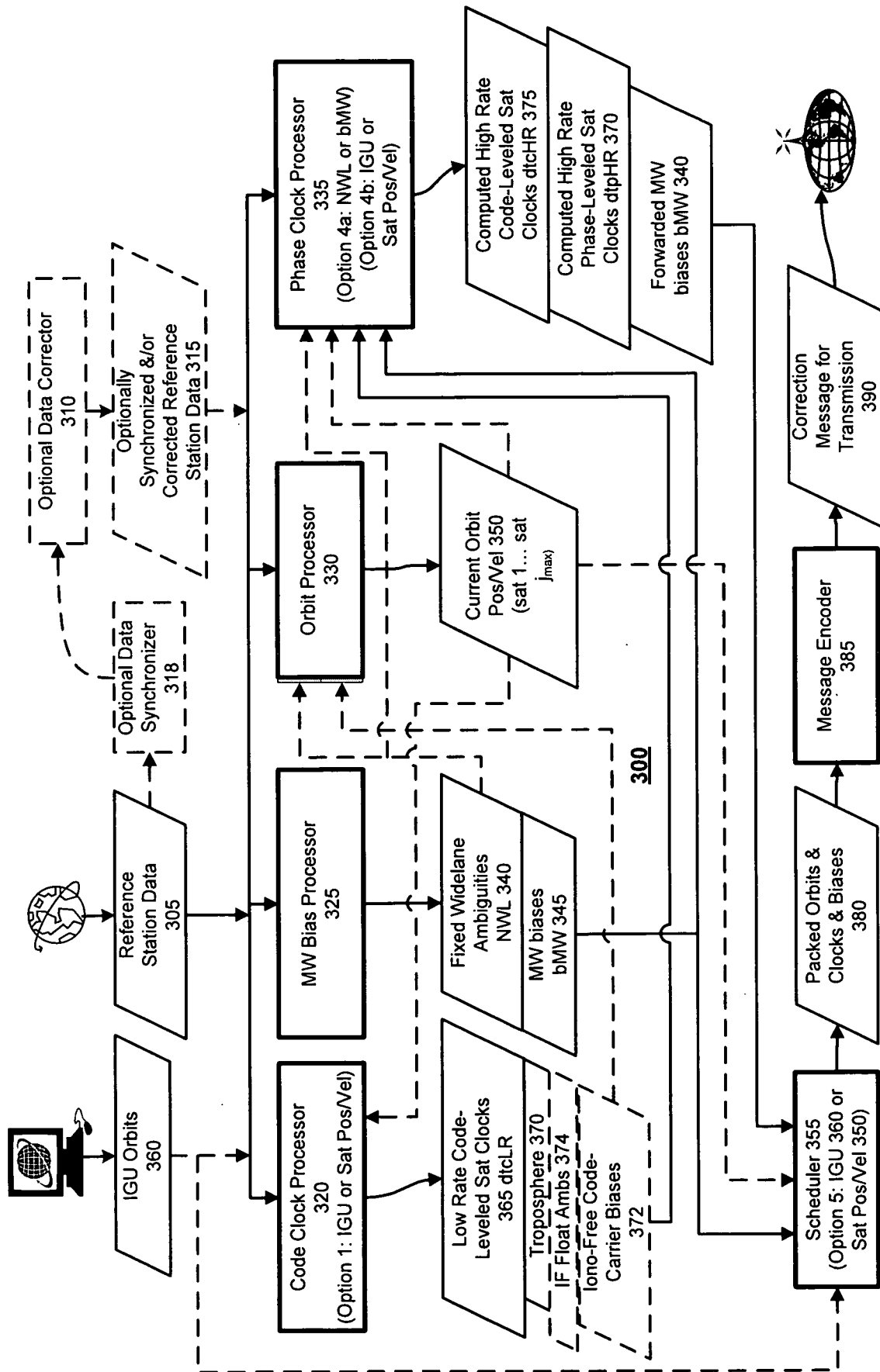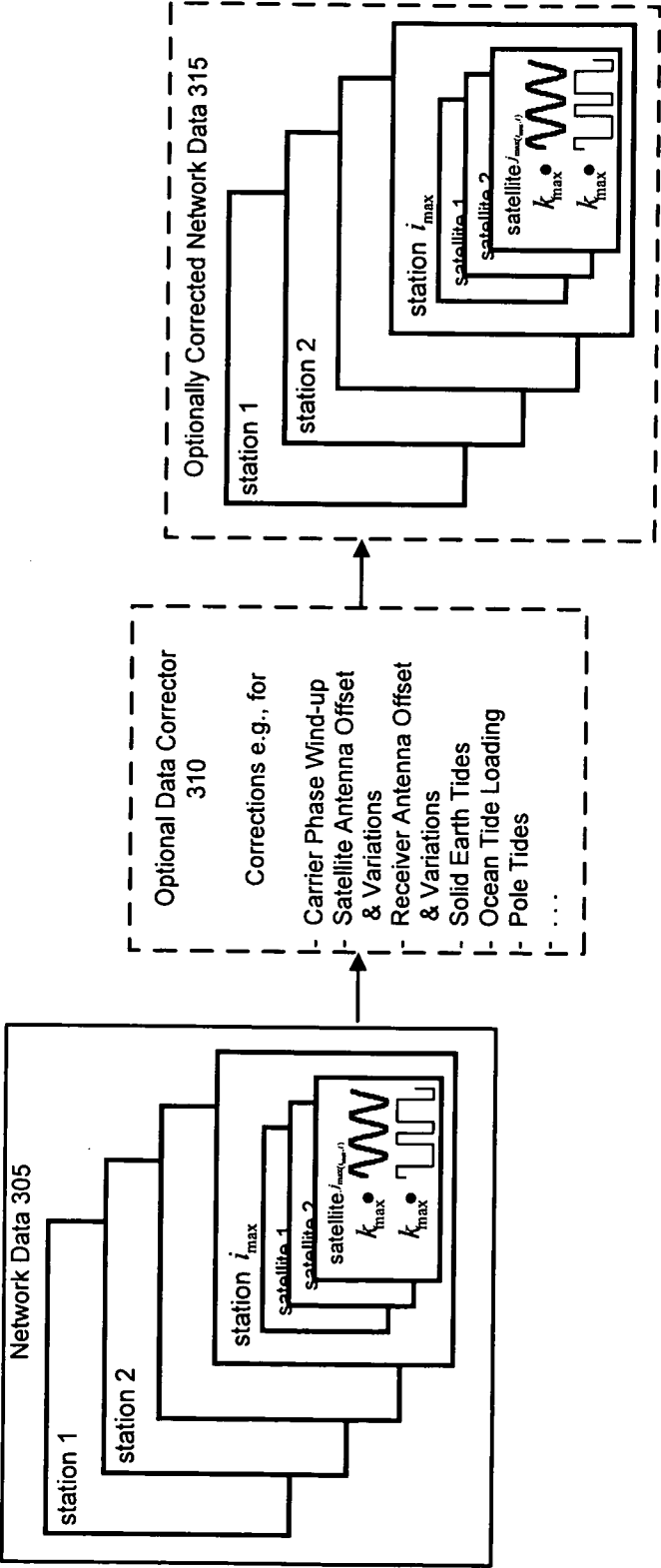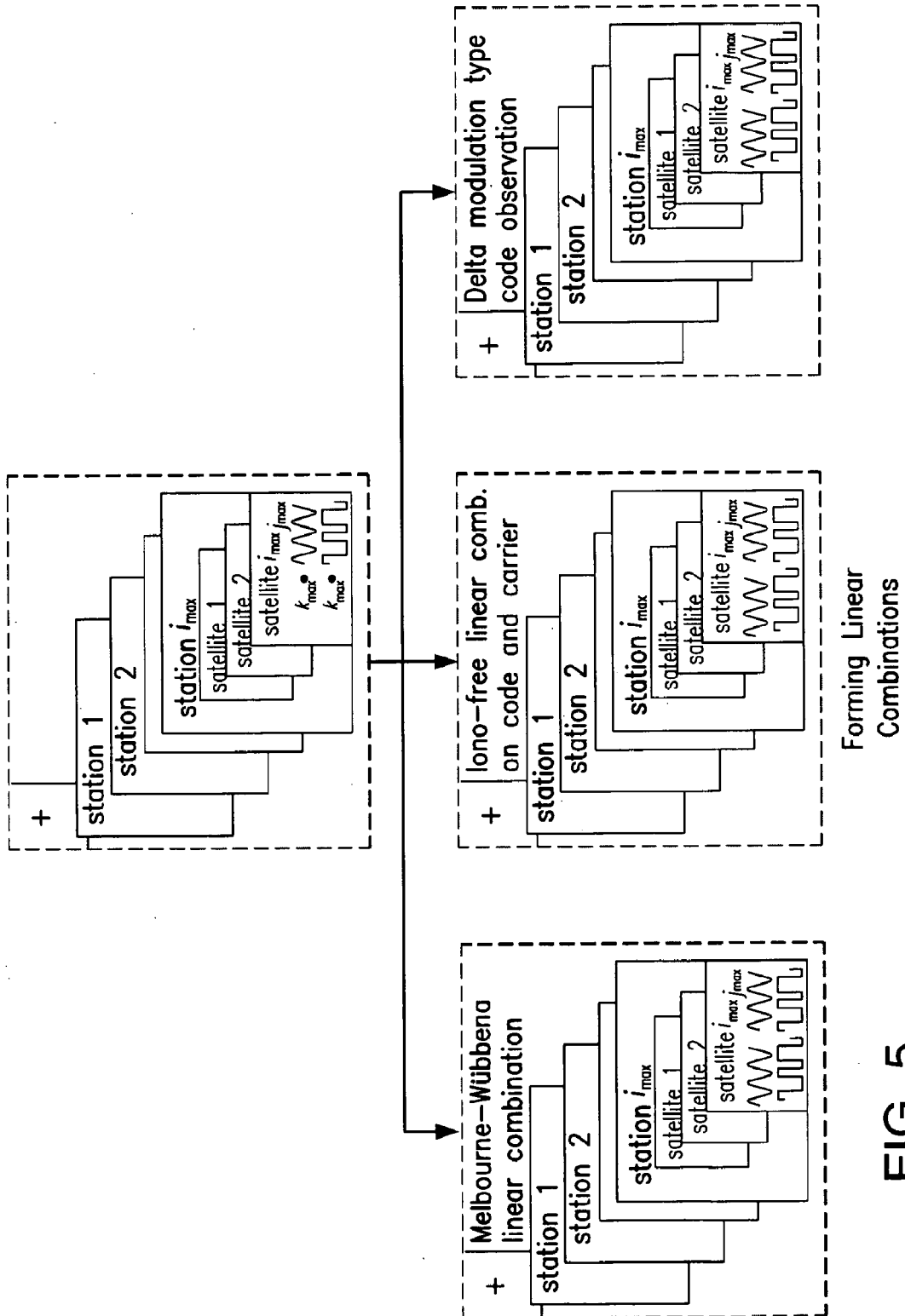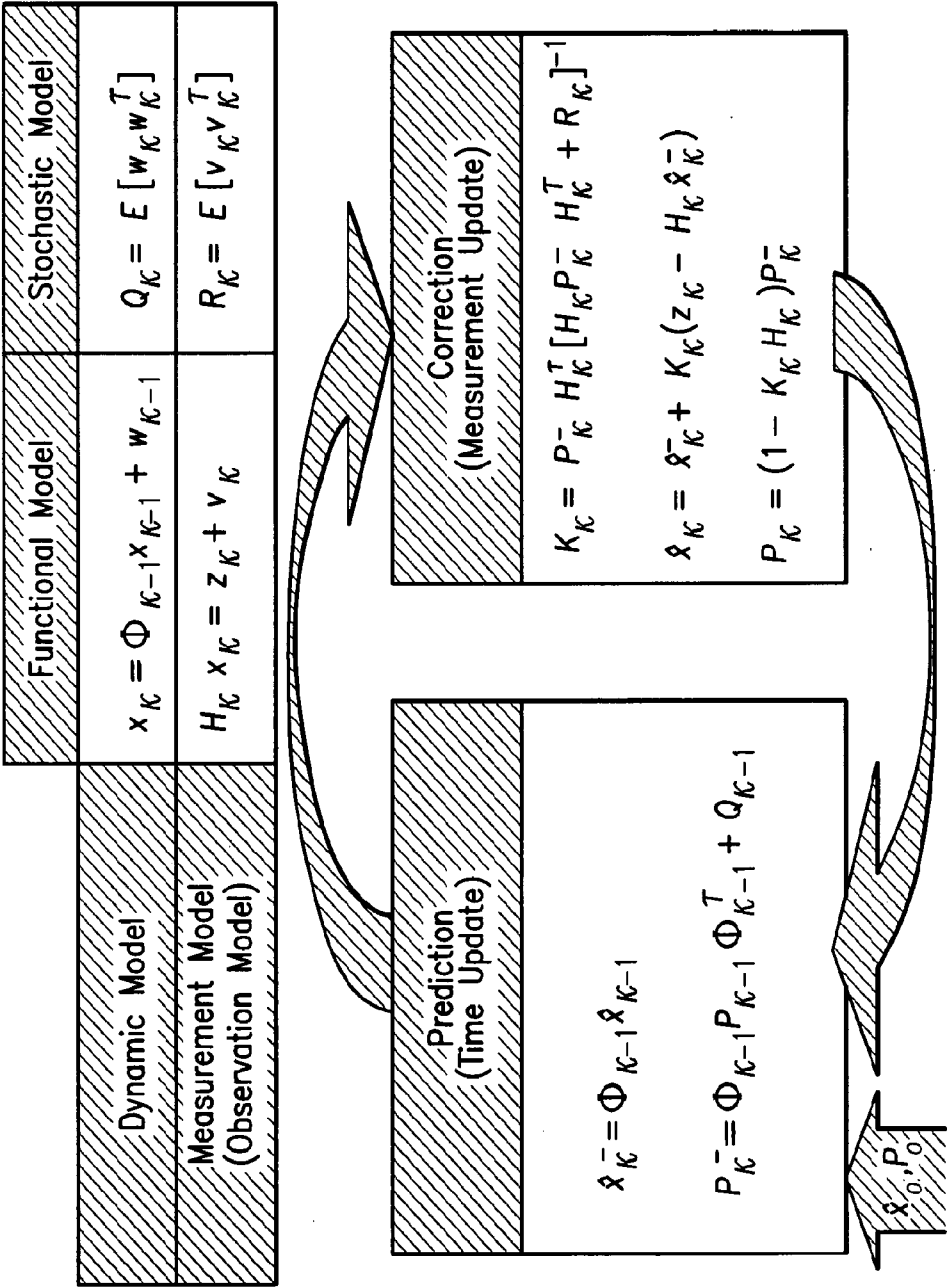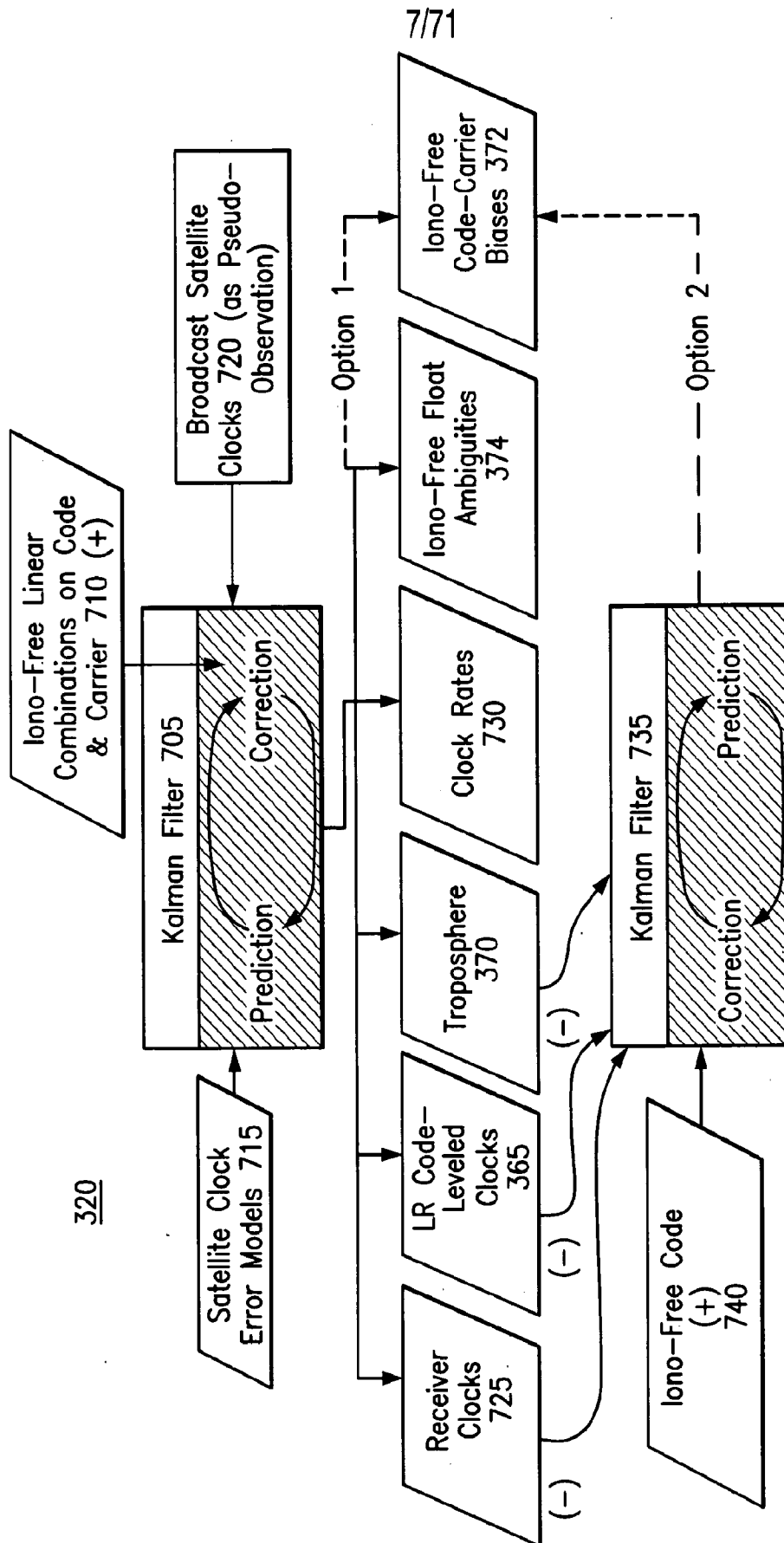
FIG. 7
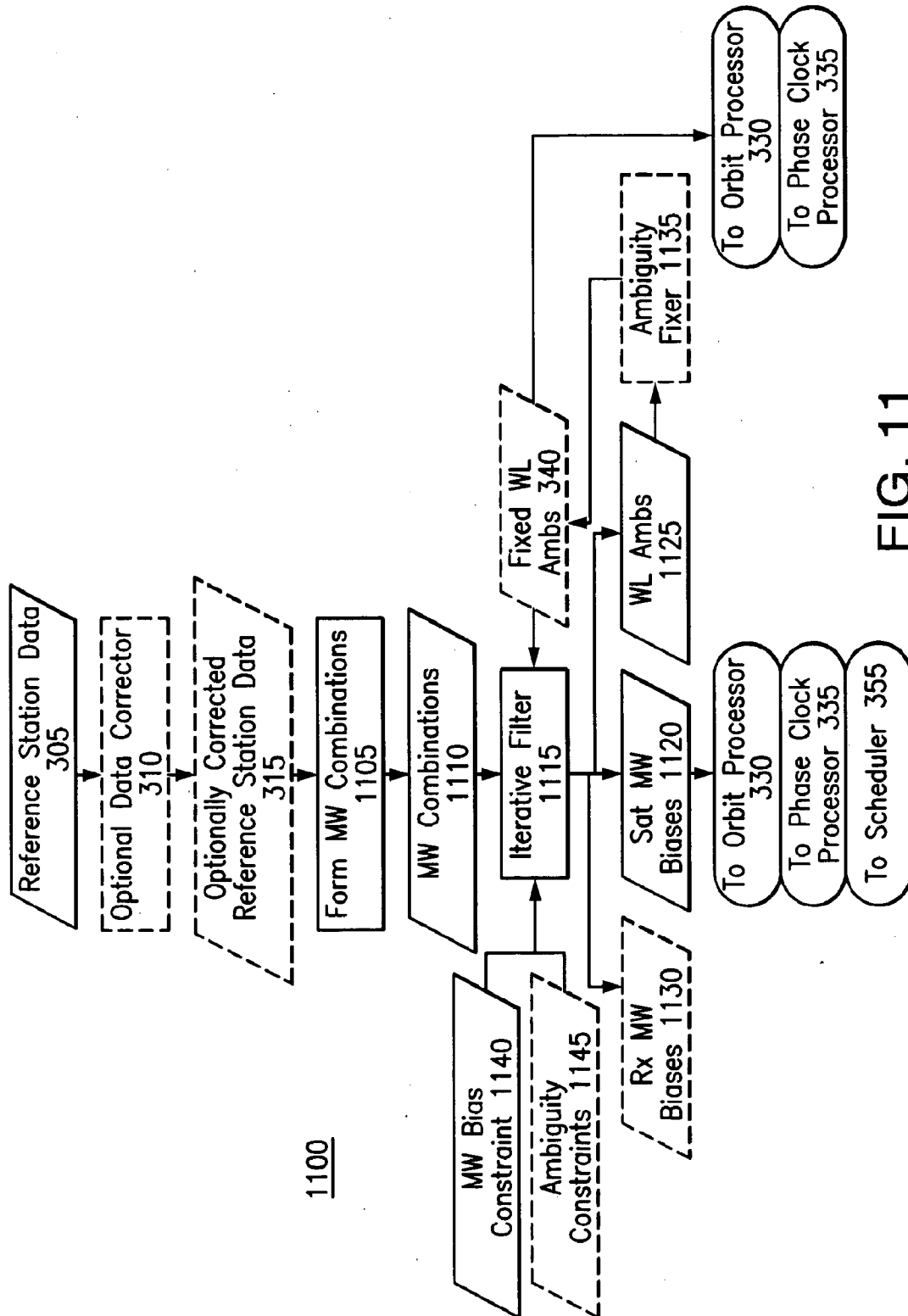
FIG. 11
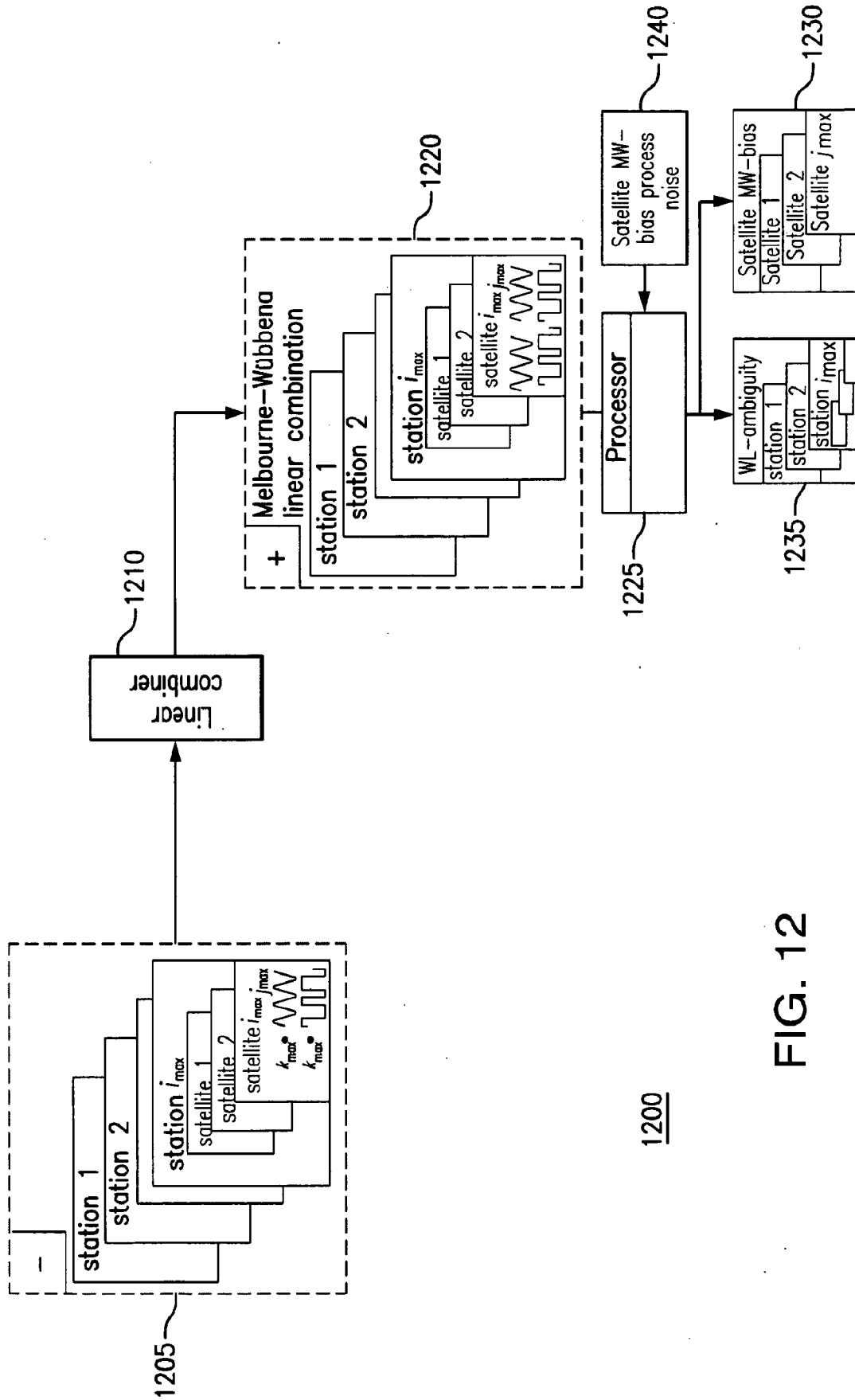
FIG. 12
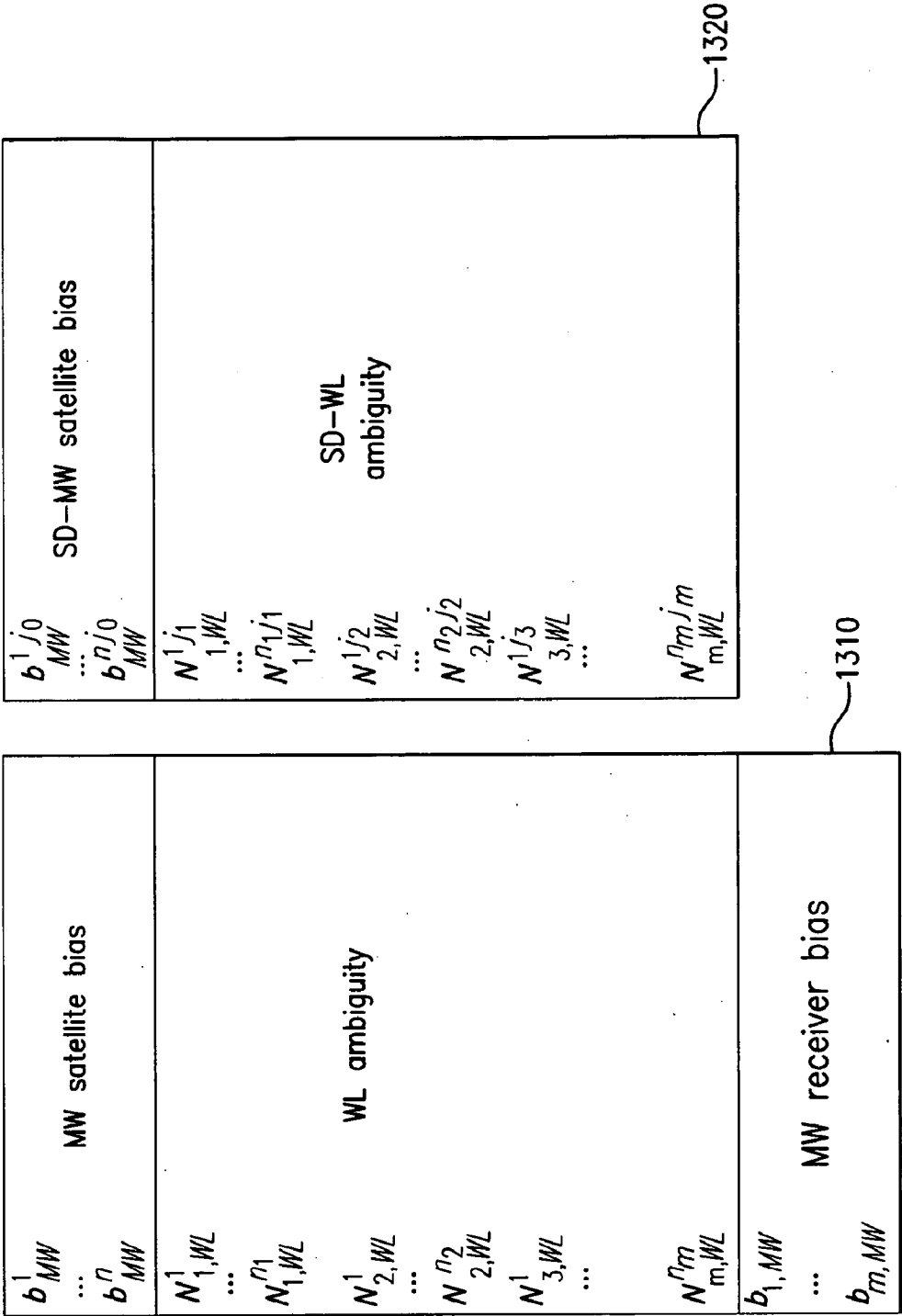
FIG. 13B

FIG. 13A

11/71
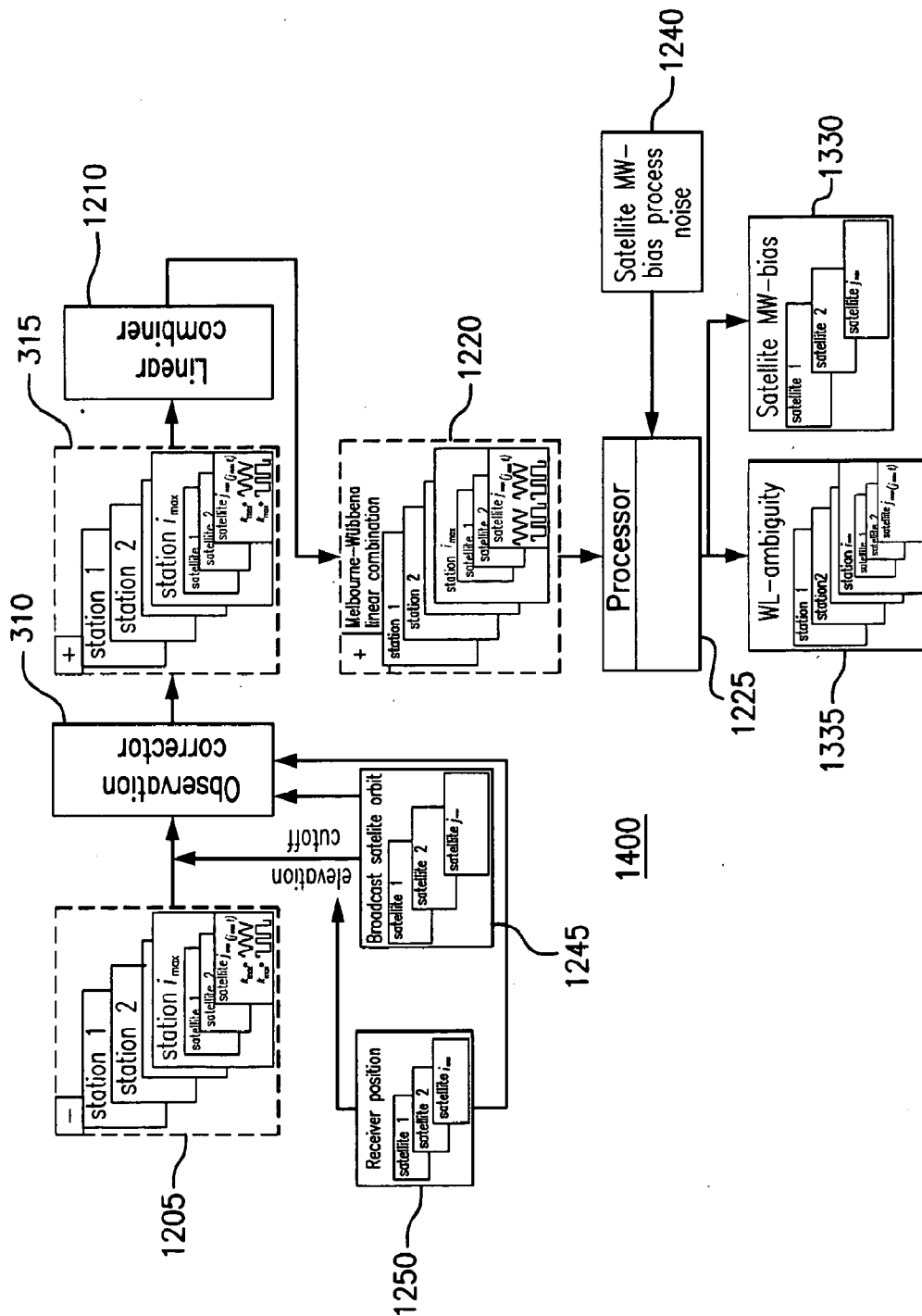
FIG. 14

12/71
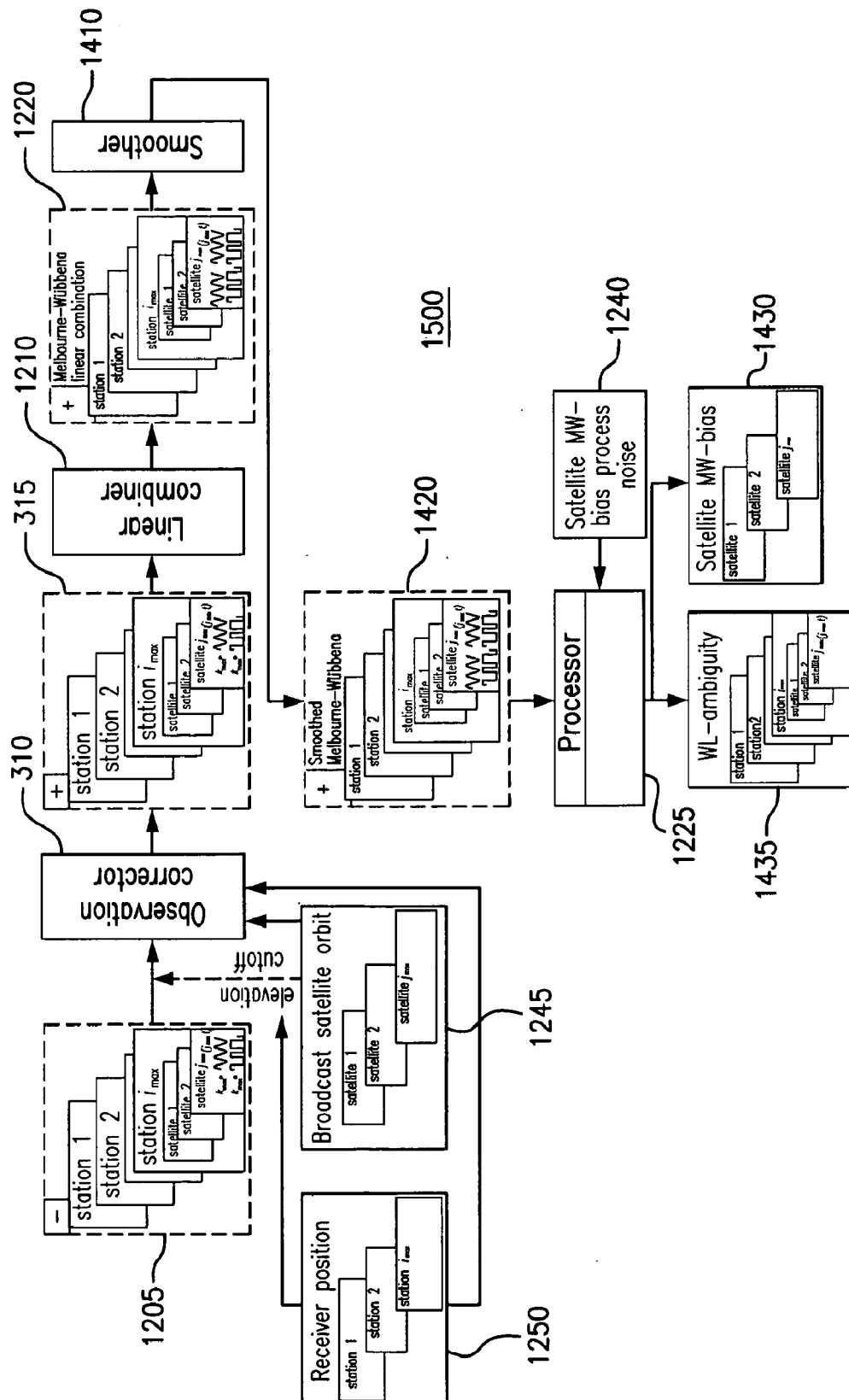
FIG. 15
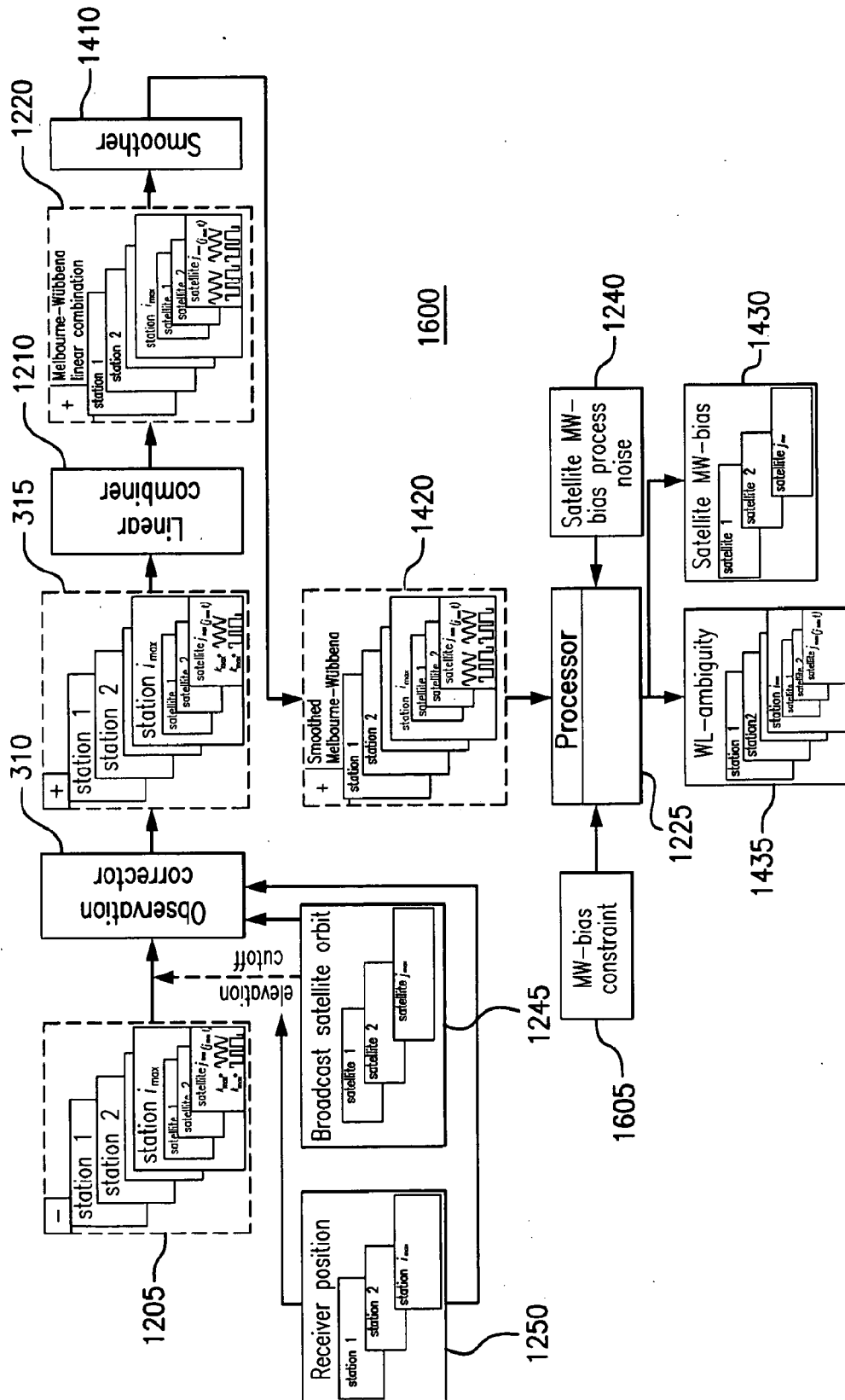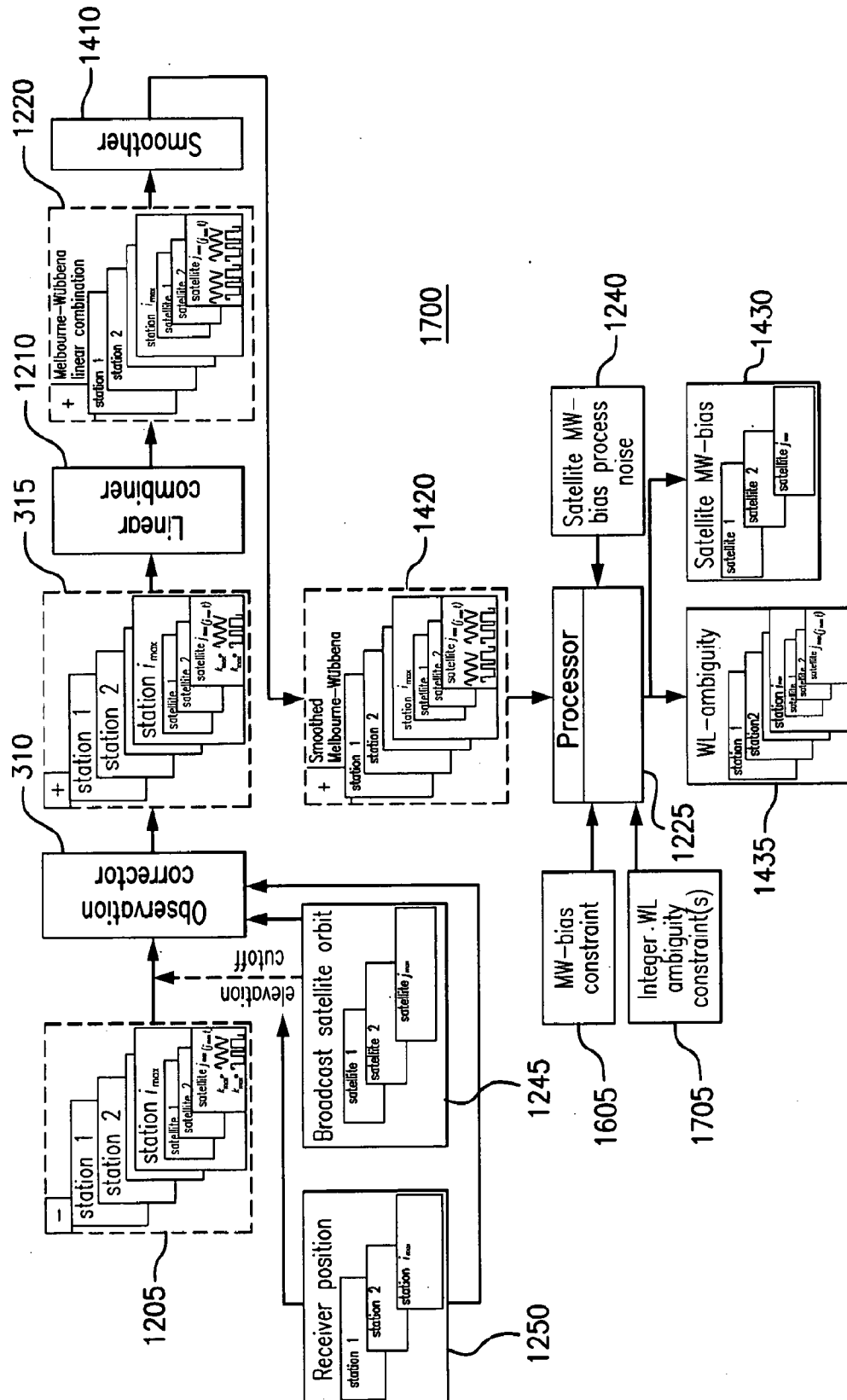
FIG. 16

14/71

FIG. 17

15/71
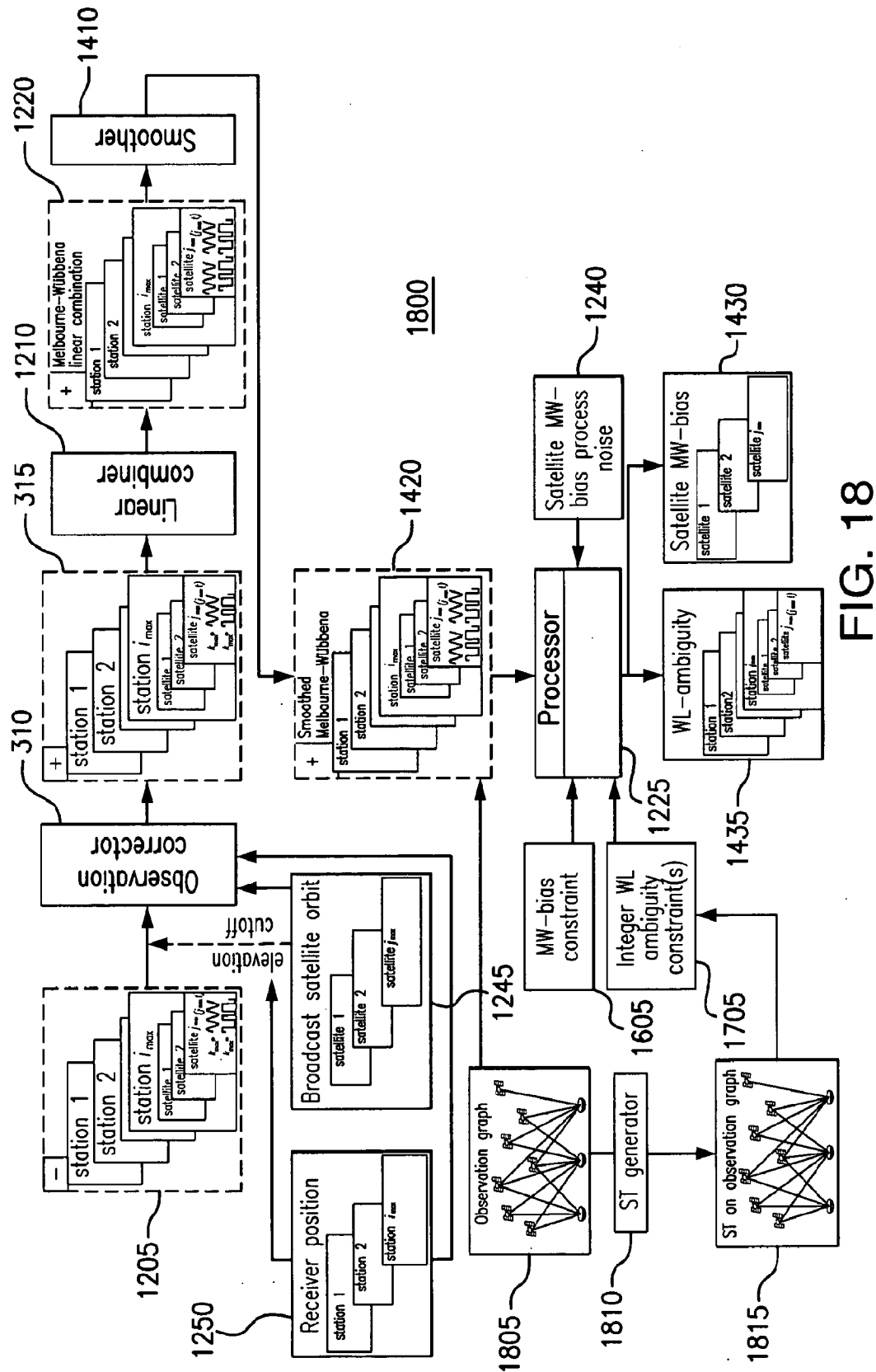
FIG. 18
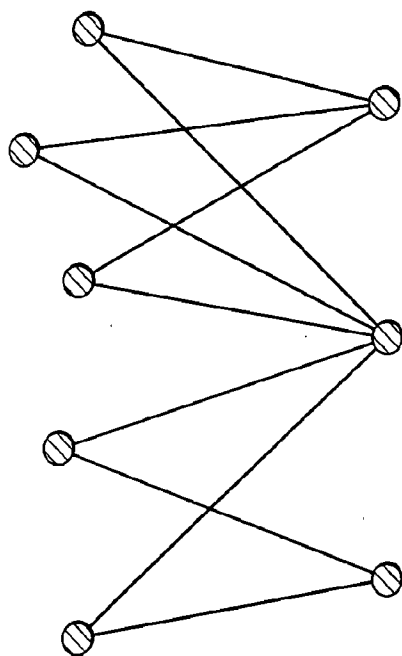
FIG. 19B

1910
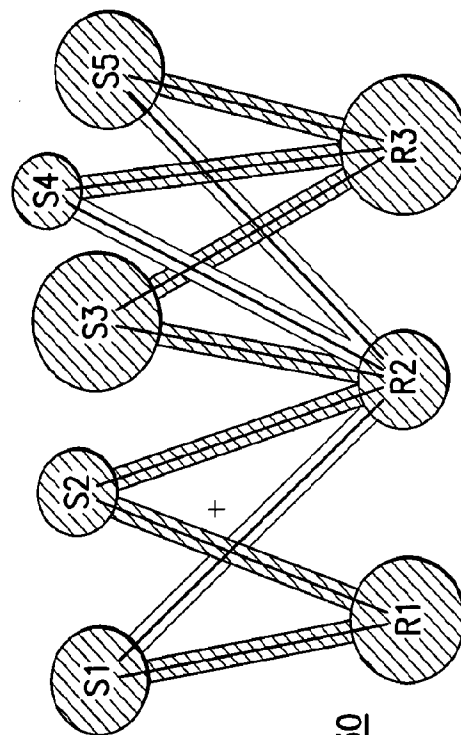
FIG. 19D

1930
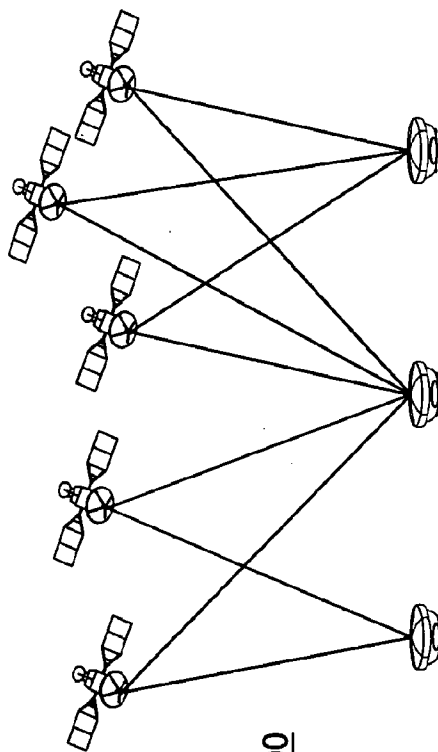
FIG. 19A

1900
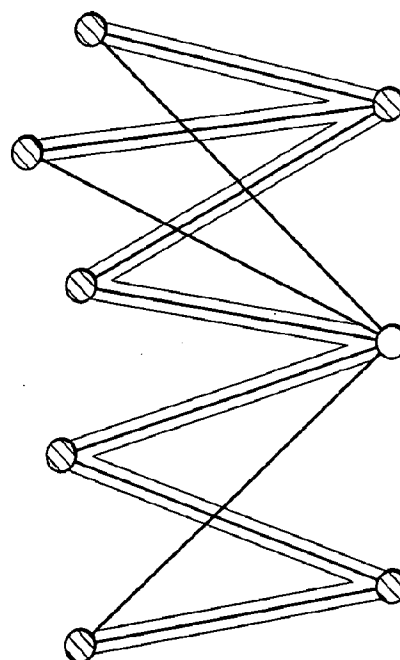
FIG. 19C

1920

Filter graph

FIG. 19F

1950
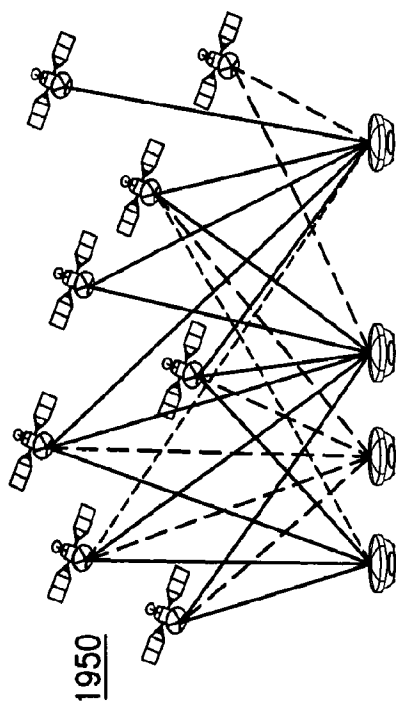
SD Filter graph

FIG. 19H

1970
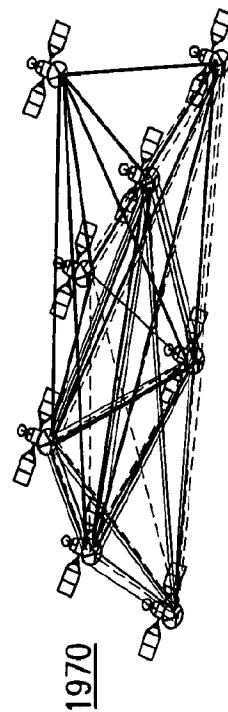
Observation graph

FIG. 19E

1940
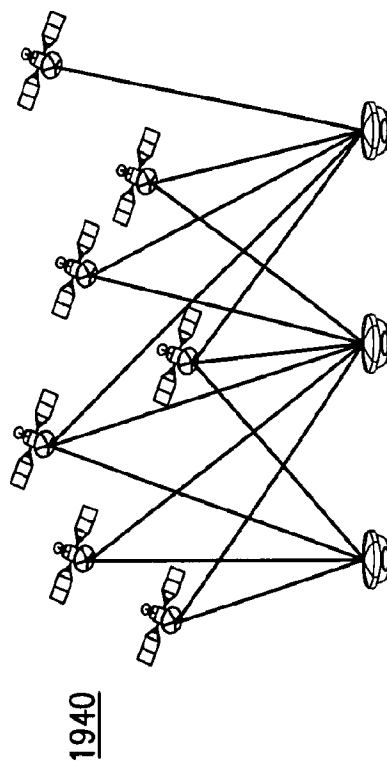
SD observation graph

FIG. 19G

1960
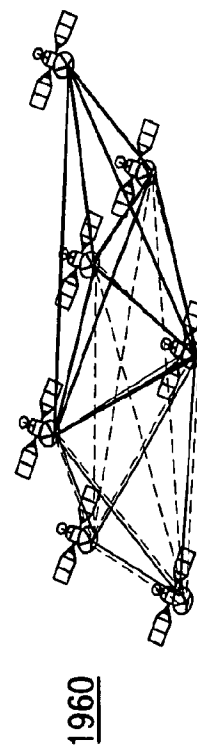
FIG. 19I
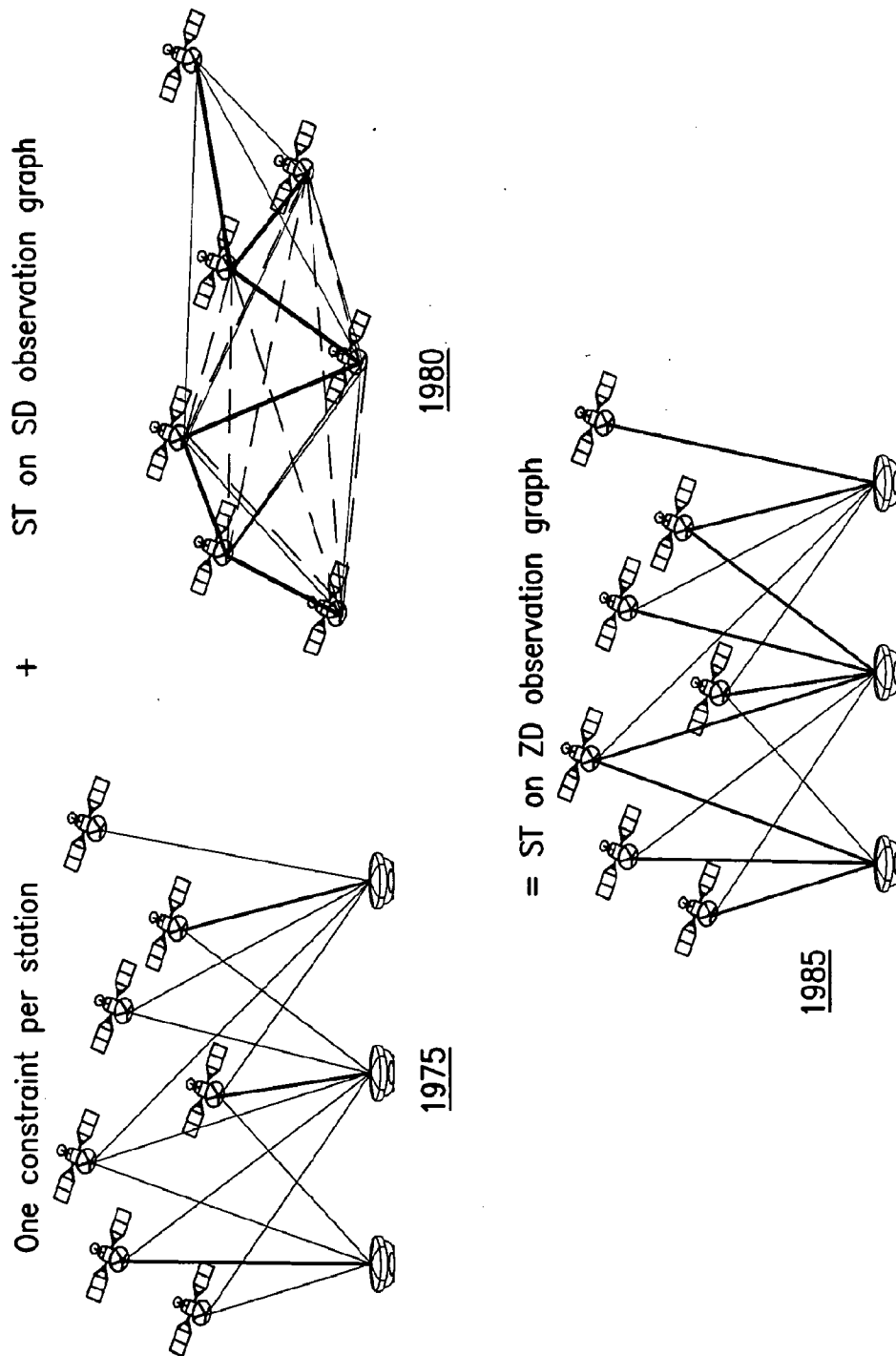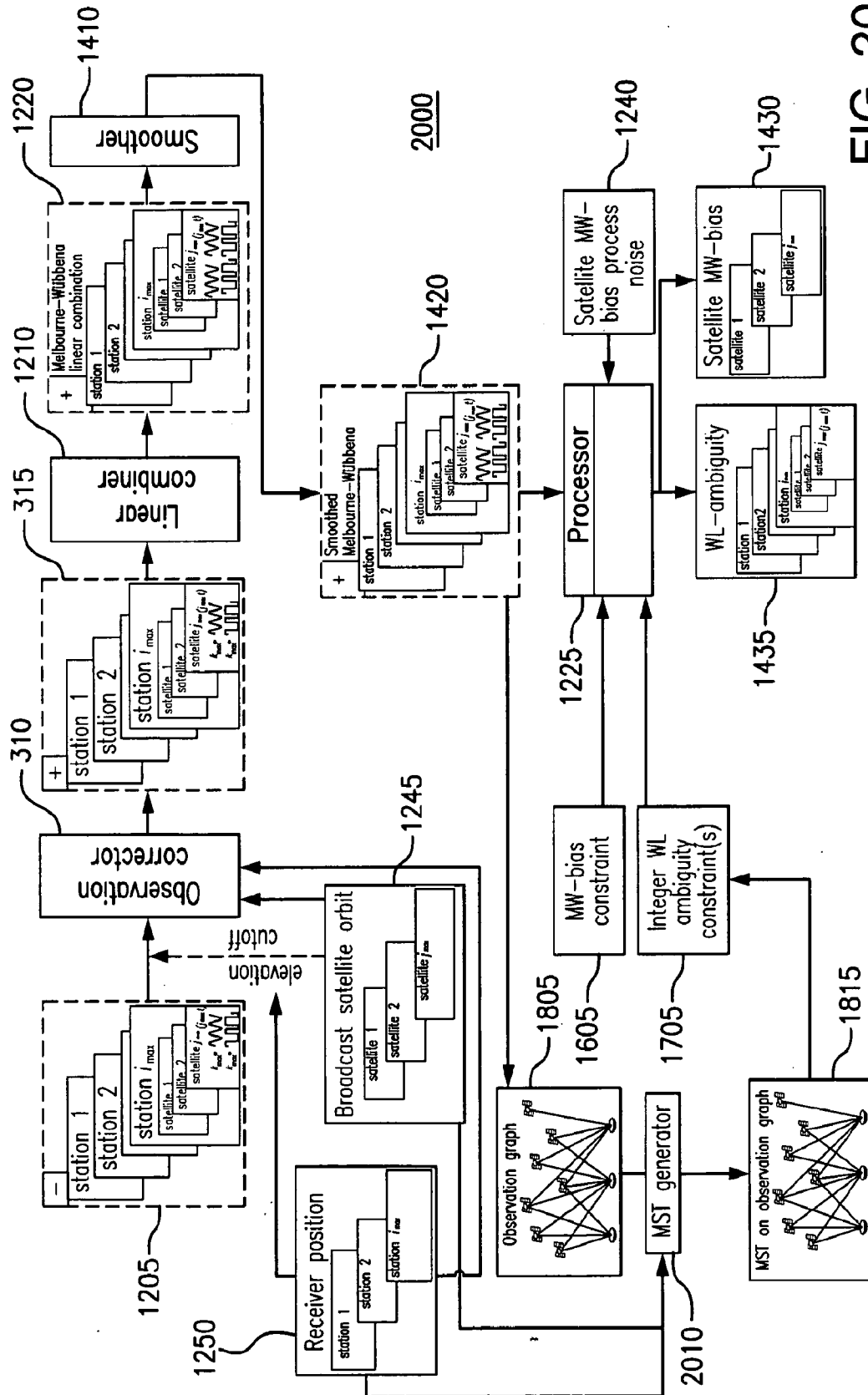
FIG. 20

MST on observation graph

FIG. 21B

2120

ST on Observation graph

FIG. 21A

2110

MST on SD Observation graph

FIG. 21D

2140

ST on SD observation graph

FIG. 21C

2130

21/71

FIG. 22

22/71

FIG. 23A

FIG. 23B

24/71

FIG. 24A

FIG. 24B

26/71

FIG. 24C

FIG. 24D

FIG. 25A

FIG. 25B

FIG. 25C

31/71

FIG. 26A

FIG. 26B

2686

Updated Orbit State Vector 2680 (sat 1 ... sat j_{max}) (with estimated EOPs xp,yp,UT1−UTC)

Orbit Mapper 2682 (Use Reference Trajectory at current epoch and Partial Derivatives at current epoch to get Updated Orbit in ECEF reference frame at current epoch)

Current Epoch Orbit Position/Velocity 350 (sat 1 ... sat j_{max})

Orbit Start Vector & Partial Derivatives 2635 (sat 1 ... sat j_{max}) (EOP: $x_p y_p$ UT1−UTC)

FIG. 26C

2688

Updated Orbit State Vector 2680 (sat 1 ... sat j_{max}) (with estimated EOPs xp,yp,UT1−UTC)

Orbit Mapper 2684 (Use Reference Trajectory at current epoch and Partial Derivatives at current epoch to get Updated Orbit in inertial reference frame at current epoch)

New Orbit Start Vector 2690 (at t0 + x hours)

Orbit Start Vector & Partial Derivatives 2635 (sat 1 ... sat j_{max}) (EOP: $x_p y_p$ UT1−UTC)

FIG. 26D

FIG. 27

FIG. 28A

36/71

FIG. 28B

37/71

FIG. 28C

38/71

2900

FIG. 29

MW Biases &/or Fixed WL Ambiguities 2905

Code-Leveled Clock per Satellite 2910

Precise Orbits Or IGS Orbits 2915

Tropo per station 2920

Receiver 1–n Observations per Satellite 2925

Phase-Leveled Clock per Satellite 2970

SD HR Code Clock per Satellite 2960

LR (only if fixed WL Ambiguities–option 2)

LR (only if MW Biases–option 1)

Compute SD Float Nif's 2945

SD Float Nif's 2950

NWL Fixer Bank 2930

SD Fixed NWL's 2935

Compute HR Code Clock 2955

SD HR Code Clocks 2960

Compute HR Phase Clock Per Satellite 2965

Phase Leveled Clocks 2970

N1 Fixer Bank 2975

SD Fixed N1's 2980

HR Phase Clocks, HR Code Clocks, HR WL biases 2990

Shift & Combine 2985

FIG. 30A

FIG. 30B

FIG. 30C

FIG. 31

FIG. 32

FIG. 33

FIG. 34

FIG. 36

47/71


FIG. 37

FIG. 38

FIG. 39

FIG. 40

Virtual Base Station Location 3840 → Save/Update Virtual Base Location 4005

Precise Satellite Data 3840 → Save Current Satellite Data 4010

Time Tag 3842 → Save Current Time Tag 4015

External Trigger 4020

Create Dataset Now? 4025 — No

Yes → Compute Satellite Position/Velocity for Current Time tag 4030 → Satellite Position/Velocity for Current Time Tag 4035 → Create Base Station Data set for Current Time Tag 4040 → Uncorrected Synthesized Base Station Data Set 4045 → Correct Synthesized Base Station Data Set 4050

4000

Synthesized Base Station Data 3850
e.g.,
L1 Code, L2 Code
L1 Phase, L2 Phase
L1 Cycle Slip, L2 Cycle Slip
Virtual Base Location

51/71

FIG. 42

FIG. 43

FIG. 44

54/71

FIG. 45

FIG. 46

FIG. 47
PPP Ambiguity Fixing
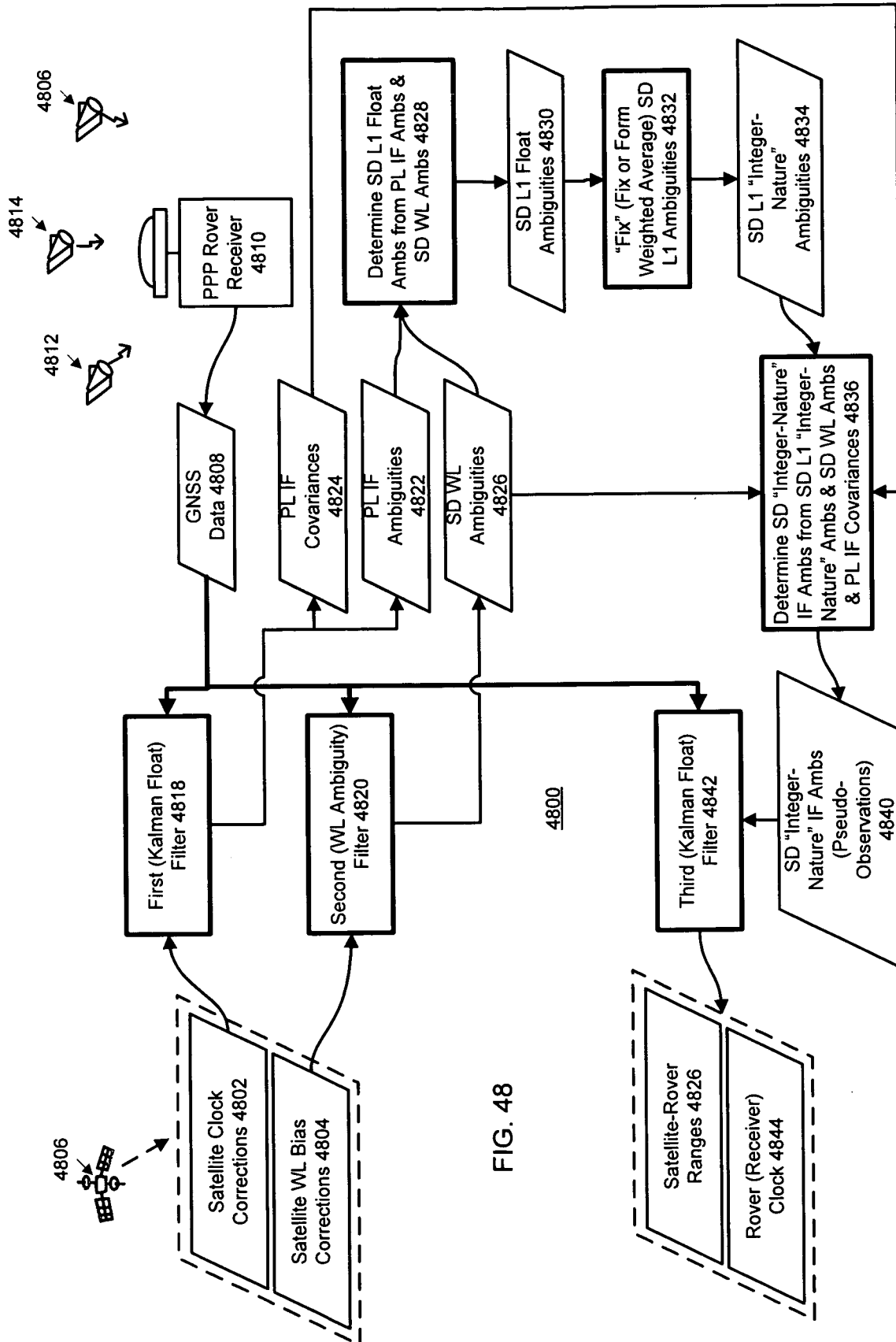
FIG. 48
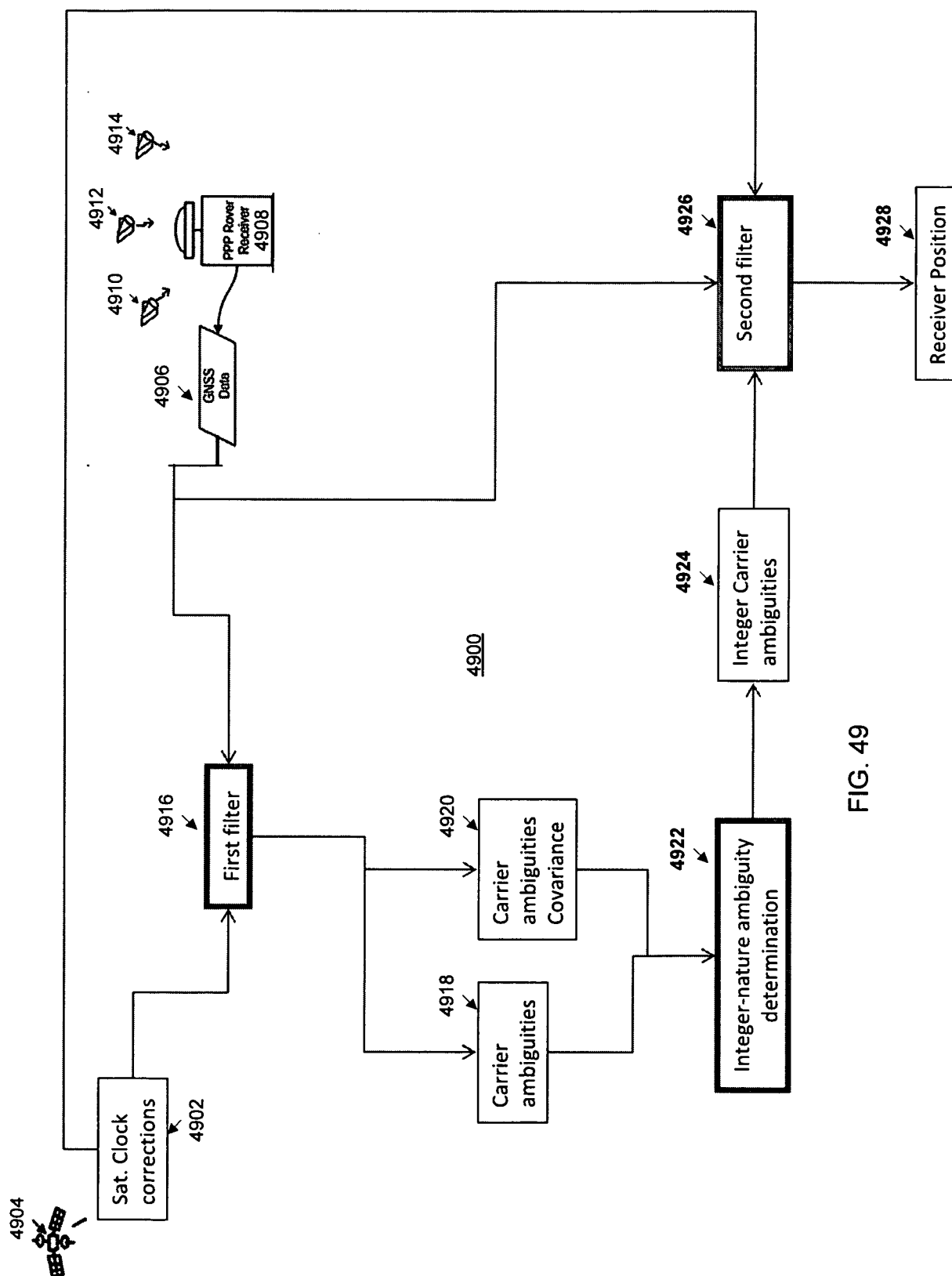
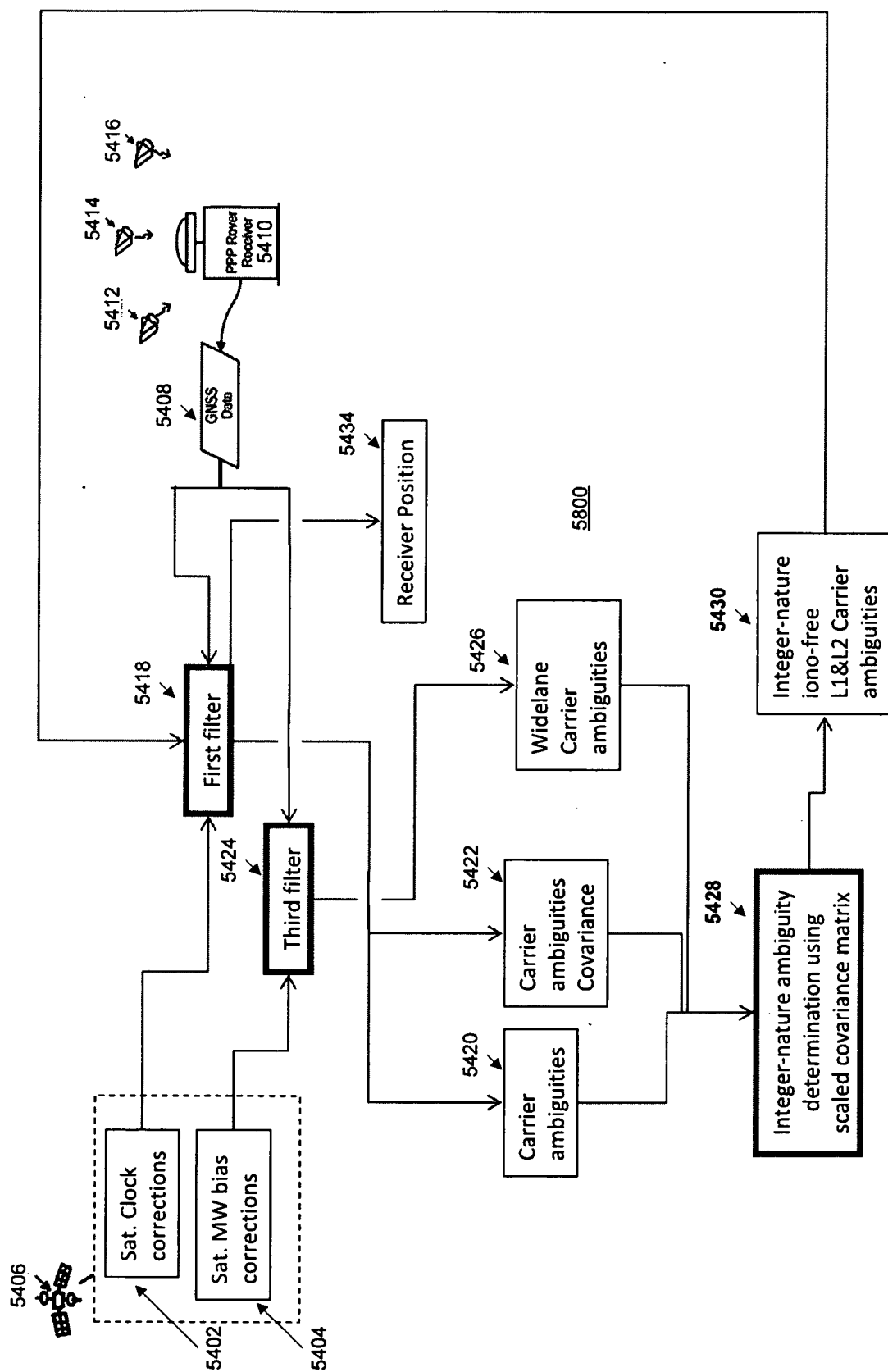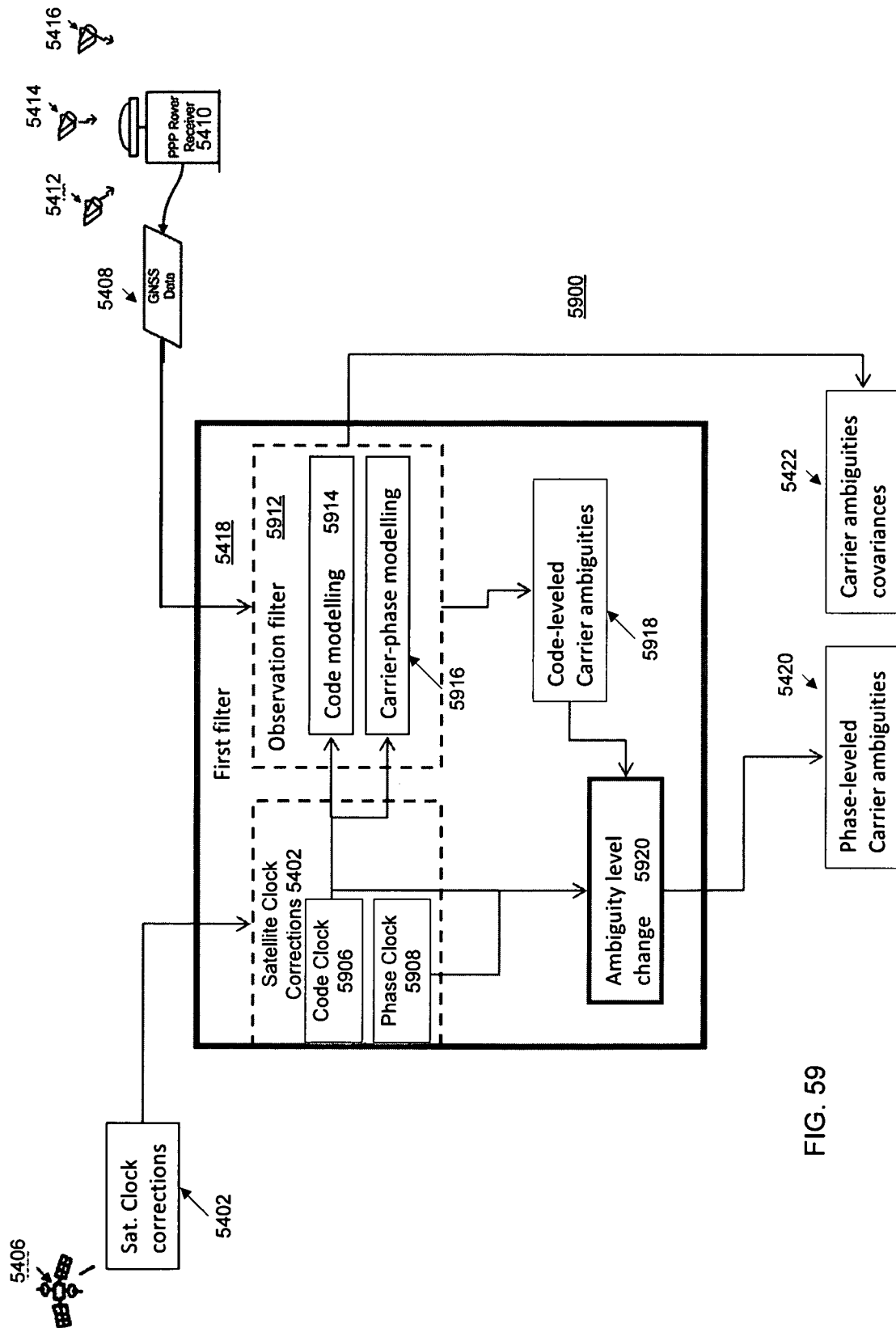FIG. 49
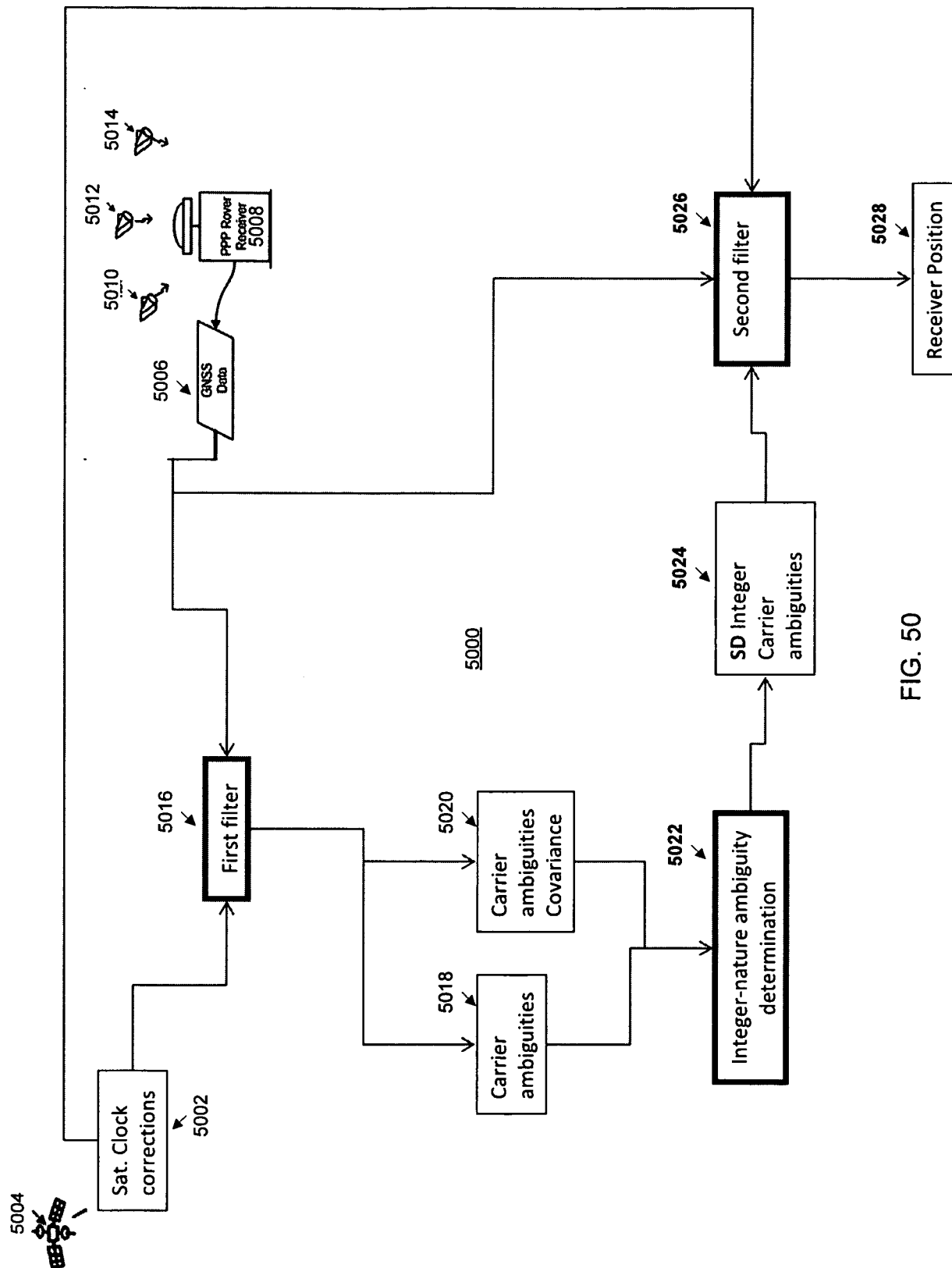
FIG. 50
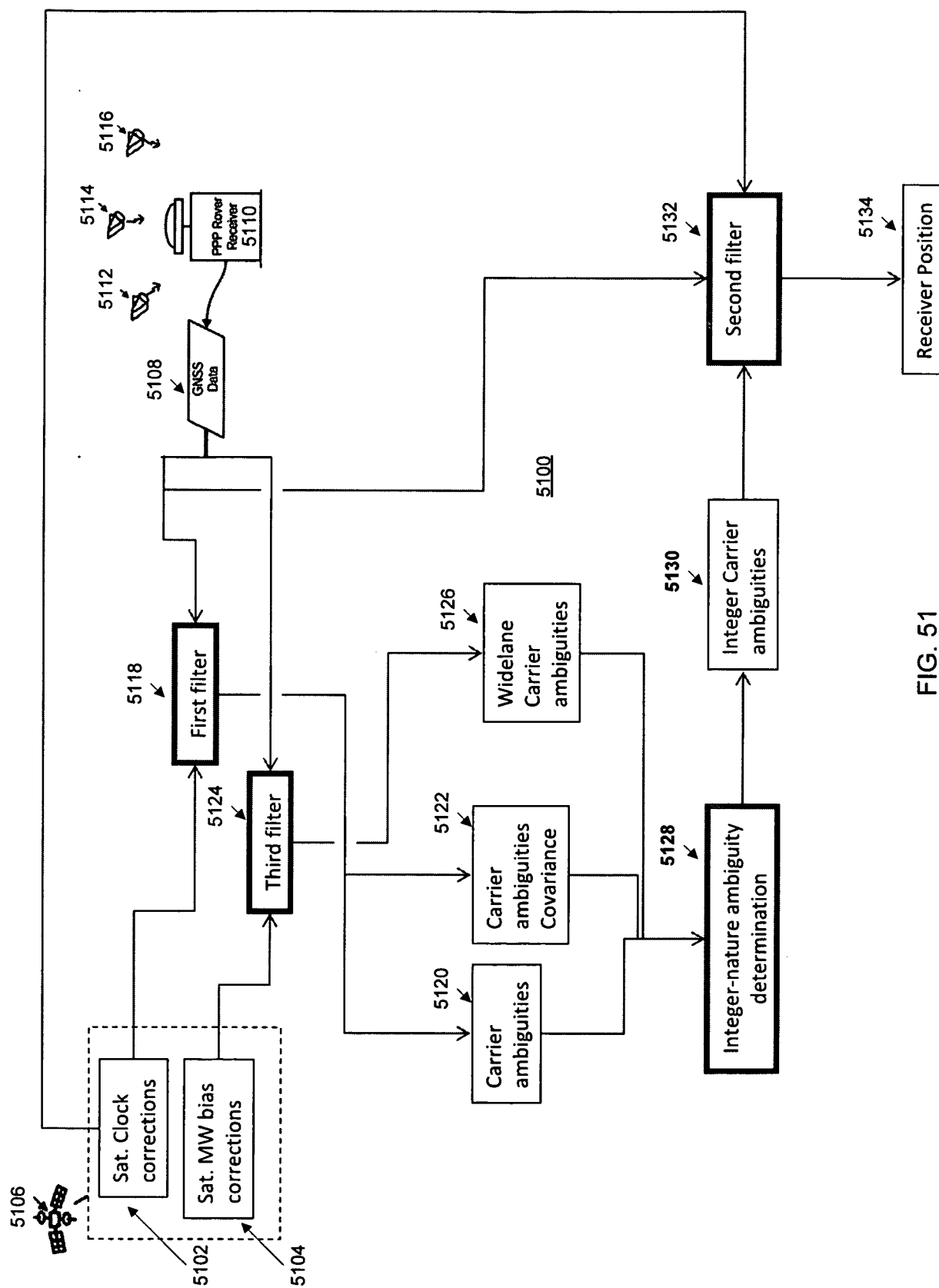
FIG. 51
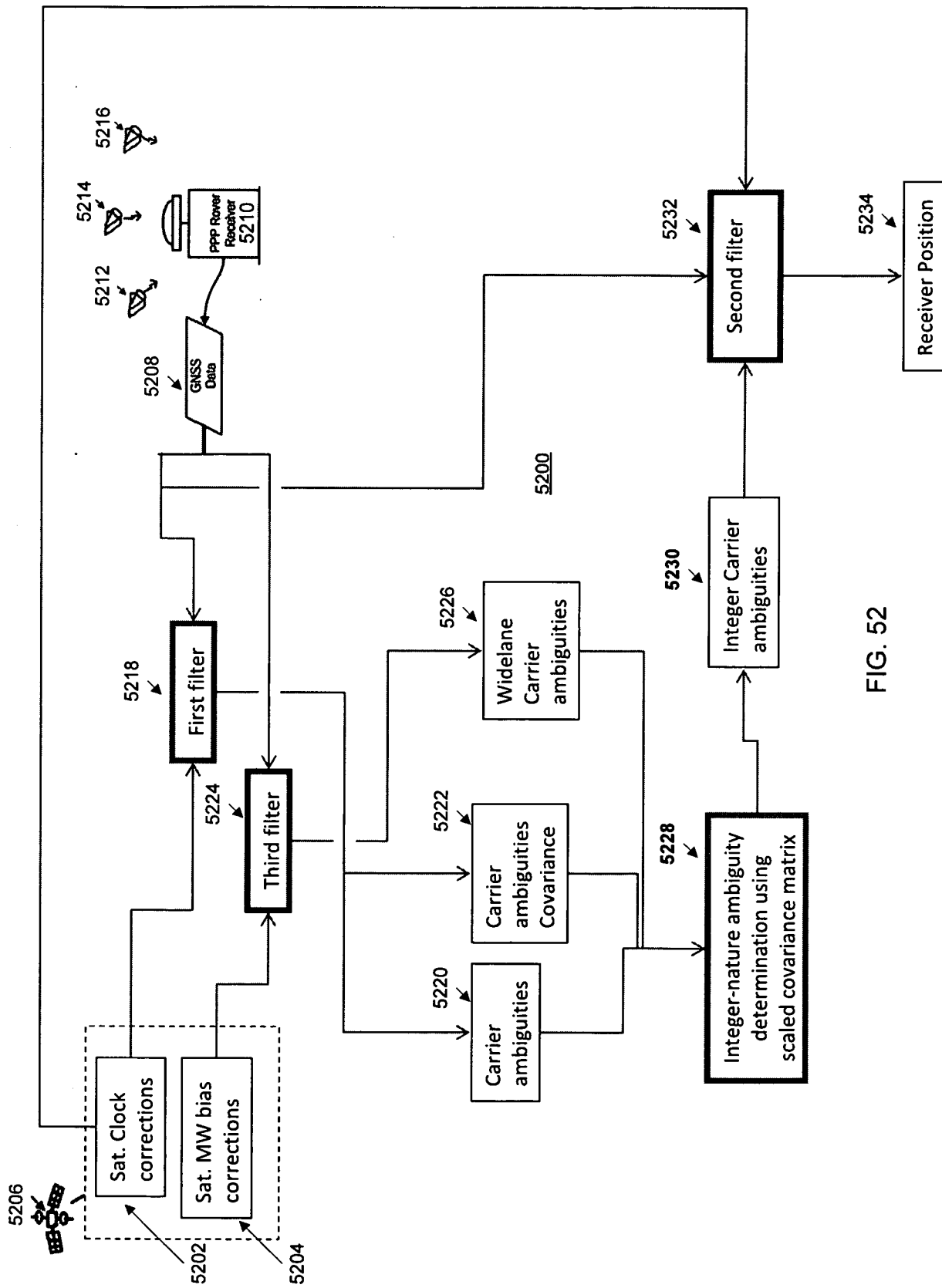
FIG. 52
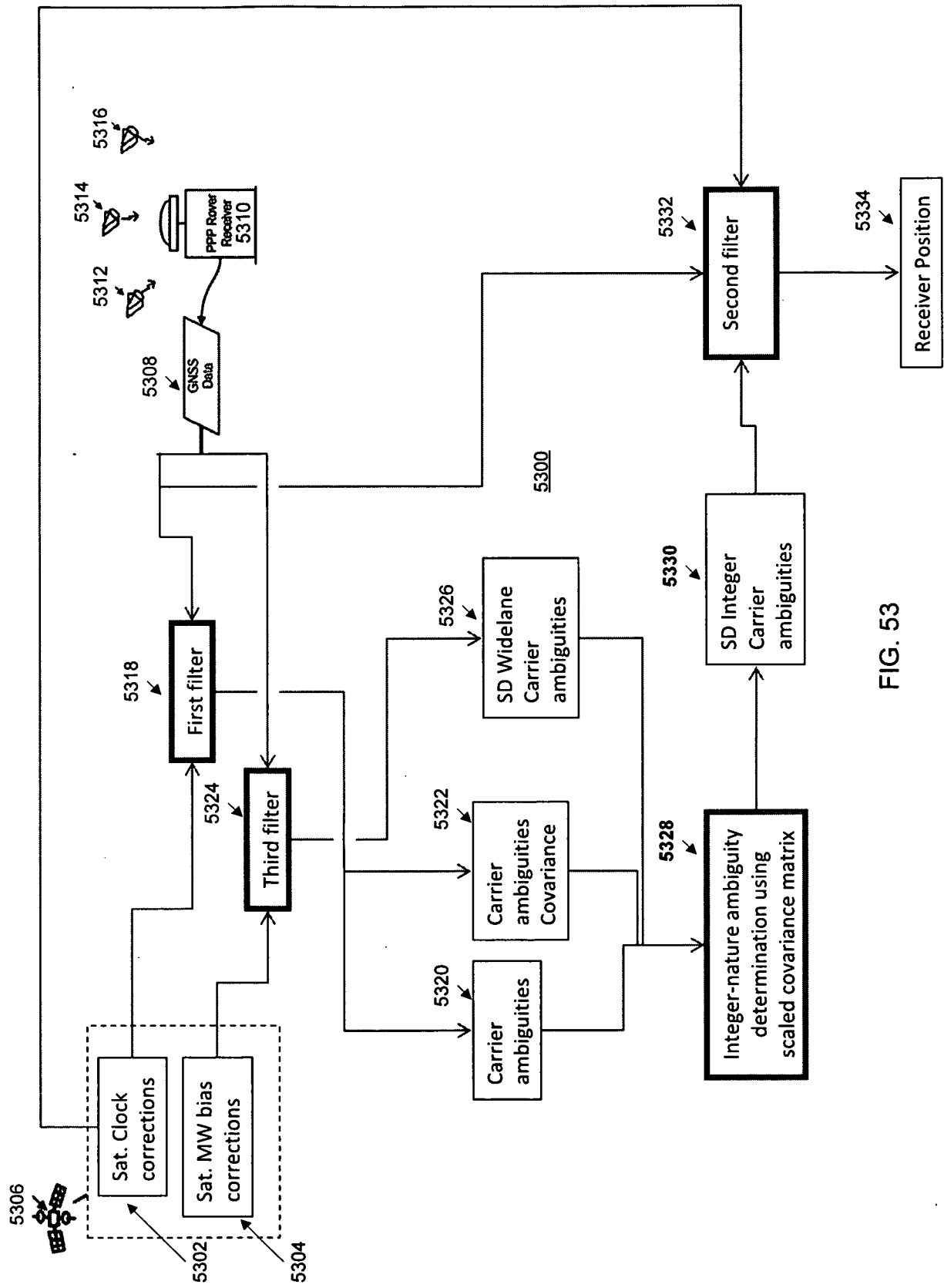
FIG. 53
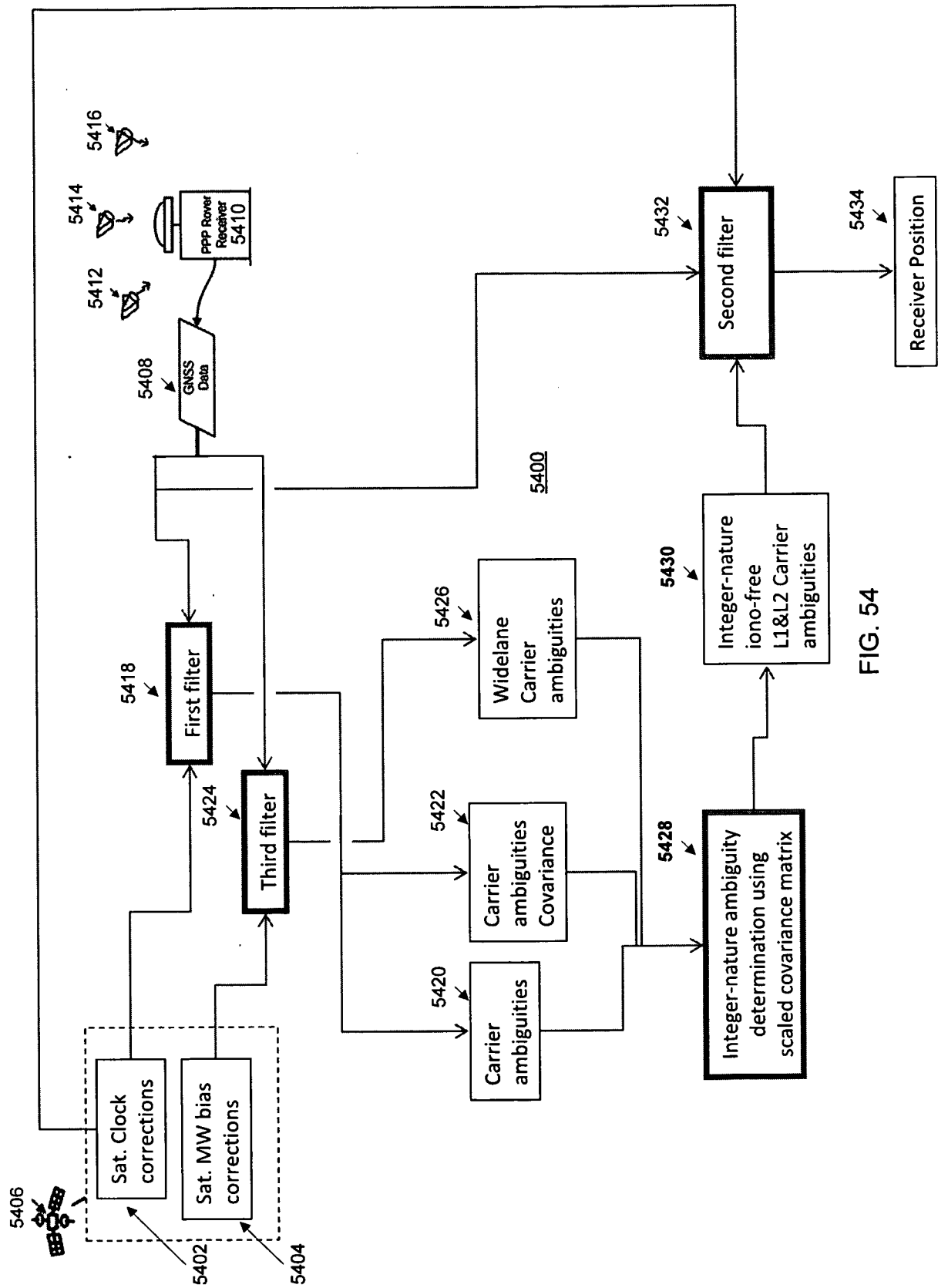
FIG. 54
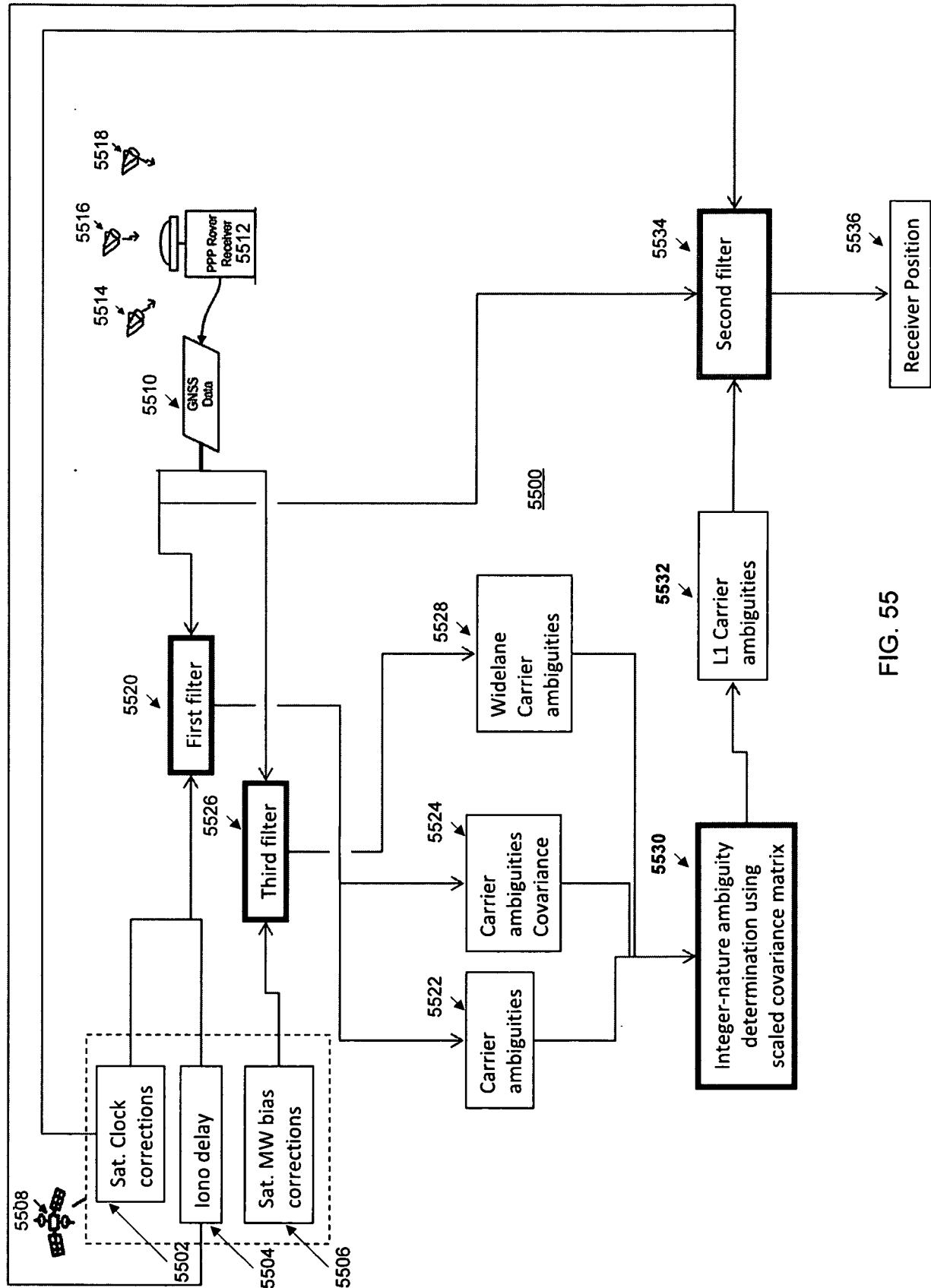
FIG. 55
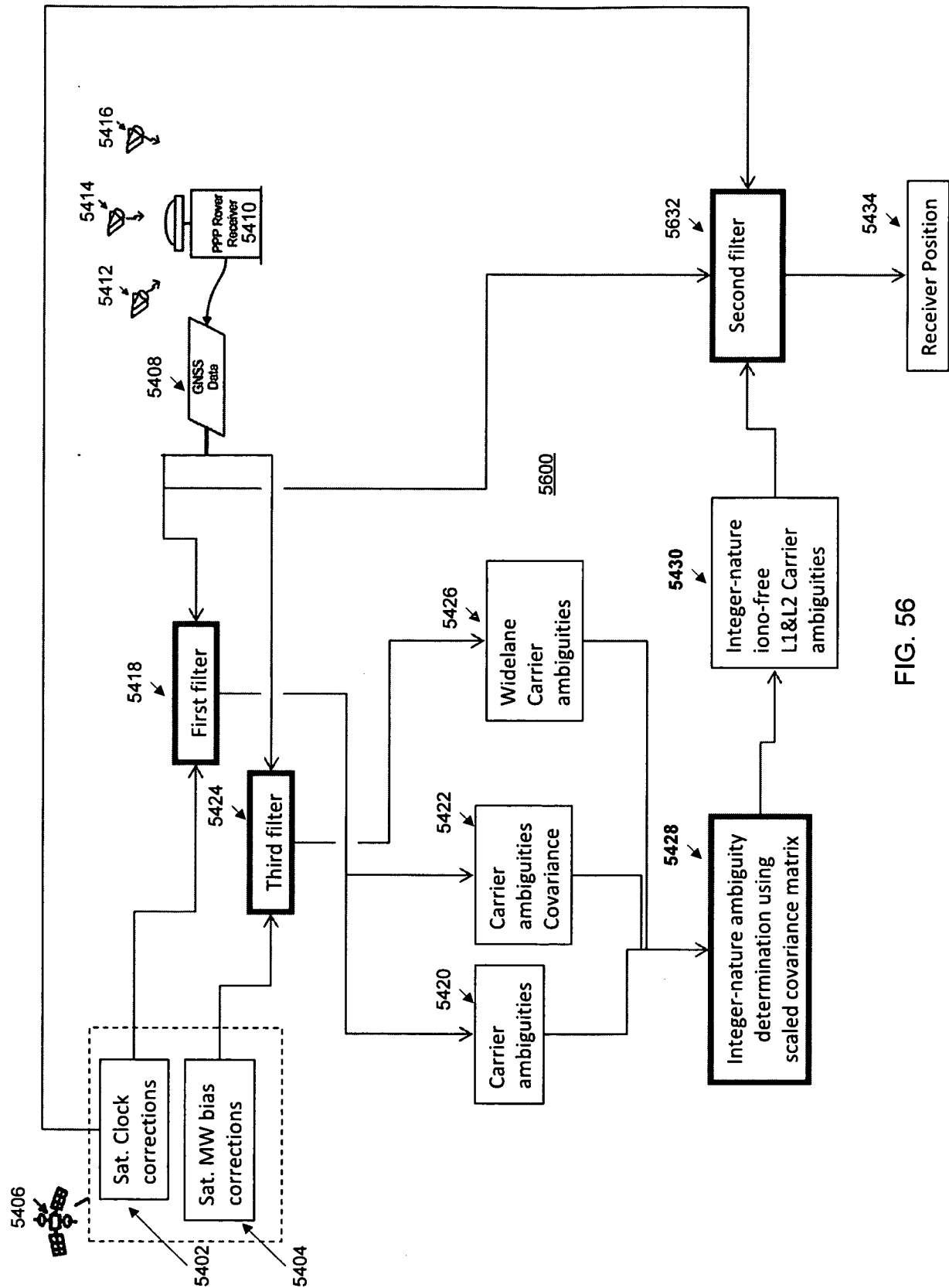
FIG. 56
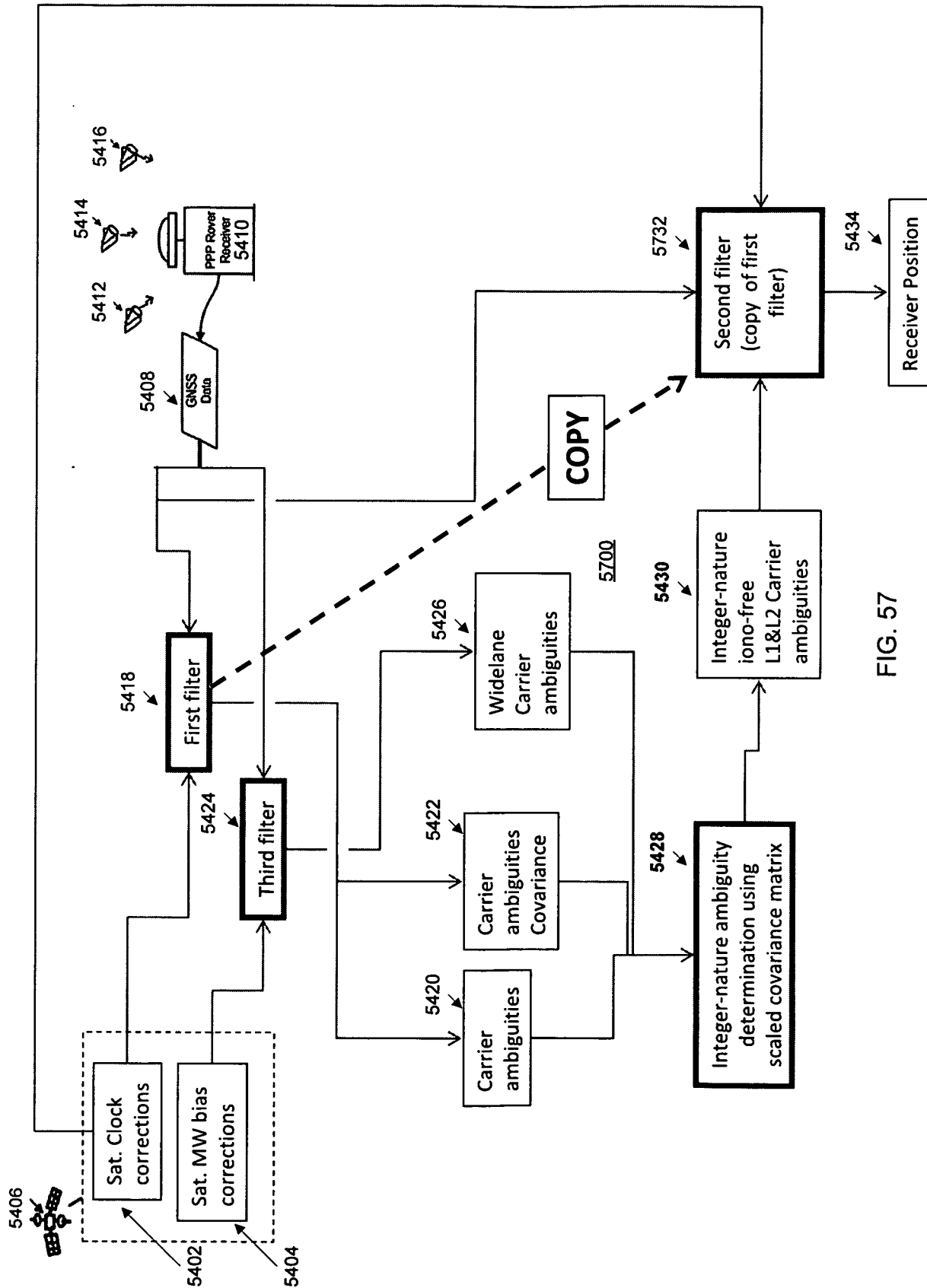
FIG. 57

FIG. 58

FIG. 59

FIG. 60

FIG. 61

FIG. 62